



# **O**verview of Approaches Used to Determine Computational Bias in Criticality Safety Assessment



# **Overview of Approaches Used to Determine Calculational Bias in Criticality Safety Assessment**

**State-of-the-Art Report (Part 1)**

**October 2013**

© OECD 2013

NUCLEAR ENERGY AGENCY

ORGANISATION FOR ECONOMIC CO-OPERATION AND DEVELOPMENT

## ORGANISATION FOR ECONOMIC CO-OPERATION AND DEVELOPMENT

The OECD is a unique forum where the governments of 34 democracies work together to address the economic, social and environmental challenges of globalisation. The OECD is also at the forefront of efforts to understand and to help governments respond to new developments and concerns, such as corporate governance, the information economy and the challenges of an ageing population. The Organisation provides a setting where governments can compare policy experiences, seek answers to common problems, identify good practice and work to co-ordinate domestic and international policies.

The OECD member countries are: Australia, Austria, Belgium, Canada, Chile, the Czech Republic, Denmark, Estonia, Finland, France, Germany, Greece, Hungary, Iceland, Ireland, Israel, Italy, Japan, Luxembourg, Mexico, the Netherlands, New Zealand, Norway, Poland, Portugal, the Republic of Korea, the Slovak Republic, Slovenia, Spain, Sweden, Switzerland, Turkey, the United Kingdom and the United States. The European Commission takes part in the work of the OECD. OECD Publishing disseminates widely the results of the Organisation's statistics gathering and research on economic, social and environmental issues, as well as the conventions, guidelines and standards agreed by its members.

*This work is published on the responsibility of the OECD Secretary-General.  
The opinions expressed and arguments employed herein do not necessarily reflect the official  
views of the Organisation or of the governments of its member countries.*

### NUCLEAR ENERGY AGENCY

The OECD Nuclear Energy Agency (NEA) was established on 1 February 1958. Current NEA membership consists of 31 OECD member countries: Australia, Austria, Belgium, Canada, the Czech Republic, Denmark, Finland, France, Germany, Greece, Hungary, Iceland, Ireland, Italy, Japan, Luxembourg, Mexico, the Netherlands, Norway, Poland, Portugal, the Republic of Korea, the Russian Federation, the Slovak Republic, Slovenia, Spain, Sweden, Switzerland, Turkey, the United Kingdom and the United States. The European Commission also takes part in the work of the Agency.

The mission of the NEA is:

- to assist its member countries in maintaining and further developing, through international co-operation, the scientific, technological and legal bases required for a safe, environmentally friendly and economical use of nuclear energy for peaceful purposes, as well as
- to provide authoritative assessments and to forge common understandings on key issues, as input to government decisions on nuclear energy policy and to broader OECD policy analyses in areas such as energy and sustainable development.

Specific areas of competence of the NEA include the safety and regulation of nuclear activities, radioactive waste management, radiological protection, nuclear science, economic and technical analyses of the nuclear fuel cycle, nuclear law and liability, and public information.

The NEA Data Bank provides nuclear data and computer program services for participating countries. In these and related tasks, the NEA works in close collaboration with the International Atomic Energy Agency in Vienna, with which it has a Co-operation Agreement, as well as with other international organisations in the nuclear field.

This document and any map included herein are without prejudice to the status of or sovereignty over any territory, to the delimitation of international frontiers and boundaries and to the name of any territory, city or area.

Corrigenda to OECD publications may be found online at:

#### © OECD 2013

---

You can copy, download or print OECD content for your own use, and you can include excerpts from OECD publications, databases and multimedia products in your own documents, presentations, blogs, websites and teaching materials, provided that suitable acknowledgment of the OECD as source and copyright owner is given. All requests for public or commercial use and translation rights should be submitted to [rights@oecd.org](mailto:rights@oecd.org). Requests for permission to photocopy portions of this material for public or commercial use shall be addressed directly to the Copyright Clearance Center (CCC) at [info@copyright.com](mailto:info@copyright.com) or the Centre français d'exploitation du droit de copie (CFC) [contact@cfcopies.com](mailto:contact@cfcopies.com).

---

## Foreword

The Working Party on Nuclear Criticality Safety (WPNCS) has been established to deal with technical and scientific issues relevant to criticality safety. Specific areas of interest include (but are not limited to) investigations of static and transient configurations encountered in the nuclear fuel cycle (fuel fabrication, transport and storage). The main objectives of the WPNCS are to exchange information on national programmes in the area of criticality safety, to guide, promote and co-ordinate high-priority activities of common interest to the international criticality safety community and to establish co-operation, publish databases, handbooks and reports, facilitate communications within the international criticality safety community through relevant websites, co-ordinate the on-going series of International Conferences on Nuclear Criticality Safety (ICNC), co-ordinate WPNCS activities with other working groups within the NEA and in other international organisations, provide a technical basis for the activities of other international organisations. This working party currently co-ordinates five expert groups and the International Criticality Safety Benchmark Evaluation Project (ICSBEP).

One of the groups is the Expert Group on Uncertainty Analysis for Criticality Safety Assessment (UACSA), whose objective is to address issues related to Sensitivity/Uncertainty (S/U) studies for criticality safety calculations and to promote exchange of information on these topics, as well as to carry out the comparison and testing of methods and computing tools for uncertainty analysis, and assist with the selection and development of safe and efficient methodologies.

The present state-of-the-art report is the first outcome of the work of EG UACSA, which, at the first stage, is focused on the description of approaches for the validation of criticality safety calculations, as contributed by the different participants of the Expert Group.

The opinions expressed in this report are those of the authors only and do not necessarily represent the position of any member country or international organisation.

## **Acknowledgements**

The authors would like to acknowledge the contributors to the benchmark, the developers of the validation methods and software codes and their sponsoring organisations. Special thanks are also due to all the members of the Expert Group on Uncertainty Analysis for Criticality Safety Assessment (UACSA) for the fruitful discussions during the Expert Group meetings. (The list of authors and contributors can be found in Appendix B.)

## Table of contents

<b>1. Introduction</b> .....	<b>7</b>
<b>2. EG UACSA area of activity</b> .....	<b>9</b>
<b>3. Criteria for assessing methodologies</b> .....	<b>11</b>
3.1 Methodology for criticality computation .....	11
3.2 Description of the validation methodology .....	11
<b>4. Approaches for criticality safety validation</b> .....	<b>13</b>
4.1 AREVA GmbH PEPA5-G, Germany .....	13
4.2 Commissariat a l'Energie Atomique (CEA), France .....	22
4.3 E Mennerdahl Systems, EMS, Sweden .....	27
4.4 Institute for Physics and Power Engineering (IPPE), Russian Federation.....	30
4.5 Institut de Radioprotection et de Sûreté Nucléaire (IRSN), France .....	33
4.6 Japan Atomic Energy Agency (JAEA), Japan .....	39
4.7 Korean Institute of Nuclear Safety (KINS), Republic of Korea .....	45
4.8 Oak Ridge National Laboratory (ORNL), US .....	47
4.9 Paul Scherrer Institute (PSI), Switzerland.....	81
<b>5. Conclusions and plans for further studies</b> .....	<b>85</b>
<b>6. References</b> .....	<b>88</b>
<b>Appendix A: Glossary of EG UACSA</b> .....	<b>93</b>
<b>Appendix B: List of authors and contributors</b> .....	<b>98</b>

### List of figures

1: Area of EG UACSA interest.....	10
2: Hierarchy of uncertainties in criticality safety analysis.....	18
3: NUDUNA and coupling of NUDUNA with MOCADATA.....	20
4: Generation of random libraries for nuclear data and chemical assay data ("exp":= experiment-based MC samples) .....	20
5: Hierarchical Bayesian Monte Carlo criticality calculation procedure ( $x_S=x$ , $x_B=y$ ) .....	21
6: Flux comparison with graphical user interface of MACSENS.....	35
7: Flux comparison with graphical user interface of MACSENS.....	35
8: Flux comparison with graphical user interface of MACSENS.....	36
9: Probability distributions of calculated $k_{eff}$ and $\bar{k} - \mu_S$ .....	41

10: Illustration of correlation coefficient trending with $USL_1$ .....	54
11: Observed $k_{eff}$ biases and uncertainties due to cross-sections for 275 benchmark experiments .....	73
12: Some important uncertainties in the SCALE 6.0 covariance library.....	79
13: Additional uncertainties in the SCALE 6.0 covariance library.....	79

**List of tables**

1: $\mu$ values for typical sample number $n$ and degrees of freedom $f = n-1$ , where $\gamma = 0.975$ and $P = 0.025$ .....	43
2: The estimated criticality multiplication factor, ECMF, and the estimated criticality lower-limit multiplication factor, ECLLMF, for the JACS code system applied to the simple uranium/plutonium systems .....	43
3: The estimated criticality multiplication factor, ECMF, and the estimated criticality lower-limit multiplication factor, ECLLMF, for the MVP code system applied to the simple uranium/plutonium systems .....	44
4: Benchmark experiments used by ORNL .....	64
5: Sensitivity types computed by TSUNAMI-1D and -3D.....	74
6: Sources of covariance data in the SCALE 6 covariance library.....	78
7: Summary table: participants, criticality codes, nuclear data, criticality validation methods, and software tools .....	87

## 1. Introduction

At this time, the necessity to formalise a procedure for validation of codes for criticality computation based on rigorous techniques has become an issue of importance. There are, among others, the following reasons to develop methodologies and tools providing an approach for such a validation: 1) extension of operations with nuclear materials, caused by the growth of industry, could face a shortage of criticality analysts; 2) the changeover to innovation nuclear systems will require staff with specific qualifications for criticality safety assessment; 3) globalisation of demand for nuclear energy in countries with insufficient experience and infrastructure to manage fission materials; 4) economic “necessity” reducing costs of the redundant safety margin.

Approaches addressing forthcoming needs are developed in different countries. Even though validation of the criticality calculation is complicated and is a multiple-factor problem, the comparison and validation of the tools for such validation is an even more sophisticated problem. The solution of this problem could answer the question whether we can trust the bias and its uncertainty predicted by a tool for criticality safety analysis validation. That is why it seems relevant to characterise and compare the techniques developed by different teams and to provide their cross-validation to profit from the variety of the developments.

Based on these facts, the EG UACSA has been created with the objective to compare the existing approaches in order to establish the best practices and provide an answer to the scepticism that some safety authorities show when faced with the practical use of these approaches.

The main objectives of the group are to:

- promote the exchange of information on topics related to sensitivity and uncertainty (S/U) analysis;
- compare methods used for S/U analysis;
- test the performance of the methods against benchmark tests;
- assist with the selection/development of “best-practice” methodologies for the validation of criticality safety calculation computations and the establishment of manufacturing/operational uncertainties .

The kick-off meeting of the Group took place on 5-6 December 2007. Twenty-five participants from nine countries discussed techniques and codes adopted or developed in their organisations for criticality safety validation and the use of these techniques and/or codes to support compliance with the standards for nuclear criticality safety. The diversity of the approaches presented has shown that their description, qualitative comparison and testing of their bias and bias uncertainty generation capability would be useful for the criticality safety community. Thus, the outcome of the meeting was to set goals to compile an overview of approaches to the validation of criticality safety calculations and to illustrate their performance through application to a set of benchmark exercises.

Accordingly, specifications were prepared [2] and participants submitted descriptions of their validation approaches. The submitted descriptions of the approaches and results of the exercises were discussed at three EG meetings.

This report provides an overview of some of the approaches used among the international criticality safety community to validate criticality calculations, which include 1) similarity assessment; 2) selection of suitable benchmark experiments; 3) determination of  $k_{\text{eff}}$  bias and bias uncertainty.

Ten approaches are described in the report, based on submissions from the participants. For each approach, the following issues are described in accordance with a proposed specification:

- methods and software tools for both criticality computation and validation of the computation;
- parameters and procedure used for similarity assessment;
- the number of experimental benchmarks available for the validation study;
- treatment of benchmark uncertainties;
- algorithm for bias and bias uncertainty establishment;
- status of the developments for the method/tool.

References supporting the validation methodology can also be found in the report.

Application of these methods is illustrated through a set of benchmark tests (Phase I Exercise). The results of the Benchmark will be published in the State-of-the-art report (Part 2).

A glossary added in Appendix A provides descriptions of some technical terms.

## 2. EG UACSA area of activity

A key part of many modern criticality safety assessments is the use of computer modelling as part of the process of identifying appropriate limits for criticality control purposes. In these cases, an allowance must be made for any bias and uncertainty in the modelling methods used. The key to providing a rigorous derivation of this allowance is the identification of suitable experimental evidence against which the calculation method can be validated.

Other sources of uncertainty may arise from modelling approximations, operation conditions, and technological or manufacturing parameters. These parameters should be estimated for the application undergoing criticality safety analysis and (in the case of technological or manufacturing uncertainties) for the experimental benchmarks used to validate the method. This typically requires comprehensive sensitivity studies. For benchmarks based on critical experiments such a study is available in the ICSBEP Handbook. The Handbook includes the treatment of uncertainties encountered in experimental data and the derivation of benchmark results.

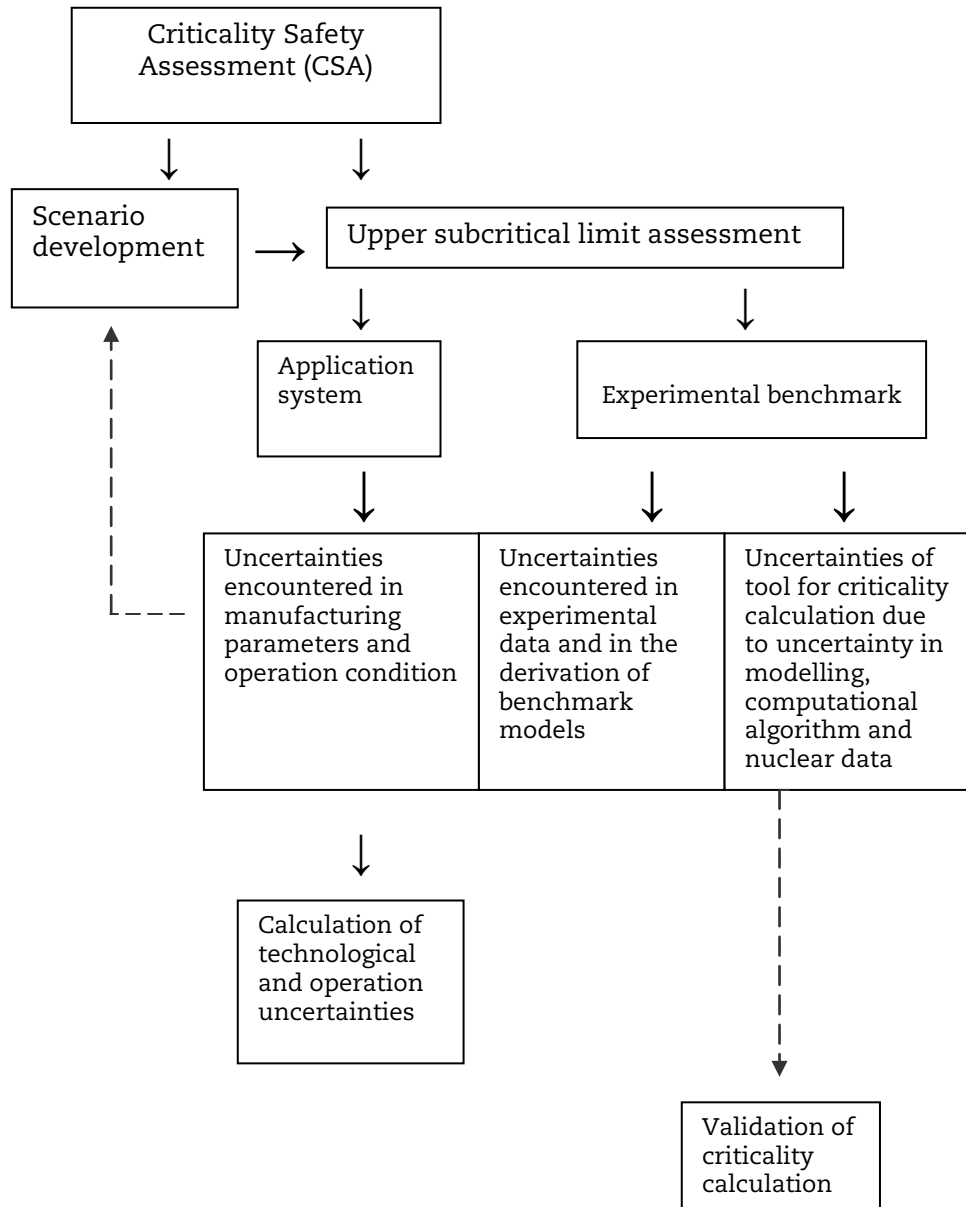
Uncertainty analysis can be applied to improve the validation of criticality safety calculation, e.g. to improve the rigor of the methodologies used for similarity assessment, benchmarks selection, and establishment of bias and bias uncertainty.

Estimation of real and potential variations in manufacturing parameters and operation condition are required to identify appropriate assumptions for criticality assessment scenarios. Methods used for the establishment of manufacturing uncertainties may also be significant in providing a complete description of uncertainties in benchmark experiments.

Figure 1 demonstrates two principal directions in EG activities: estimation of the bias (and its uncertainty) for criticality safety calculations and the assessment of manufacturing/operational (including depletion when applicable) uncertainties.

At the current stage, the work of the UACSA group focuses on approaches for validation of criticality safety calculations. Methodologies that establish uncertainties related to operational as well as technological or manufacturing parameters for applications/design systems will be the subject of further study. Special attention will also be paid to the establishment of uncertainties related to depletion calculations for burn-up credit validation.

**Figure 1: Area of EG UACSA interest**



### 3. Criteria for assessing methodologies

The objective of the descriptive part (Part 1) of the report is to gather information about methods used for validation of criticality safety assessments in different countries and to outline their current status. Validation methods determine an appropriate bias and bias uncertainty for use in determining subcriticality with a specified confidence level. The following sources of uncertainties are typically evaluated in validation methods: uncertainty associated with nuclear data, uncertainties associated with criticality experiment descriptions, uncertainty associated with nuclear data and computational methods, uncertainties related to modelling approximations, and uncertainties related to technological or manufacturing parameters.

Criteria for assessing the different methodologies have been defined and agreed upon by all the contributors to the report. They fall into the following categories: criticality computation and validation of criticality computation.

Contributors to the report were requested to provide the following information.

#### 3.1 Methodology for criticality computation

- criticality package (codes system) title and version (e.g. SCALES.1, CRISTAL V1);
- modules utilised for neutron cross-section treatment and neutron transport calculation (methods employed and titles);
- nuclear data source and energy structure;
- validation of criticality calculations;
- main sources of uncertainty [e.g. nuclear data, technological parameters (specify the parameters)];

#### 3.2 Description of the validation methodology

- Approach for selection of benchmark experiments:
  - parameters used for similarity assessment of a benchmark-experiment relative to a test application;
  - criteria and process used for similarity assessment (expert judgement, similarity parameter, parameter range comparison, etc.);
- Implementation of the validation method used to determine bias and bias uncertainty (if available):
  - software tool title;
  - algorithm;
- Initial data for the bias and bias uncertainty determination:
  - number of benchmarks available for calculation-to-experiment comparison;
  - uncertainties treatment for experimental data;

- other data used in validation method (nuclear data covariance, sensitivity coefficients, etc.);
- source of data;
- preprocessing tools and methods used;
- amount of data available for the analyses (for example, sensitivity coefficients are available for 400 configurations);
- History of the validation methodology :
  - primarily purpose;
  - experience of use;
  - status of the development/validation;
  - published references supporting the validation methodology;
  - additional information/notes.

These criteria have been submitted to the participants together with specification for Benchmark Phase I [2]. The responses are provided in Chapter 4.

## 4. Approaches for criticality safety validation

### 4.1 AREVA GmbH PEPA5-G, Germany

Participants: Jens Christian Neuber, Axel Hofer

#### 4.1.1 Criticality calculations

##### 4.1.1.1 Criticality package (codes system) title and version

- SCALE 5.1 and SCALE 6.0 [3];

##### 4.1.1.2 Modules utilised for neutron cross-section treatment and neutron transport calculation (methods employed and titles)

- SCALE 5.1 and SCALE 6.0 control sequences CSAS25/CSAS26, including the modules;
- BONAMI, NITAWL, KENO Va / KENO VI;
- BONAMI, CENTRM/PMC, KENO Va / KENO VI, [3].

##### 4.1.1.3 Nuclear data source and energy structure

Cross-section libraries:

- 238GROUPNDF5;
- 44GROUPNDF5;
- V6-238 plus continuous energy, [3].

#### 4.1.2 Validation of criticality calculations

##### 4.1.2.1 Introduction

It is an indispensable part of the Criticality Safety Analysis (CSA) of a Nuclear Fuel System (NFS) performed by using numerical methods for calculating the neutron multiplication factor  $k_{\text{eff}}$  of the system to demonstrate that the probability that this neutron multiplication factor exceeds the maximum allowable value  $k_{\text{max}}$  is not greater than an administratively established margin  $\gamma$ , i.e. it meets the following inequality:

$$\pi_{\text{NFS}} = P((k_{\text{eff}} + \Delta k_{\text{B}}) > k_{\text{max}} | \text{NFS}) \leq \gamma. \quad (1)$$

The term  $\Delta k_{\text{B}}$  in this inequality denotes the bias of the numerical result obtained for  $k_{\text{eff}}$  by means of a specific calculation procedure adequately chosen with respect to the NFS of interest. The bias  $\Delta k_{\text{B}}$  being characteristic of the employed calculation procedure with respect to the NFS of interest is obtained from a statistical analysis of the deviations of the numerical results  $(k_{\text{B}})_i$  obtained by means of this calculation procedure for a set of  $N_{\text{B}}$  benchmark systems (e.g. critical experiments) from the respective benchmark values  $B[(k_{\text{B}})_i]$  (reference solutions).

$$(\Delta k_B)_i = B[(k_B)_i] - (k_B)_i, \quad i = 1, \dots, N_B, \quad (2)$$

$\pi_{\text{NFS}}$  in inequality (1) denotes the probability  $P((k_{\text{eff}} + \Delta k_B) > k_{\text{max}} | \text{NFS})$  that, for the given NFS,  $(k_{\text{eff}} + \Delta k_B)$  is greater than  $k_{\text{max}}$  given by an adequate administrative margin  $\Delta k_m$  according to  $k_{\text{max}} = 1 - \Delta k_m$ .

The sum:

$$\kappa \equiv k_{\text{eff}} + \Delta k_B \quad (3)$$

is a function of:

- the set of the parameters  $\mathbf{x}_{\text{NFS}} \equiv \mathbf{x} = (x_1, x_2, \dots)^T$  describing the material compositions and the geometrical arrangement of the materials forming the NFS of interest (named as “application case” in the following);
- the joint set  $\mathbf{y}_B \equiv \mathbf{y} = (y_1, y_2, \dots)^T$  of all the parameters  $y_j$  characterising the whole set of evaluated benchmarks  $i = 1, \dots, N_B$ , i.e. describing the material compositions and the geometrical arrangements of these materials of all the benchmarks analysed;
- the set of nuclear data  $\boldsymbol{\xi} = (\xi_1, \xi_2, \dots)^T$  (cross-sections, neutron-per-fission quantities etc.) involved due to the isotopic compositions of the NFS and the benchmark systems:

$$\kappa = \kappa(\boldsymbol{\xi}, \mathbf{x}, \mathbf{y}) = k_{\text{eff}}(\boldsymbol{\xi}, \mathbf{x}) + \Delta k_B(\boldsymbol{\xi}, \mathbf{y}) \quad (4)$$

Due to the experimental and calculation procedures used for their estimation the nuclear data are random variables, i.e. the nuclear data vector  $\boldsymbol{\xi} = (\xi_1, \xi_2, \dots)^T$  is completely defined by the probability distribution:

$$P(\boldsymbol{\xi} \in \Xi \subset \Omega(\boldsymbol{\xi})) = \int_{\Xi} d\boldsymbol{\xi} \psi(\boldsymbol{\xi}) \quad (5)$$

where  $\Xi$  denotes some region in the  $\boldsymbol{\xi}$ -space  $\Omega(\boldsymbol{\xi})$ , and  $\psi(\boldsymbol{\xi})$  is the joint probability density function of the nuclear data  $\boldsymbol{\xi} = (\xi_1, \xi_2, \dots)^T$ . The expectation of a matrix or vector function  $\mathbf{g} = \mathbf{g}(\boldsymbol{\xi})$  is given by Equation (6):

$$E[\mathbf{g}(\boldsymbol{\xi})] = \int_{\Omega(\boldsymbol{\xi})} d\boldsymbol{\xi} \mathbf{g}(\boldsymbol{\xi}) \psi(\boldsymbol{\xi}) \quad (6)$$

With  $\mathbf{g}(\boldsymbol{\xi}) = \boldsymbol{\xi}$  Equation (6) gives the expectation  $E[\boldsymbol{\xi}]$  of  $\boldsymbol{\xi}$ . With  $\mathbf{g}(\boldsymbol{\xi}) = (\boldsymbol{\xi} - E[\boldsymbol{\xi}]) (\boldsymbol{\xi} - E[\boldsymbol{\xi}])^T$  Equation (6) gives the covariance matrix  $\text{cov}(\boldsymbol{\xi})$  of the nuclear data  $\boldsymbol{\xi}$ :

$$\text{cov}(\boldsymbol{\xi}) = E[(\boldsymbol{\xi} - E[\boldsymbol{\xi}]) (\boldsymbol{\xi} - E[\boldsymbol{\xi}])^T] \quad (7)$$

The numerical values of the nuclear data given in a nuclear data library are estimates yielded by estimators  $\hat{\boldsymbol{\xi}}$  related to the experimental and calculation procedures used for the estimation of the nuclear data. Due to these procedures the estimators may be biased, i.e. the expectation  $E[\hat{\boldsymbol{\xi}}]$  of  $\hat{\boldsymbol{\xi}}$  may deviate from the vector of the true values  $\boldsymbol{\xi}_t = E[\boldsymbol{\xi}]$ :

$$\mathbf{b}[\hat{\xi}] = E[\hat{\xi}] - \xi_i \neq \mathbf{0} \quad (8)$$

As appears from Equations (7) and (8), nuclear data “uncertainty” due to  $\text{cov}(\xi)$  and nuclear data bias are completely different characteristics and must not be confused. The covariance matrix  $\text{cov}(\xi)$  represents important numerical characteristics of the joint probability density function  $\psi(\xi)$ . Bias is a property of an estimator  $\hat{\xi}$ . The desirable property is unbiasedness, of course, i.e.  $\mathbf{b}[\hat{\xi}] = \mathbf{0}$ . However, possible biases in the nuclear data as well as algorithmic and numerical weaknesses of the applied criticality calculation code may result in a non-zero bias  $\Delta k_B$ . The covariance matrix  $\text{cov}(\xi)$  results in a covariance matrix  $\mathbf{V}[k_{\text{eff}}, (\Delta k_B)_1, \dots, (\Delta k_B)_{N_B}]$  of the vector  $(k_{\text{eff}}, (\Delta k_B)_1, \dots, (\Delta k_B)_{N_B})^T$ , i.e.  $\text{cov}(\xi)$  generates correlations between the neutron multiplication factor  $k_{\text{eff}}$  of the application case and all the benchmark results  $(\Delta k_B)_i$ ,  $i = 1, \dots, N_B$  [see Equation (2)] as well as mutual correlations between all these benchmark results.

In addition, since characterised by uncertainties due to variations, manufacturing tolerances, measurement uncertainties etc. the vectors  $\mathbf{x}_{\text{NFS}} \equiv \mathbf{x} = (x_1, x_2, \dots)^T$  and  $\mathbf{y}_B \equiv \mathbf{y} = (y_1, y_2, \dots)^T$  are random vectors as well. The joint probability density function  $p(\xi, \mathbf{x}, \mathbf{y})$  of  $\xi$ ,  $\mathbf{x}$ , and  $\mathbf{y}$  is given by the product:

$$p(\xi, \mathbf{x}, \mathbf{y}) = \psi(\xi) p(\mathbf{x}) p(\mathbf{y}) \quad (9)$$

of the individual probability density functions  $\psi(\xi)$ ,  $p(\mathbf{x})$ , and  $p(\mathbf{y})$ , respectively since  $\xi$ ,  $\mathbf{x}$ , and  $\mathbf{y}$  are mutually independent.

As specified above, the vector  $\mathbf{y}$  describes the isotopic compositions and the geometrical arrangements of all the materials of the whole set of evaluated benchmarks  $i = 1, \dots, N_B$ . The use of such a joint vector of the experimental parameters  $y_j$  of all the benchmarks is usually required because benchmarks very often consist of a series of experiments employing the same materials (e.g. same fuel rods, same absorber plates, etc.) in different geometrical configurations. The use of the same materials in different experiments results, due to the uncertainties in the isotopic composition and the geometrical dimensions of these materials, in correlations of the results  $(k_B)_i$  obtained for these experiments and hence of the bias values  $(\Delta k_B)_i$  [see Equation (2)].

As a function of the random vectors  $\xi$ ,  $\mathbf{x}$ , and  $\mathbf{y}$  the bias-corrected neutron multiplication factor  $\kappa = \kappa(\xi, \mathbf{x}, \mathbf{y})$  defined by Equation (3) is a random variable defined by its probability distribution:

$$F(k_0) = P(\kappa \leq k_0) = \int_0^{k_0} d\kappa f(\kappa) \quad (10)$$

where  $f(\kappa)$  denotes the probability density function of  $\kappa = \kappa(\xi, \mathbf{x}, \mathbf{y})$ . The probability density function  $f(\kappa | \text{NFS})$  of a given nuclear fuel system remains unknown due to the very fact that a functional relation  $\kappa = \kappa(\xi, \mathbf{x}, \mathbf{y} | \text{NFS})$  cannot be given in general. The consequence is that the probability  $\pi_{\text{NFS}}$  on the right-hand side of inequality (1) cannot be calculated since this probability is only given by the probability distribution of  $\kappa$ :

$$\pi_{\text{NFS}} = P((k_{\text{eff}} + \Delta k_B) > k_{\text{max}} | \text{NFS}) = P(\kappa > k_{\text{max}} | \text{NFS}) = \int_{k_{\text{max}}}^{\infty} d\kappa f(\kappa | \text{NFS}) \leq \gamma \quad (11)$$

However, each and every numerical result:

$$\kappa_j \equiv [k_{\text{eff}} + \Delta k_B]_j = \{k_{\text{eff}}\}_j + \{\Delta k_B\}_j \quad (12)$$

is a sample of the probability distribution of  $\kappa$ . As shown in [7], with a sufficient number  $M$  of independently drawn samples Equation (12),  $j = 1, \dots, M$ , it becomes possible to calculate the probability  $(1 - \alpha)$  that the probability  $\pi_{\text{NFS}}$  meets inequality (11):

$$1 - \alpha = P(\pi_{\text{NFS}} \leq \gamma) = P(F(\kappa > k_{\text{max}} | \text{NFS}) \leq \gamma) = P\left(\int_{k_{\text{max}}}^{\infty} d\kappa f(\kappa | \text{NFS}) \leq \gamma\right) \quad (13)$$

The probability  $(1 - \alpha)$  expresses the confidence that one has in the statement that the probability that  $\kappa$  exceeds the value  $k_{\text{max}}$  is not greater than an administratively established margin  $\gamma$ . It is obvious that  $\alpha$  as well as  $\gamma$  will be sufficiently small.

In case that definite values are prescribed for  $\gamma$  and  $\alpha$  Equation (13) can be rewritten as

$$1 - \alpha = P(F(\kappa \leq k(\gamma, \alpha) | \text{NFS}) \geq (1 - \gamma)) = P\left(\int_0^{k(\gamma, \alpha)} d\kappa f(\kappa | \text{NFS}) \geq (1 - \gamma)\right) \quad (14)$$

This expression defines the integration limit  $k(\gamma, \alpha)$  such that the probability that  $\kappa \equiv k_{\text{eff}} + \Delta k_B$  does not exceed  $k(\gamma, \alpha)$  amounts at least to  $(1 - \gamma)$  with a probability (confidence) of  $(1 - \alpha)$ . Accordingly,  $k(\gamma, \alpha)$  is often named as “one-sided upper  $(1 - \gamma) / (1 - \alpha)$  tolerance limit” of  $\kappa \equiv k_{\text{eff}} + \Delta k_B$  (e.g. for  $\gamma = \alpha = 0.05$  the “one-sided upper 95%/95% tolerance limit” the use of which is prescribed by many criticality safety regulatory standards). Equation (13) is met if  $k(\gamma, \alpha) \leq k_{\text{max}}$  is obtained for the application case.

#### 4.1.2.2 Hierarchy of uncertainties

The set of samples Equation (12) used for solving Equation (13) or Equation (14) [7] has to take account of:

- the uncertainties and correlations due to  $\text{cov}(\xi)$ ;
- the uncertainties arising from the uncertainties and possible correlations in the parameters  $\mathbf{x} = (x_1, x_2, \dots)^T$  describing the application case;
- the uncertainties and possible correlations due to the uncertainties in the parameters  $\mathbf{y} = (y_1, y_2, \dots)^T$  characterising the set of evaluated benchmarks.

For this purpose, it is necessary to consider the hierarchy of uncertainties. Figure 2 gives an overview of this hierarchy. This overview refers to the general case of criticality safety analysis, i.e. it includes application cases which make use of burn-up credit.

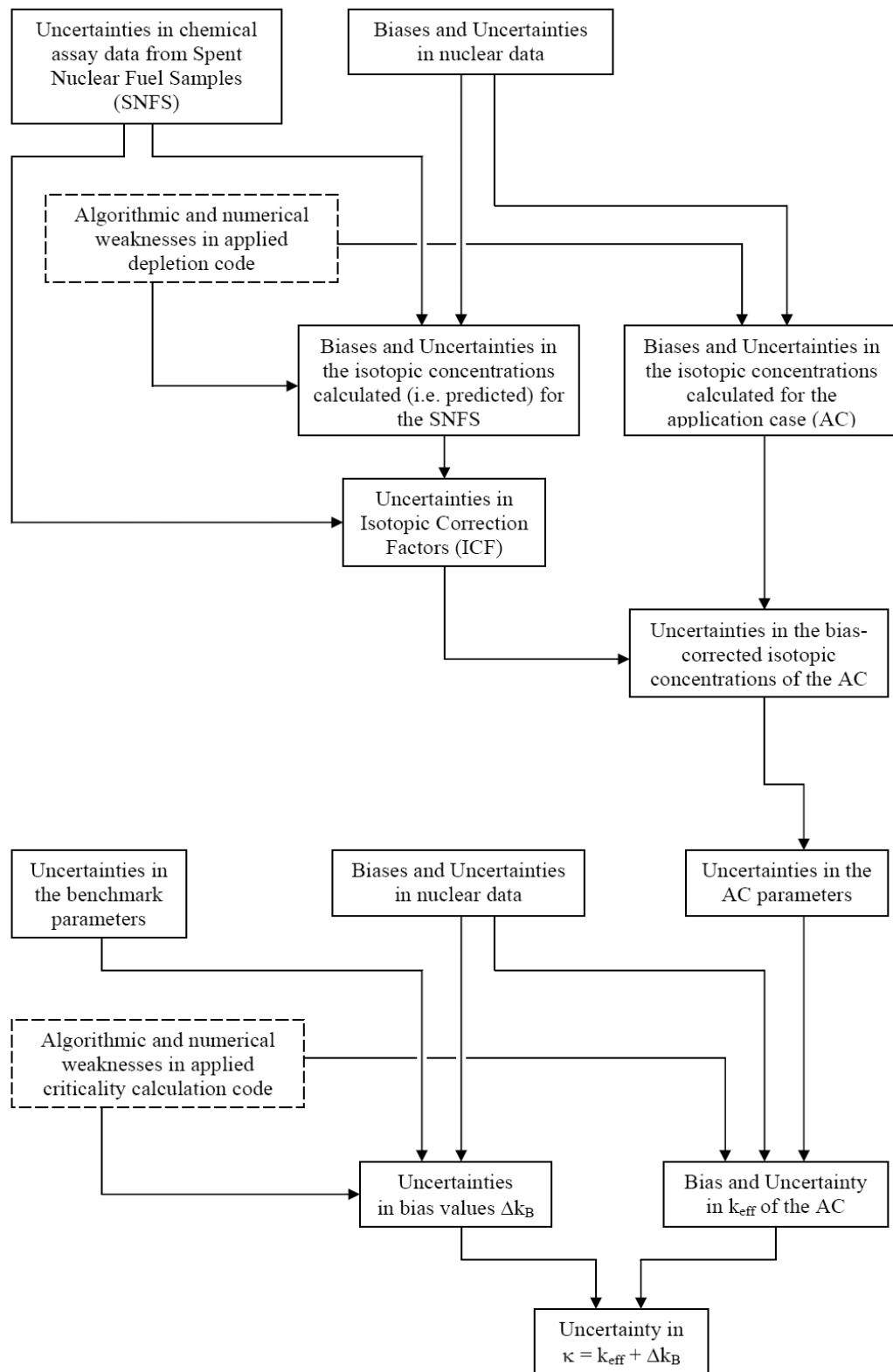
Figure 2 therefore splits up into two blocs:

- the bloc of calculating and validating the isotopic number densities of irradiated nuclear fuel (upper part of Figure 2);
- the bloc of performing and validating the criticality calculations (lower part of Figure 2).

Possible biases in the nuclear data  $\xi$  as well as algorithmic and numerical weaknesses in the applied depletion calculation code may result in biases of the isotopic number densities calculated for the irradiated nuclear fuel of the application case, and the uncertainties and correlations in the nuclear data  $\xi$  result in uncertainties and correlations of these number densities. To validate the depletion calculations and to eliminate the biases in the isotopic number densities, isotopic correction factors are derived from comparisons between measured isotopic concentrations obtained from chemical assays of samples from irradiated fuel and calculated isotopic concentrations predicted for these samples. The isotopic correction factors are mutually correlated because of:

- the uncertainties and correlations in the nuclear data  $\xi$  ;
- the uncertainties and correlations in the measured concentrations arising from the applied assay methods [77];
- the uncertainties in the information about the depletion conditions required to predict the isotopic concentrations by means of re-calculating the respective irradiation histories of the assayed fuel samples.

**Figure 2: Hierarchy of uncertainties in criticality safety analysis**



The importance of considering the correlations between the isotopic correction factors has been demonstrated in [78]. In addition, it has to be considered that due to  $\text{cov}(\xi)$ , the isotopic correction factors and the isotopic number densities calculated for the application case are correlated.

Therefore, the bias-corrected number densities obtained for the application case by means of the isotopic correction factors are mutually correlated. These number densities are components of the vector  $\mathbf{x}$  representing the application case in the criticality calculations. This brings us to the lower part of Figure 2. The uncertainties and correlations of the components of the vector  $\mathbf{x}$  as well as the uncertainties and correlations of the nuclear data  $\xi$  and the uncertainties and possible correlations of the components of the vector  $\mathbf{y}$  have to be considered in the estimation of the neutron multiplication factor  $k_{\text{eff}}$  and the bias values  $(\Delta k_B)_i = B[(k_B)_i] - (k_B)_i$ ,  $i = 1, \dots, N_B$ , see Equation (2).

In conclusion, the flow of all the information required for solving Equation (13) or Equation (14) has to follow the hierarchy of uncertainties outlined in Figure 2. The uncertainties (i.e. variances and possible covariances or correlation coefficients) of the parameters related to some level in that hierarchy determine the uncertainties of the parameters of the following level. The most efficient way in following the complete hierarchy of all the uncertainties which have to be considered consists in application of hierarchical Monte Carlo (MC) procedures.

#### 4.1.2.3 Use of hierarchical Monte Carlo procedures

A complete uncertainty analysis for criticality safety analysis including burn-up credit applications can be performed by means of the codes NUDUNA and MOCADATA developed by AREVA NP GmbH, Germany, [79] [80].

NUDUNA makes it possible to consider the uncertainties in neutron physics calculations due to the variances and covariances of the nuclear data  $\xi$  applied. This is achieved by means of Monte Carlo techniques used for varying the nuclear data information randomly according to the covariance matrices of the data. Nuclear data from several basic nuclear data libraries formatted in the ENDF 6 standard can be used [79]. NUDUNA focuses on basic data and covariance matrices of multiplicities of produced secondary particles, resonance parameters, cross-sections, and angular distributions of final state particles.

Each Monte Carlo (MC) draw on these multivariate data sets results in a random library. By means of the basic data code NJOY [81], each random library can be transformed to both an ACE tape and a GENDF tape. The ACE tape can be used in calculations performed by means of the Monte Carlo particle transport code MCNP. The GENDF tape can be transformed by means of the module SMILER of the code PUFF IV [82] which converts multi-group formatted data into an AMPX working format which can be used in calculations performed by means of the SCALE system (Figure 3).

NUDUNA is integrated in the MOCADATA Bayesian Monte Carlo framework [7] [80]. The combined NUDUNA plus MOCADATA calculation procedure, called CONCERT, takes into account all the analysis uncertainties, the uncertainties in the nuclear data  $\xi$ , the uncertainties in the chemical assay data evaluated for validation of depletion calculations (to be performed in burn-up credit applications), the uncertainties in the parameters  $\mathbf{x}$  describing the application case, and the uncertainties in the parameters  $\mathbf{y}$  characterising the benchmark systems evaluated for validation of the criticality calculation. Because of the use of the Bayesian methodology, this procedure considers all these uncertainties in a consistent and robust way without any approximations. In addition, it takes account of the fundamental uncertainties due to the finiteness of sample sizes (e.g. finite number of benchmark systems) and the necessity of choosing

distribution models in order to be able to evaluate empirical data (e.g. the chemical assay data).

Figure 3: NUDUNA [79] and coupling of NUDUNA with MOCADATA [7]

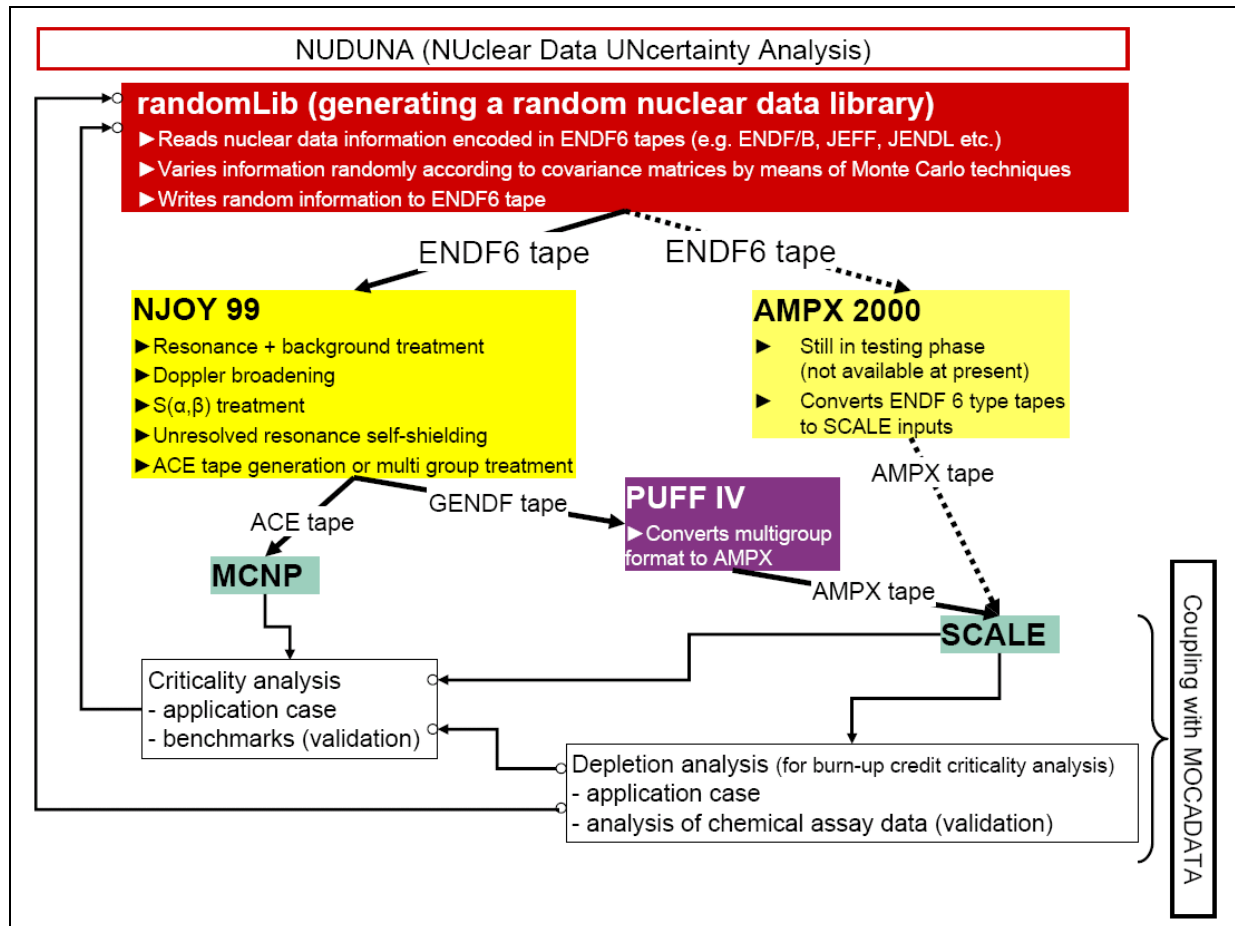


Figure 4: Generation of random libraries for nuclear data and chemical assay data (“exp”:= experiment-based MC samples [7])

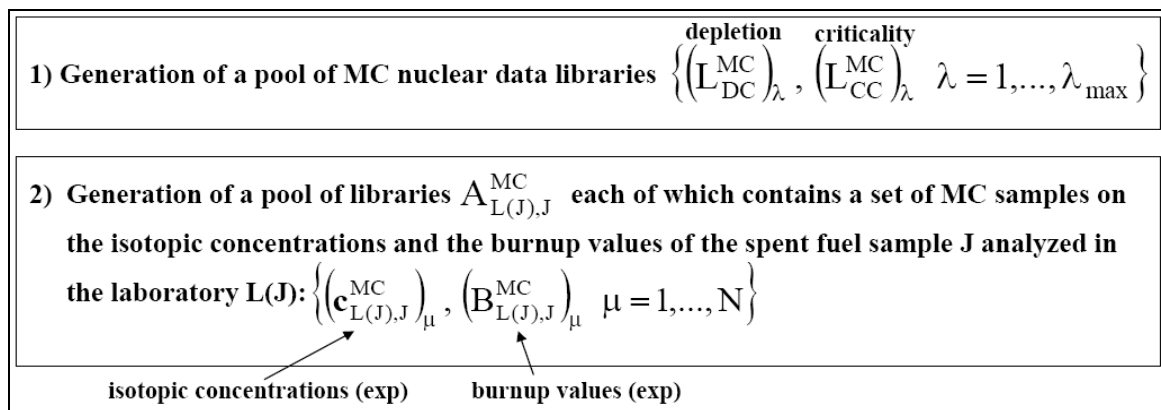
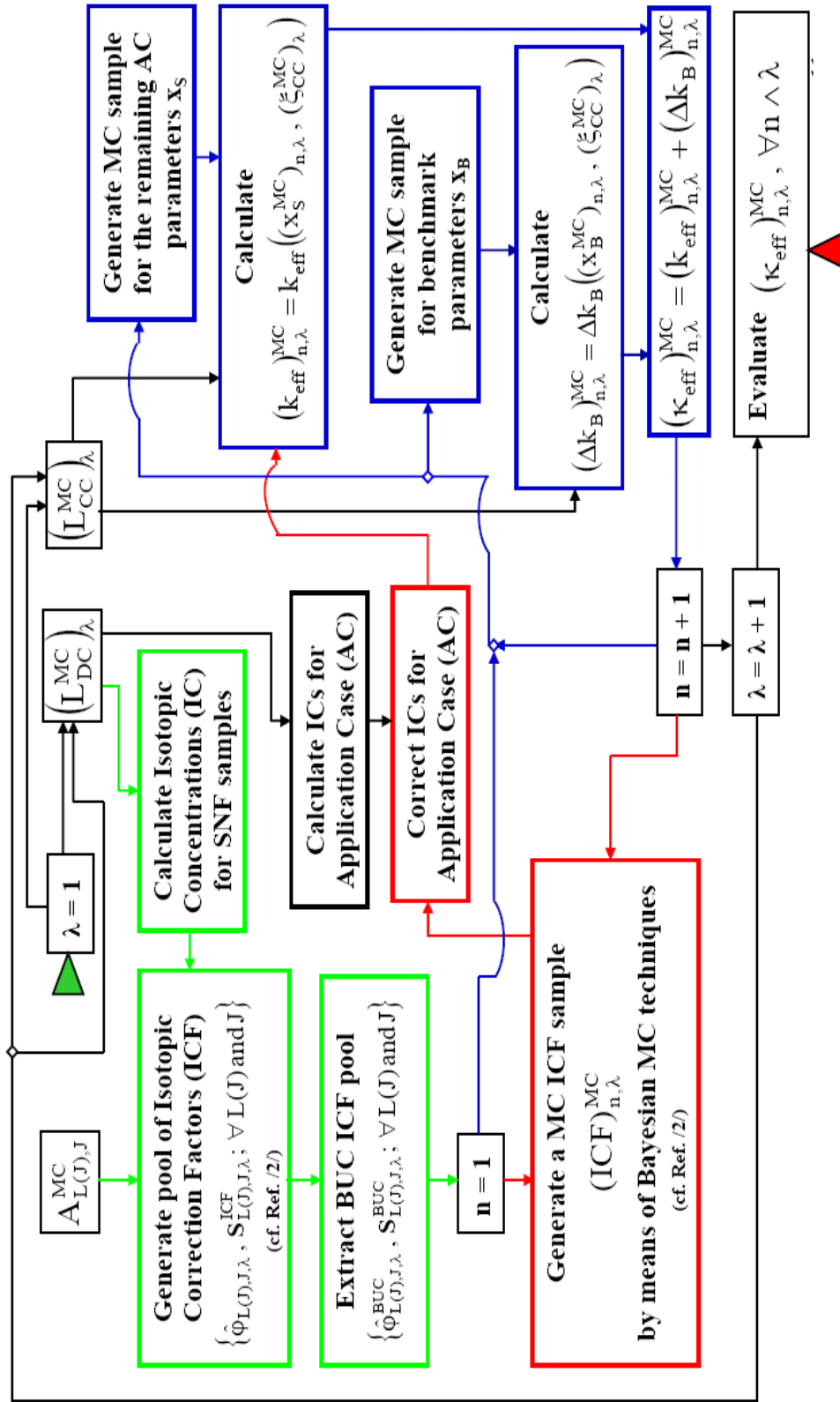


Figure 5: Hierarchical Bayesian Monte Carlo criticality calculation procedure ( $\mathbf{xS}=\mathbf{x}$ ,  $\mathbf{xB}=\mathbf{y}$ )



The complete procedures for criticality calculations including burn-up credit analysis are summarised in Figures 4 and 5:

- The first step (Figure 4) consists in generating a sufficient number  $\lambda_{\max}$  of random libraries by means of NUDUNA. Each random library can be transformed in a library  $(L_{DC}^{MC})_{\lambda}$  for depletion calculations (DC) and a library  $(L_{CC}^{MC})_{\lambda}$  for criticality calculations (CC). For example, the library used for depletion analysis performed by means of the SCALE sequence TRITON/NEWT may have a 44-group-energy structure, the library used for the criticality calculations performed with the aid of MCNP may have the continuous energy format. But both libraries must originate from one and the same random library; that is a must.
- The second step (Figure 4) consists in the generation of a pool of libraries  $A_{L(J),J}^{MC}$  each of which contains Monte Carlo (MC) samples of isotopic concentrations and burn-up values related to a selection of spent nuclear fuel samples. The chemical assay data of these samples are used to validate the depletion code used for calculations of the spent fuel system for which sufficient subcriticality has to be proved [7].
- Then, as shown in Figure 5, an outer Monte Carlo sampling loop ( $\lambda$ -loop) related to the consideration of the nuclear data uncertainties and an inner Monte Carlo sampling loop (n-loop) related to the consideration of all the other uncertainties can be carried out until the number of samples in Equation (12) is sufficiently large. Using these samples, Equation (13) or Equation (14) can be solved.

## 4.2 Commissariat a l'Energie Atomique (CEA), France

Contributors: Christophe Venard, Alain Santamarina, Claude Mounier (Saclay)

### 4.2.1 Criticality calculations

#### 4.2.1.1 Criticality package (codes system) title and version

CRISTAL V1.1

#### 4.2.1.2 Modules utilised for neutron cross-section treatment and neutron transport calculation

- Reference route: Monte Carlo TRIPOLI4.3;
- Standard route: APOLLO2 Release 5.5 is used for self-shielding and homogenisation CPM and Sn calculations, 20 or 172 groups, anisotropy up to P5. MORET4.3 Monte Carlo code is used for neutron transport calculation. User interface CIGALES3.1 is used for APOLLO2 input generation.

In this exercise, k-effective is computed with the CRISTAL reference route (continuous-energy Monte Carlo) to minimise computing method biases.

#### 4.2.1.3 Nuclear data source and energy structure

- Reference route: European JEF2.2 Continuous energy library;
- Standard route: 172-group CEA93v6 library, processed by NJOY from JEF 2.2.

### 4.2.2 Validation of criticality calculations

#### 4.2.2.1 Sources of bias and uncertainties

- nuclear data uncertainty;

Modelling biases when using multi-group calculations (CRISTAL standard route) are determined from comparison to reference MC continuous-energy calculations.

#### 4.2.2.2 Description of the validation methodology

The CRISTAL package allows the user to select either a multi-group calculation or a continuous-energy calculation ('reference route'). When using the multi-group route for a new and challenging criticality calculation, the user has to carry out first a numerical validation based on the comparison to reference continuous-energy calculation (using the same library, currently JEF 2.2). This first step allows the calibration of the modelling calculational bias. Therefore, the second step corresponds to the experimental validation. This CRISTAL V1 validation database is made up of 2132 critical experiments either performed in French facilities or issued from the OECD/ICSBEP Handbook. The experiments are selected according to the fissile media and the configurations involved, which must be as representative as possible of those encountered in the nuclear fuel cycle. Moreover, the diversity of experimental facilities and laboratories and the quality of benchmark's data are also taken into account in the selection criteria. This selection is facilitated by the automated calculation of the experiment representativity. The C/E discrepancies and the experimental uncertainties  $\delta E$ , are used in the representativity method to derive rigorously the calculational bias and the posterior uncertainty (bias uncertainty) for the application.

#### 4.2.2.3 Approach for selection of benchmark experiments

##### 4.2.2.3.1 Parameters used for similarity assessment

The representativity  $r_{AE}$  of an experiment E, whose measurement value is  $I_E \pm \delta$ , with respect to application A is given by the following expression:

$$r_{AE} = \frac{(S_A^+ DS_E)}{\varepsilon_A \cdot \varepsilon_E}. \quad (15)$$

This correlation coefficient  $r_{AE}$  represents the share of information provided by experiment E common with the parameter  $I_A$ . A value of 0.0 means that the experiment and the application are not correlated. Experimental information provided by experiment E will not be of any use for the validation of the application parameter I. A value of 1.0 indicates a full correlation between experiment and application. Experimental information will be advantageous.

##### 4.2.2.3.2 Criteria and process used for similarity assessment

#### 4.2.2.4 Implementation of the validation method used to determine bias and bias uncertainty (if available)

##### 4.2.2.4.1 Software tool title

R.I.B.

##### 4.2.2.4.2 Algorithm

The representativity method is the rigorous method, accounting for both nuclear data uncertainties and integral experiment uncertainties, to project the experimental information from the selected integral measurements to the application. The methodology allows the assessment of the calculational bias and the posterior uncertainty on the application parameter ( $k_{eff}$ , here in safety-criticality).

Notation:

I: 'a priori' calculated integral parameter,  $i = A$  for industrial application,  $i = E$  for experiment;

$\varepsilon_i$ : 'a priori' computation uncertainty,  $i = A$  for industrial application,  $i = E$  for experiment;

$I_{E}^m$ : measured integral parameter;

$\delta_E$ : experimental uncertainty;

$I_A$ : "a posteriori" calculated integral parameter;

$\varepsilon_A^*$ : "a posteriori" computation uncertainty;

$S_i$ : sensitivity coefficient vector,  $i = A$  for industrial application,  $i = E$  for experiment;

$\sigma$ : nuclear data vector;

$\sigma^*$ : re-estimated nuclear data vector;

$D$ : prior nuclear data uncertainty (covariance matrix);

$D^*$ : posterior covariance matrix corresponding to re-estimated nuclear data.

In the industrial application the parameter  $I_A$  is calculated (best-estimate based on the reference route). Its prior calculation uncertainty  $\varepsilon_A$ , due to the nuclear data, is given by:

$$\varepsilon_A = \left( S_A^+ D S_A \right)^{1/2} \quad (16)$$

with,  $S_A = \frac{\sigma^j}{I_A} \cdot \frac{dI_A}{d\sigma^j}$  with  $j=1, N$ , where  $N = \text{group number} \times \text{nuclear reaction number} \times \text{isotope number}$ .

The nuclear data re-estimation, using both differential measurements and integral experiments  $I_{Ei}$ , is based on the maximum likelihood principle.

From the nuclear data re-estimation, the vector  $Y_\sigma$  of nuclear data modifications and the posterior covariance matrix  $D^*$  are given by:

$$Y_\sigma = D S_E^+ \left( D_E + S_E D S_E^+ \right)^{-1} Y_E \quad (17)$$

$$D^* = D - D \cdot S_E \cdot \left[ S_E^T \cdot D \cdot S_E + D_E \right]^{-1} \cdot S_E^T \cdot D \quad (18)$$

where  $D_E$ : experiment covariance matrix,

$Y_E$ : Calculation-experiment discrepancies vector.

The correction to apply to the prior calculated value  $I_A$  is:

$$\Delta I_A = \frac{I_A^* - I_A}{I_A} = S_A \cdot Y_\sigma \quad (19)$$

And, the posterior uncertainty, to associate with the corrected value  $I_A^*$ , is:

$$\varepsilon_A^* = \left( S_A^+ D^* S_A \right)^{1/2} \quad (20)$$

This formula allows derivation of the calculational bias  $\Delta I_A$  and the associated bias uncertainty  $\varepsilon_A^*$  as a function of the representativity factors  $r_{AEi}$ . For example, in the framework of this exercise where we used only two integral experiments  $I_{E1, \pm \delta_{E1}}^m$  and  $I_{E2, \pm \delta_{E2}}^m$ , which yield the following calculational bias and bias uncertainty :

$$\frac{\delta(A)}{\varepsilon_A} = \frac{1}{1 - \hat{r}_{E_1 E_2}^2 w_1 w_2} \cdot \left[ r_{AE_1} w_1 \frac{\delta(E_1)}{\varepsilon_{E_1}} + r_{AE_2} w_2 \frac{\delta(E_2)}{\varepsilon_{E_2}} - \hat{r}_{E_1 E_2} w_1 w_2 \left( r_{AE_2} \frac{\delta(E_1)}{\varepsilon_{E_1}} + r_{AE_1} \frac{\delta(E_2)}{\varepsilon_{E_2}} \right) \right] \quad (21)$$

$$\frac{\varepsilon_A^{*2}}{\varepsilon_A^2} = 1 - \frac{1}{1 - \hat{r}_{E_1 E_2}^2 w_1 w_2} \left( r_{AE_1} \sqrt{w_1} - r_{AE_2} \sqrt{w_2} \right)^2 - \frac{2 \sqrt{w_1 w_2}}{1 + \hat{r}_{E_1 E_2} \sqrt{w_1 w_2}} r_{AE_1} r_{AE_2} \quad (22)$$

Where the “weight”  $w$ , associated with each experiment  $E_i$  (decreasing with increasing experimental uncertainty  $\delta_{E_i}$ ) is defined as:  $w = \frac{1}{1 + \delta_E^2 / \varepsilon_E^2}$

$\hat{r}_{E_1, E_2}$  is the correlation coefficient between experiment 1 and experiment 2. It gathers the representativity  $r_{E_1, E_2}$  between experiments and the technological/measurement correlation. It is recommended to choose two independent integral measurements, so  $\hat{r}_{E_1, E_2} = r_{E_1, E_2}$ .

#### 4.2.2.5 Initial data for the bias and bias uncertainty determination

##### 4.2.2.5.1 Number of benchmarks available for calculation-to-experiment comparison

For this UACSA benchmark, two experiments among the CRISTAL experimental validation database are selected to determine the computing bias and its uncertainty.

##### 4.2.2.5.2 Uncertainties treatment for experimental data

The uncertainties treatment for experimental data follows the ICSBEP uncertainty guide. The measurement and technological uncertainties are considered. No correlated experiments are selected.

##### 4.2.2.5.3 Other data used in the validation method (nuclear data covariance, sensitivity coefficients, etc.)

- Nuclear-data covariances

Using reliable nuclear data uncertainties and correlations is of importance for the quality of the results. Correlations between energy groups, cross-sections and isotopes should be in principle considered. However, in the most recent libraries, obtaining reliable error information on cross-sections is still difficult. Thus, realistic uncertainties have been estimated using both differential information (comparison between evaluated files, review of cross-section measurements, information given by the standard cross-section committee and nuclear data compilations) and feedback from targeted integral measurements. The uncertainties values are available for the following isotopes:  $^{235}\text{U}$ ,  $^{238}\text{U}$ ,  $^{238}\text{Pu}$ ,  $^{239}\text{Pu}$ ,  $^{240}\text{Pu}$ ,  $^{241}\text{Pu}$ ,  $^{242}\text{Pu}$ ,  $^{241}\text{Am}$ ,  $\text{H}_2\text{O}$ ,  $^{10}\text{B}$ ,  $\text{C}$ ,  $^{16}\text{O}$ ,  $\text{CH}_2$ ,  $\text{Si}$ ,  $^{23}\text{Na}$ ,  $^{27}\text{Al}$ ,  $\text{Ca}$ ,  $^{56}\text{Fe}$ ,  $^{58}\text{Ni}$ ,  $^{52}\text{Cr}$ .

Realistic assumptions are made on the correlations:

- concerning energy groups, a total correlation is assumed ( $C_{g, g'} = 1$ ) between thermal groups, and long range correlation for epithermal and fast groups ( $C_{g, g+1} = 0.75$ ,  $C_{g, g+2} = 0.5$ ,  $C_{g, g+3} = 0.25$ );
- There are correlations ( $C \approx 0.5$ ) between isotopes  $^{235}\text{U}$ ,  $^{239}\text{Pu}$ ,  $^{241}\text{Pu}$  on the neutron multiplicity and the fission cross-section (coming from the standards used in the normalisation of differential measurements).

The JEF 15-groups structure is used for covariance matrices.

- Sensitivity coefficients

$K_{\text{eff}}$  sensitivity profiles to nuclear data are performed with the CRISTAL standard route APOLLO2-Sn using the 172-group nuclear data library CEA93v6 based on JEF 2.2. They were easily obtained from the first-order perturbation theory implemented in APOLLO2. Sensitivity coefficients to the cross-sections and multiplicities were derived from the European JEF 15-group structure.

Set of  $k_{\text{eff}}$  sensitivity coefficients comprises data for 350 benchmark experiments.

#### 4.2.2.6 History of the validation methodology

##### 4.2.2.6.1 Primary purpose

The representativity method was first used in the French Fast Breeder Reactor Programme (Phénix and Superphénix reactors) to adjust the nuclear data library and to derive realistic uncertainty on design parameter prediction ( $K_{\text{eff}}$ , sodium void coefficient, etc.). The re-estimation of nuclear data and the representativity method have been in use since 1990 to conceive representative LWR experiments in Eole and to produce the APOLLO2 Validation-Qualification Report for both PWR and BWR.

##### 4.2.2.6.2 Experience of use

This methodology was also implemented in criticality-safety assessment to validate criticality studies and to obtain the bias and uncertainty bias of the CRISTAL calculations: MELOX fuel fabrication plant, MOX assembly storage, CEA spent-fuel storage plant, and others.

##### 4.2.2.7 Status of the development/validation

##### 4.2.2.8 Published references supporting the validation methodology

See [11] through [18].

##### 4.2.2.9 Additional information/notes

The proposed validation methodology is easy to use and does not require strong qualification for criticality practitioner. However, a minimum background on integral experiments will be useful. The choice of the relevant experiments, to evaluate bias and uncertainties, is clear and it is based on:

- experiment representativity ( $r > 0.7$ );
- experiment accuracy: the experimental uncertainty has to be lower than computational uncertainty ( $\delta E / \varepsilon E < 1$ );
- attention must be paid to correlation between experiments (for example: use of the same fuel pins).

The proposed representativity methodology is the unique rigorous way to use integral experiments and to derive the  $k_{\text{eff}}$  bias and uncertainty in a criticality-safety calculation. This efficient method has been used for a long time by Russian and French engineers to obtain reliable correction factors and uncertainties in their FBR and LWR Reactor design calculations.

### 4.3 E Mennerdahl Systems, EMS, Sweden

Contributor: Dennis Mennerdahl

#### 4.3.1 Criticality calculations

##### 4.3.1.1 Criticality package (codes system) title and version

The computer software package SCALE 5.1 was used in this project.

##### 4.3.1.2 Modules used for neutron cross-section treatment and neutron transport calculation (methods employed and titles)

The “multi-region” resonance treatment model and the code CENTRM were used for fissile material and sometimes for other materials. The “inhommedium” resonance treatment model and the code CENTRM were sometimes used for other materials. This was sometimes necessitated by a lack of computer random access memory.

KENO V.a was used to determine  $k_{\text{eff}}$  and EALF values.

TSUNAMI-3D was used to determine sensitivities for applications and benchmarks.

The TSUNAMI-IP code was used to determine indices for similarity between application and benchmarks, based on the TSUNAMI-3D calculations.

##### 4.3.1.3 Nuclear data source and energy structure

The 238-group SCALE 5.1 ENDF/B-VI library was used in all calculations.

#### 4.3.2 Validation of criticality calculations

##### 4.3.2.1 Sources of bias and uncertainties

Various sources of error lead to biases and uncertainties that need to be estimated. A bias is a measure of accuracy while an uncertainty is a measure of precision. Main sources of error include the accuracy and precision of benchmarks, of basic evaluated cross-sections, of group-averaged cross-sections, of resonance modelling, of adequate numerical/statistical calculation parameters, of simulation of the application, of simulation of the benchmarks and of subjective judgement in selecting and evaluating benchmarks.

##### 4.3.2.2 Description of the validation methodology

The validation methodology is very subjective. All information sources are in principle acceptable. This includes taking advantage of experience from other specialists. Validation may be based on the evaluation of a single benchmark if this benchmark is considered reliable and is similar to the application. Analytical benchmarks, including those that are based on calculations using validated methods, may be acceptable. Agreement between expected results and obtained results during routine use of SCALE 5.1 is used as a verification process which supports validation. Benchmarks are weighted according to uncertainty (quality), similarity to application and to correlations between benchmarks.

##### 4.3.2.3 Approach for selection of benchmark experiments

###### 4.3.2.3.1 Parameters used for similarity assessment

The approach for selection of benchmark experiments is to aim for quality benchmarks, without necessarily restricting them to experiment-based benchmarks. Small benchmark result uncertainties are given high priority. The SCALE 5.1 TSUNAMI-IP code is used to verify that the subjectively selected benchmarks are appropriate.

- 4.3.2.3.2 Criteria and process used for similarity assessment

The main parameter used for similarity assessment of a benchmark relative to a test application is the Ck index determined by TSUNAMI-IP. Other index values obtained from TSUNAMI-IP may be used. The nuclide concentrations, reactivities, absorption fractions, EALF values, moderation ratios, neutron flux distributions and neutron leakage may also be used.

#### 4.3.2.4 Implementation of the validation method used to determine bias and bias uncertainty (if available)

- 4.3.2.4.1 Software tool title

None

- 4.3.2.4.2 Algorithm

Implementation of the validation method used to determine bias and bias uncertainty is made on a case-by-case basis.

#### 4.3.2.5 Initial data for the bias and bias uncertainty determination

- 4.3.2.5.1 Number of benchmarks available for calculation-to-experiment comparison

The ICSBEP Handbook is used as the main source for validation. For this project, most of the input data have been taken from the ICSBEP DVD or from Appendix A of the Handbook. This input has been examined. Experience from other specialists in applying the benchmarks, SCALE 5.1 and in using ENDF/B-VI cross-sections is taken advantage of.

- 4.3.2.5.2 Uncertainties treatment for experimental data

The applied subjective validation method has been applied successfully for many years. Correlations between benchmarks have always been considered in the evaluation of the overall uncertainty. Sensitivities to significant parameters have also been estimated and have influenced the conclusions. Acceptable uncertainties can be as large as one percent in  $k_{eff}$ . During the evaluation of the OECD/NEA study on minimum critical values, attempts were made to obtain as accurate and precise values as possible. That evaluation showed that the specified uncertainties in benchmarks often appear not to be very reliable. Methods used to determine atomic number densities, in particular for solutions, had unexpectedly large biases for some concentrations.

- 4.3.2.5.3 Other data used in the validation method (nuclear data covariance, sensitivity coefficients, etc.)

Expert judgement is always a significant component of validation. However, with more experience and testing of tools like TSUNAMI, the reliability of “formal” validation procedures will increase. This should lead to more accurate bias corrections (positive or negative) and to the fact that smaller margins to account for uncertainties can be applied.

#### 4.3.2.6 History of the validation methodology

- 4.3.2.6.1 Primary purpose

The validation methodology has been developed for two main criticality safety purposes. One purpose is licensing of nuclear fuel cycle facilities and transport. The other purpose is participation in international studies and development of standards and regulations. In both cases, it is essential to know the performance of the methods. It is not sufficient to have conservative methods; best-estimate methods are also needed.

#### 4.3.2.6.2 Experience of use

Several years before the code package SCALE-0 was released in 1980, the computer codes and cross-sections were available. Installation on a main-frame computer required more work and validation than later software packages since the software often had to be slightly modified before being compiled into a final system. In the late 1970s, the current validation method varied from many others by comparing the benchmark and application sensitivities to design parameters such as neutron absorbers. Many critical experiments were considered essentially useless since their sensitivities were much lower than the applications. Another difference to published validation methods was that correlations between different critical experiments were considered.

#### 4.3.2.7 Status of the development/validation

New methods such as TSUNAMI and GLLSM fit very well with the previous methods.

#### 4.3.2.8 Published references supporting the validation methodology

See [19] with its appendices, covers the method well.

#### 4.3.2.9 Additional information/notes

The selection of benchmarks and weighting based on benchmark uncertainties and correlations requires extensive experience, understanding of the neutron physics and of systematic effect uncertainties.

Application of the method typically involves some months of an experienced practitioner's time.

A subcritical limit accounts for biases and uncertainties in determination of the best-estimate critical value. The subcritical limit is set so that the probability for criticality, due to calculation uncertainties not being accounted for correctly, is acceptably low. The subcritical limit is often related to  $k_{\text{eff}}$  but may also be related to other parameters.

A subcritical limit is not a safety limit. A safety limit accounts for additional uncertainties in operations with fissile material. Such considerations require additional margins to the subcritical limit. A safety limit is normally expressed in engineering or administrative terms but may also be expressed as a  $k_{\text{eff}}$  limit.

The requirements on design system subcriticality, accounting for bias and bias uncertainty determinations, depend on the application. Under normal operation conditions, the probability for criticality due to a calculation error must be essentially zero. For extreme accident conditions, the requirements on calculation accuracy may be lower since it is the total probability of criticality that is of importance. Under emergency conditions, a higher subcritical limit may be justified if special precautions are taken.

The requirement for essentially zero probability for criticality due to only a calculation error can be translated into a high coverage factor<sup>1</sup>, e.g. six. Bias corrections (positive and negative<sup>2</sup>) are applied when biases are found. The uncertainties are expressed as one standard uncertainty (one standard deviation) to simplify comparison

<sup>1</sup> The coverage factor is a factor to be combined with the standard deviation to produce a confidence interval. The product provides a probability distribution. Different coverage factors are used for different purposes and their values determine how to apply an uncertainty allowance in criticality safety. A factor of only two or three allows a significant probability for calculation error outside the uncertainty allowance.

<sup>2</sup> Bias corrections that are negative (account for positive biases in calculated results) are necessary in licensing since the applicant may have a more accurate method (supported by solid validation) than the reviewer. The applicant must not be punished because the reviewer overestimates  $k_{\text{eff}}$ . The applicant should be allowed to apply bias corrections, whatever the sign, when solid validation supports this.

with other participants. The subcritical  $k_{\text{eff}}$  limits are determined as the results after accounting for bias corrections and for reducing  $k_{\text{eff}}$  with an appropriate margin, e.g. six standard deviations.

It is important that the degree of conservatism in setting the subcritical limits is known. This information is needed in licensing to avoid rejecting perfectly adequate applications and in emergency response when conservatism can be a danger to human life and to the environment.

In the validation process, it is necessary to weigh the benchmarks in order to consider:

- correlations between benchmarks;
- similarities between benchmarks and applications;
- the quality of the benchmarks.

#### **4.4 Institute for Physics and Power Engineering (IPPE), Russian Federation**

Contributors: Yury Golovko, Evgeny Rozhikhin, and Anatoly Tsiboulia

##### **4.4.1 Criticality calculations**

###### *4.4.1.1 Criticality package (codes system) title and version*

SKALA

###### *4.4.1.2 Modules used for neutron cross-section treatment and neutron transport calculation (methods employed and titles)*

- CONSYST Code used for cross-section processing;
- 3D MMKKENO Monte Carlo code was used for neutron transport calculation.

###### *4.4.1.3 Nuclear data source and energy structure*

299-group ABBN-93.1 cross-section library processed from FOND-2.2 evaluated nuclear data files.

##### **4.4.2 Validation of criticality calculations**

###### *4.4.2.1 Sources of bias and uncertainties*

Assumed sources of uncertainty are:

- uncertainties in neutron cross-section data;
- uncertainties in benchmark  $k_{\text{eff}}$  values;
- methodical uncertainty in  $k_{\text{eff}}$  calculations with MMKKENO code (statistical uncertainties).

###### *4.4.2.2 Description of the validation methodology*

The validation methodology is based on the calculation of benchmark experiments and a subsequent evaluation of the obtained  $k_{\text{eff}}^{\text{calc}}/k_{\text{eff}}^{\text{bench}}$  values. The obtained  $k_{\text{eff}}$  calculated with group-wise cross-sections are compared with the continuous energy code version for some typical experiments to estimate methodological uncertainty. The obtained  $k_{\text{eff}}^{\text{calc}}/k_{\text{eff}}^{\text{bench}}$  values are then used for bias and uncertainty estimation using the Generalised Linear Least-Square (GLLS) Method. The source of the criticality benchmarks is the MMKKENO database.

#### 4.4.2.3 Approach for selection of benchmark experiments

##### 4.4.2.3.1 Parameters used for similarity assessment

The benchmarks selected for method validation should be representative relative to a test application in terms of the fuel form, typical dimensions and physical properties (neutron spectrum). The benchmarks should also be accurately evaluated.

- fuel content;
- fuel form;
- spectral characteristics;
- presence/material of absorber;
- quality of the evaluated benchmark  $k_{\text{eff}}$  uncertainty.

Benchmarks selected should be known as not containing strongly correlated cases or correlation of uncertainty should be established.

##### 4.4.2.3.2 Criteria and process used for similarity assessment

The initial benchmark selection is based on the comprehensive analysis of the parameters specified in Section 4.4.2.3.1 supported by expert judgement.

Afterwards, GLLSM statistical procedure is employed to test quality (experimental data are well evaluated and not mutually contradictory) and efficiency (benchmark data used in validation procedure decrease priori uncertainty originated from nuclear data) of the selected benchmark data.

#### 4.4.2.4 Implementation of the validation method used to determine bias and bias uncertainty (if available)

##### 4.4.2.4.1 Software tool title

INDECS

##### 4.4.2.4.2 Algorithm

Algorithm is based upon the Generalised Linear Least-Squares Method (GLLSM). Such an approach (sometimes referred to as “adjustment”) considers potential variations in nuclear cross-sections that minimise the differences in measured and calculated  $k_{\text{eff}}$  for a suite of integral experiments, taking into account uncertainties and correlations in nuclear data and in the measured data. A detailed description of the algorithm is described in the references provided below.

#### 4.4.2.5 Initial data for the bias and bias uncertainty determination

##### 4.4.2.5.1 Number of benchmarks available for calculation-to-experiment comparison

The evaluation database comprises more than 4 000 benchmark experiments. The majority of them are selected from the ICSBEP Handbook. The validation set includes cases that represent the whole spectrum of the configurations available in the ICSBEP Handbook. The validation data base also includes a vast set of experiments performed at the IPPE's experimental facilities.

##### 4.4.2.5.2 Uncertainties treatment for experimental data

Uncertainties of the benchmark  $k_{\text{eff}}$  are tested using GLLSM based procedure. Some doubtful uncertainties are re-evaluated. Correlations of the experimental uncertainties are established and tested using the GLLSM method.

- 4.4.2.5.3 Other data used in the validation method (nuclear data covariance, sensitivity coefficients, etc.)

Energy-dependent sensitivity coefficients for all the materials and reaction types calculated using: 1) 3D MMK-KENO Monte Carlo code (to model configuration with complex geometry) or 2) ONE- or TWODANT based code employing first-order perturbation theory.

Both codes produce 299-group sensitivities of  $k_{\text{eff}}$  for the following neutron data: fission, capture, elastic and inelastic scattering cross-sections, nu-bar, mu-bar, and fission spectrum. Then the sensitivities are collapsed into 30 groups.

30-group nuclear data covariance matrices are available from the ABBN-93 cross-section library. 30-group matrices are also processed from ENDF/B-V, ENDF/B-VI, and JENDL-3 evaluated nuclear data files.

#### 4.4.2.6 History of the validation methodology

- 4.4.2.6.1 Primary purpose

The GLLSM-based validation methodology was developed in the 1970s for the nuclear data evaluation and fast reactor design studies. A recent application of this method has been in the area of criticality safety analysis validation.

- 4.4.2.6.2 Experience of use

The presented validation methodology has been applied to fast reactor design and safety studies of the following fast reactors: BN-600, BN-800, BREST-300 (Russian Federation), CEFR (China) and others. In the area of criticality safety it has been used for studies and to test the quality of the evaluated benchmark  $k_{\text{eff}}$  uncertainties for some configurations available in the ICSBEP Handbook. The validation database includes data from both critical and reactor-type experiments.

#### 4.4.2.7 Status of the development/validation

The methodology is developed and validated for fast reactor design and safety study. A variety of configurations used for criticality safety assessment requires additional efforts to validate the sensitivity calculations for heterogeneous configurations with intermediate and thermal spectra, namely, correct interpretation of sensitivities' explicit component.

#### 4.4.2.8 Published references supporting the validation methodology

See [20] through [29].

#### 4.4.2.9 Additional information/notes

Once the methodology is validated, the recommended qualification for criticality practitioners is the same as for the criticality safety calculations and evaluations.

The software tool development and validation took about 30 years. Remarkable effort was devoted to the database creation and validation of the technique. Recently being applied to criticality safety study, significant efforts are required to validate computation of  $k_{\text{eff}}$  sensitivity coefficients to neutron cross-sections, namely, for heterogeneous configurations with intermediate and thermal spectra.

The presented methodology and software tool has been successfully used in practice for fast reactor design and safety study. The recent application of the method in the area of criticality safety requires significant effort to test the validation methodology itself and additional input data that participate in the validation process. Special attention should be paid to: 1) evaluation of uncertainties and establishment of their correlation for the experimental benchmark selected for the validation study, 2) computation of  $k_{\text{eff}}$  sensitivity coefficients to neutron cross-sections for heterogeneous configurations with

intermediate and thermal spectra, 3) selection of cross-section covariances for isotopes and energy regions that are not covered by sufficient integral experiments.

#### **4.5 Institut de Radioprotection et de Sûreté Nucléaire (IRSN), France**

Participants: Frédéric Fernex, François Willem

##### **4.5.1 Criticality calculations**

###### *4.5.1.1 Criticality package (codes system) title and version*

CRISTAL V1.1

###### *4.5.1.2 Modules utilised for neutron cross-section treatment and neutron transport calculation (methods employed and titles)*

- APOLLO 2 P<sub>ij</sub> Code for cross-section treatment;
- Monte Carlo MORET 4 code for neutron transport calculation.

###### *4.5.1.3 Nuclear data source and energy structure*

- JEF 2.2 based 172-group CEA93 V6 library.

##### **4.5.2 Validation of criticality calculations**

###### *4.5.2.1 Sources of bias and uncertainties*

The sources of uncertainty are:

- uncertainties in neutron cross-section data;
- uncertainties in benchmark  $k_{\text{eff}}$  values (due to uncertainties/model simplifications in the benchmark configurations, methodical uncertainties introduced in the benchmark evaluation process);
- uncertainty originating from computational algorithm: uncertainty associated with group-wise cross-sections and cross-section processing, statistical uncertainties.

###### *4.5.2.2 Description of the validation methodology*

The validation methodology is based on the calculation of benchmark experiments and a subsequent evaluation of the obtained  $k_{\text{eff}}$  values. The source of the benchmark experiments is the APOLLO2-MORET 4 validation database.

###### *4.5.2.3 Approach for selection of benchmark experiments*

###### ▪ 4.5.2.3.1 Parameters used for similarity assessment

The benchmarks selected for method validation should be at least of the application case in terms of fuel form, fuel type and neutron spectrum. Moreover, the validation work performed at IRSN showed that some additional parameters may induce a bias in the APOLLO2-MORET 4 calculations. Therefore, the following parameters are currently considered relevant for the benchmark selection:

- fuel type;
- fuel form;
- neutron spectrum;
- reflector material;
- thickness of reflector;
- moderator material;

- moderation ratio;
  - benchmark  $k_{\text{eff}}$  uncertainty (should be reasonably small, e.g. less than 500 pcm).
- 4.5.2.3.2 Criteria and process used for similarity assessment

Once a set of representative experiments are chosen using the selection criteria, the similarity assessment is performed, using the following parameters processed by APOLLO2-MORET 4 simultaneously with criticality computations:

- flux;
- leakages;
- production rate;
- absorption rate in fuel;
- excess rate in fuel (n,xn);
- total rate in fuel;
- absorption rate in structural materials;
- excess rate in structural materials.

All these parameters are vectors with a length equalling the number of group of the energy mesh. Depending on the complexity of the benchmark, the number of parameters can reach many thousand.

A reduction of the number of parameters is required to operate easily with the data. Some reaction rates are selected for this along with energy group collapse.

In order to simplify this work, a characterisation tool developed at IRSN contains a graphical user interface allowing comparing flux and reaction rate profiles. An example of the comparison is given in Figure 6. The most representative parameters and group structure can be also selected, as shown in Figure 7.

When sets of representative experiments and parameters are selected, they create a vast number of data, which is too important to perform either a graphical 3D representation or an interpolation to determine the calculational bias. Two statistical methods are used to provide an optimisation and visualisation of data treatment and to calculate bias.

The first is the principal components analysis applied to display a three-dimensional view of experiments and application case. This visualisation is important to verify whether the application case is well surrounded by the experiments to prove the application of interpolation method. Figure 8 represents a three-dimensional graph where positions of experimental cases reflect similarity of the experiment to the application case. The benchmark experiments are shown as blue points and they form a cloud surrounding the application case marked with red.

Figure 6: Flux comparison with graphical user interface of MACSENS

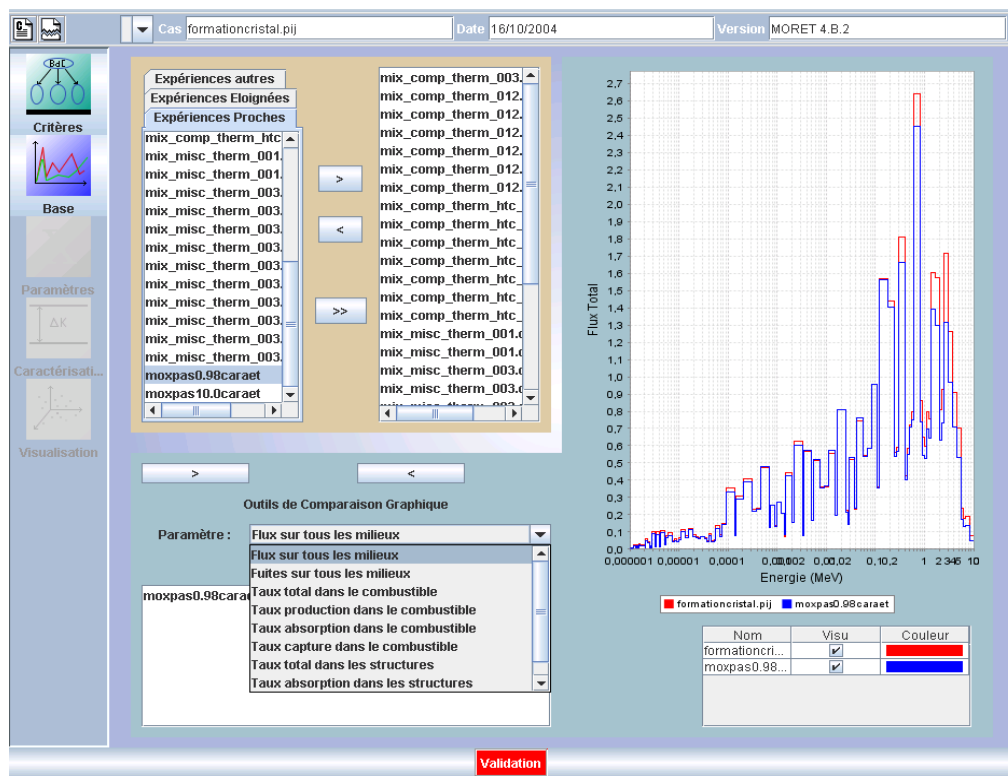


Figure 7: Flux comparison with graphical user interface of MACSENS

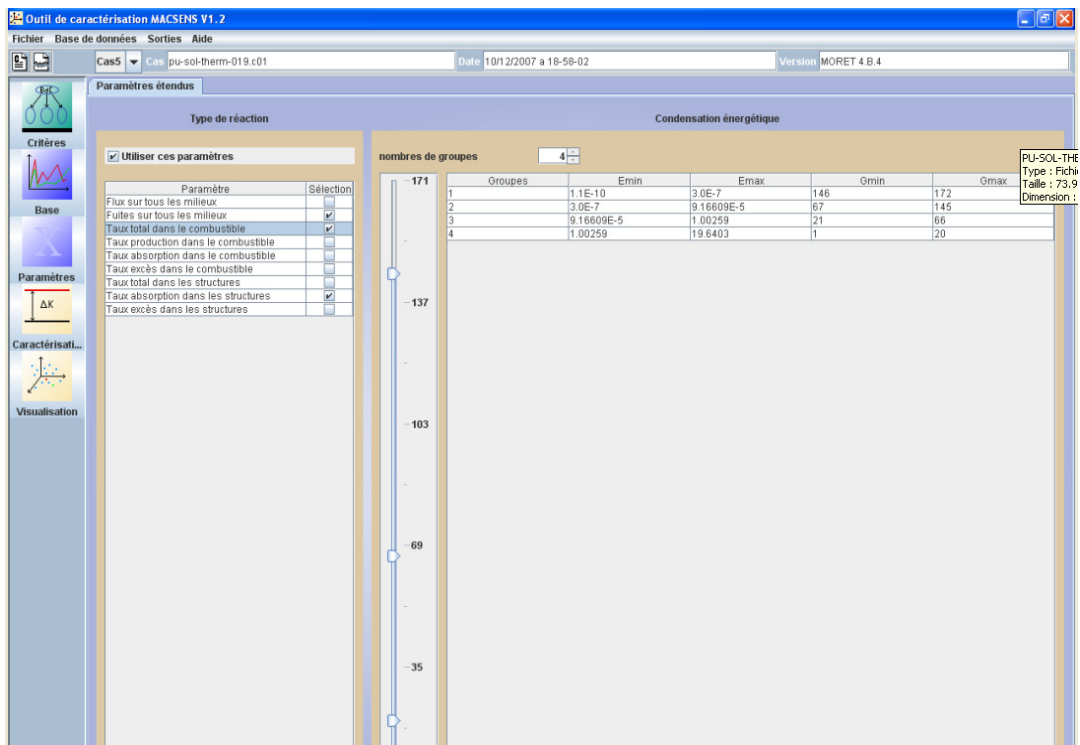
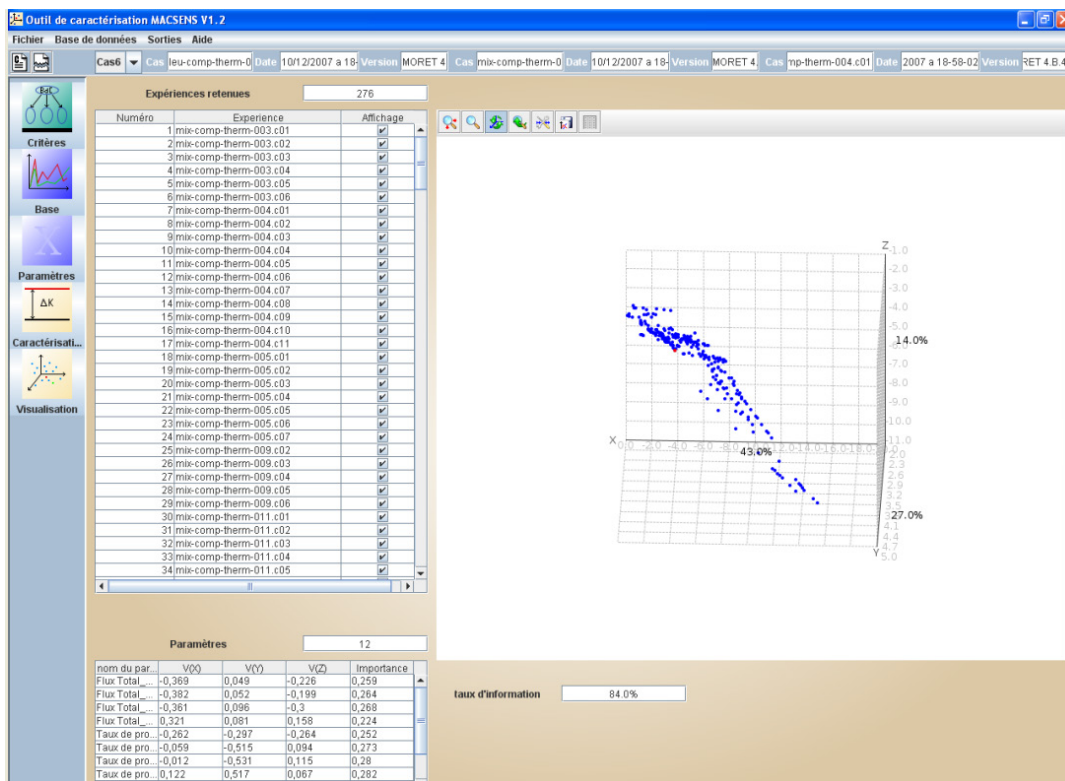


Figure 8: Flux comparison with graphical user interface of MACSENS



The second is the Sliced Inverse Regression and Kernel smoothing that allow performing a multi-dimensional interpolation on the C/E to evaluate the calculational bias for the application case.

#### 4.5.2.4 Implementation of the validation method used to determine bias and bias uncertainty (if available)

##### 4.5.2.4.1 Software tool title

MACSENS

##### 4.5.2.4.2 Algorithm

- Principal Component Analysis Method

If X is considered as a (m,n) matrix, m being the number of experiments retained and n the number of selected parameters, the PCA method is defined by the following equation:

$$C = \text{cov } X = X^t \cdot X = PDP^{-1} \tag{23}$$

where P is the eigenvector matrix of C and D is the eigenvalue matrix of C.

The eigenvectors provide the coefficients of the linear combination of parameters. These combinations of parameters define the new base of representation. The eigenvalues, the diagonal values of D matrix, represent the quantity of information kept by corresponding eigenvectors. This D matrix is sorted and it is then possible to define P as a new base, only keeping the three first vectors. All the experiments and the industrial case are then projected on this new three-dimensional space. Thus, the principal component analysis enables changing the base in establishing an orthonormal base to better discriminate the experiments. This method allows positioning the industrial case in the experimental database.

The technique of the multivariate analysis provides a set of parameters that are linear combinations of the provided parameters. All the new parameters are uncorrelated and are sorted following the ratio of information kept by each parameter.

The PCA method is equivalent to the building of a new geometric space, where axes are sorted in terms of information ratio.

- Sliced Inverse Regression and Kernel smoothing method

Because of the high number of remaining parameters, an interpolation with classical tools such as linear regression is not possible. The Sliced Inverse Regression (SIR) is designed to reduce the large number of parameters while keeping maximum information.

Let us define  $a_{ij}$  the parameters values of the  $i^{\text{th}}$  experiment and  $\Delta k_{\text{eff},i}$ , the corresponding calculation bias :

$$X = \begin{vmatrix} a_{11} & \cdots & a_{1n} \\ \vdots & \ddots & \vdots \\ a_{m1} & \cdots & a_{mn} \end{vmatrix}, \text{ and } Y = \begin{vmatrix} \Delta k_{\text{eff},1} \\ \vdots \\ \Delta k_{\text{eff},m} \end{vmatrix}, \quad (24)$$

where  $n$  is the number of parameters and  $m$  the number of experiments.

The SIR method defines a new database  $W$  using the major part of information of  $X$  with a minimum parameters number  $n'$ .

$$W = \begin{vmatrix} b_{11} & \cdots & b_{1n'} \\ \vdots & \ddots & \vdots \\ b_{m1} & \cdots & b_{mn'} \end{vmatrix} \text{ with } n' \ll n \quad (25)$$

The  $b_{ij}$  parameters are obtained by the following method:

First, the experiments of close  $\Delta k_{\text{eff}}$  are grouped. Ten groups per 100 experiments are used. Each group is characterised by a set of parameters, each of which is the average value of each parameter for all the experiments belonging to the group. The group matrix  $G$  is then the following:

$$G = \begin{vmatrix} \frac{1}{n_{g_1}} \sum_{i \in g_1} x_{i,1} & \cdots & \frac{1}{n_{g_1}} \sum_{i \in g_1} x_{i,n} \\ \vdots & \ddots & \vdots \\ \frac{1}{n_{g_k}} \sum_{i \in g_k} x_{i,1} & \cdots & \frac{1}{n_{g_k}} \sum_{i \in g_k} x_{i,n} \end{vmatrix} \quad (26)$$

The result of the PCA is a new set of parameters with their associated information rate. The SIR method consists in selecting only enough parameters to keep a certain amount of information (for instance 80%). The former parameters are projected on this new base and the SIR matrix is defined as follows:

$$W = X.SIR_{X,Y} = X \cdot \begin{vmatrix} S_{1,1} & \cdots & S_{1,p} \\ \vdots & \ddots & \vdots \\ S_{m,1} & \cdots & S_{m,p} \end{vmatrix}, \quad (27)$$

where the  $S_{i,p}$  are the  $p$  first principal components of the  $i^{\text{th}}$  experiment.

Once the dimension reduction is performed, classic interpolation methods can be used. In the present case, Kernel smoothing method is used to establish the bias. This method consists in of a weighted average calculation of  $\Delta k_{\text{eff}}$  that partially takes into account the distance between the real case and the experiment. If all experiments are “far” from the real case, all experiments will have the same weight and the tool will behave as a simple average.

$$y = f(x) = \frac{\sum_i \omega_i(x) y_i}{\sum_i \omega_i(x)} \quad (28)$$

The weighing function is defined in the following equation for a single parameter:

$$\omega_i(x) = e^{-\frac{(x-x_i)^2}{\sigma}}, \quad \text{where } \sigma = \frac{x_m - x_0}{k}$$

#### 4.5.2.5 Initial data for the bias and bias uncertainty determination

- 4.5.2.5.1 Number of benchmarks available for calculation-to-experiment comparison

About 1 580 experiments, presented in the ICSBEP Handbook and the validation database of APOLLO2-MORET 4, are available for validation studies of criticality calculations.

- 4.5.2.5.2 Uncertainties treatment for experimental data

In the given approach, the uncertainties of the experimental data are taken from the ICSBEP Handbook benchmark specifications as the  $k_{\text{eff}}^{\text{bench}}$  uncertainties. It is assumed that these correspond to random uncertainties at the  $1\sigma$  level, if not otherwise specified in the Handbook.

- 4.5.2.5.3 Other data used in validation method (nuclear data covariance, sensitivity coefficients, etc.)

The following parameters are used to assess similarity and quantify bias:

- flux;
- leakages;
- production rate;
- absorption rate in fuel;
- excess rate in fuel (n, xn);
- total rate in fuel;
- absorption rate in structural materials;
- excess rate in structural materials.

The data are processed by APOLLO2-MORET 4 simultaneously with criticality computations.

#### 4.5.2.6 History of the validation methodology

##### 4.5.2.6.1 Primary purpose

The purpose of the validation methodology is to provide data to be used for criteria to establish subcriticality and range of applicability for criticality safety evaluations for systems with fissionable materials of interest, which are various configurations met in the laboratories, during transport and at the fuel cycle facilities.

##### 4.5.2.6.2 Experience of use

The tool has been recently distributed to industrial partners for testing.

#### 4.5.2.7 Status of the development/validation

The tool is under development and verification.

#### 4.5.2.8 Published references supporting the validation methodology

See [30].

#### 4.5.2.9 Additional information/notes

The MACSENS validation methodology requires a skilled user to assign parameters for selection of the experiments and review a list of selected experiments. Bias and uncertainty set by the current version of the MACSENS are required as a guess of the user.

The described method implemented in MACSENS code is currently used by criticality safety practitioners mostly to select the benchmark experiments and determine the area of applicability.

## 4.6 Japan Atomic Energy Agency (JAEA), Japan

Participant: Yasunobu Nagaya

### 4.6.1 Criticality calculations

#### 4.6.1.1 Criticality package (codes system) title and version

MVP II

#### 4.6.1.2 Modules utilised for neutron cross-section treatment and neutron transport calculation (methods employed and titles)

Neutron cross-section treatment: LICEM code system for generation of MVP cross-section data such as point-wise cross-sections, thermal scattering data and probability tables in the unresolved resonance region.

Neutron transport calculation: continuous-energy Monte Carlo neutron transport code MVP II.

#### 4.6.1.3 Nuclear data source and energy structure

JENDL-3.2, continuous energy.

### 4.6.2 Validation of criticality calculations

#### 4.6.2.1 Sources of bias and uncertainties

- nuclear data;
- technological parameters (material constituents and location).

4.6.2.2 Description of the validation methodology

- Statistical method using the non-central t-distribution

▪ 4.6.2.2.1 Traditional prescription

In the report [31], the following three requirements were imposed for determining the estimated criticality lower-limit multiplication factor, ECLLMF, which was symbolised as  $k_{<}$ :

- any calculated  $k_{eff}$  obtained by benchmark calculations will be larger than  $k_{<}$ ;
- $k_{<}$  will not exceed 0.98;
- statistical methods should be employed to analyse the behaviour of calculation errors.

Rule (1) was required to assure that any critical experiments selected for validation shall not be misjudged to be subcritical. Rule (2) was required to prevent  $k_{<}$  from being specified to a too large value. Rule (3) declared that the expression for ECLLMF should be based on mathematical reasoning, which was summarised as follows.

The calculated  $k_{eff}$ 's in the same group were regarded as statistical samples. The samples were assumed to follow the normal distribution. The population mean and variance were designated as  $m$  and  $\sigma^2$ , respectively. The distribution of  $n$  samples,  $k_{eff,1}, k_{eff,2}, \dots, k_{eff,n}$ , were characterised by sample mean and variance,  $\bar{k}$  and  $s^2$ , respectively, defined by:

$$\bar{k} = \frac{1}{n} \sum_{i=1}^n k_{eff,i} \tag{29}$$

$$s^2 = \frac{1}{n-1} \sum_{i=1}^n (k_{eff,i} - \bar{k})^2, (n \geq 2) \tag{30}$$

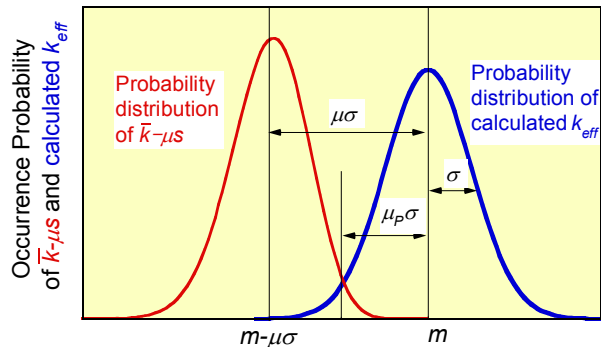
$\bar{k}$  and  $s^2$  have the following statistical characteristics:

The mean of samples,  $\bar{k}$ , follows the normal distribution, the mean and variance of which are  $m$  and  $\sigma^2/n$ , respectively.

The variance of samples,  $s^2$ , is related to the  $\chi^2$ -distribution. More specifically,  $n \cdot s^2 / \sigma^2$  is distributed according to a  $\chi^2$ -distribution with  $(n - 1)$  degrees of freedom.

The lower 100 P percentile of the normal distribution  $N(m, \sigma^2)$  is expressed as  $m - \mu_P \sigma$ . A parameter value  $\mu$  can be determined by the non-central t distribution with  $(n-1)$  degrees of freedom, and percentiles 100  $\gamma$  and 100 P. The meaning of the percentiles 100  $\gamma$  and 100 P is given below. When a constant  $\mu'$  is selected to be no smaller than  $\mu$ , then the lower 100  $\gamma$  percentile of  $\bar{k} - \mu'$ 's can be set smaller than  $m - \mu_P \sigma$  (see Figure 9).

**Figure 9: Probability distributions of calculated  $k_{eff}$  and  $\bar{k} - \mu s$**



Based on the three characteristics mentioned above, two kinds of neutron multiplication factors were introduced:

- The estimated criticality multiplication factor, ECMF, which is equal to  $\bar{k}$ , at which value of the calculated neutron factor the system is estimated to be most probably critical.
- The estimated criticality lower-limit multiplication factor, ECLLMF, which is statistically equal to  $\bar{k} - \mu s$ , for which value or less of the calculated neutron multiplication factor, the probability of the system becomes critical or supercritical is 100 P% or less for the confidence level of 100  $\gamma$ %.

In order to satisfy the three requirements mentioned in this section, a set of rates  $P = 0.025$  and  $\gamma = 0.975$  was adopted to determine the  $\mu$  value. A list of  $\mu$  values for various sample number  $n$  is given in Table 1.

The ECMF and ECLLMF values for the JACS code system, which is a combination of 137-group cross-section library based on the ENDF/B-IV and KENO-IV code, applicable to the uranium/plutonium systems in simple geometry, which were determined in the way mentioned above, are given in Table 2. The values of ECMF and ECLLMF for the MVP code system are shown in Table 3.

▪ 4.6.2.2.2 Basis for Expression of ECLLMF

When the  $k_{eff}$  of uranium/plutonium system calculated by a specified criticality code system has a value of ECLLMF, it means that there is a probability  $P$  that the system becomes critical or supercritical or less for the confidence level of  $\gamma$ , as was defined in the preceding subsection. We can express this statement in another way by finding some number  $k_<$  of  $k_{eff}$  that satisfies the following probabilistic relation:

$$\Pr(k_< \leq m - \mu_p \sigma) = \gamma \tag{31}$$

where it was assumed that  $k_{eff}$  followed the normal distribution  $N(m, \sigma^2)$ . As shown in Figure 9, we then introduce a number  $\mu$ , which will be determined in later in this subsection by use of the non-central t-distribution, and express  $k_<$  as  $k_< = \bar{k} - \mu s$ , where  $\bar{k}$  and  $s$  are the sample mean and standard deviation of  $k_{eff}$ , respectively. Equation (31) then becomes:

$$\Pr(\bar{k} - \mu s \leq m - \mu_p \sigma) = \gamma \tag{32}$$

This equation means the probability that  $\bar{k} - \mu s$  becomes no larger than  $m - \mu_p \sigma$ , which is characterised by the parent distribution of the calculated  $k_{eff}$ , is  $\gamma$ . By dividing

both sides of the inequality relation by  $\sigma$  and by transposing some terms, we can find the following equation:

$$\Pr\left(\frac{\bar{k} - m}{\sigma} + \mu_p \leq \mu \frac{s}{\sigma}\right) = \gamma \quad (33)$$

The inequality relation is eventually changed into the following form to show that it is related to the non-central t-distribution:

$$\Pr\left(\frac{\frac{\bar{k} - m}{\sigma/\sqrt{n}} + \mu_p \sqrt{n}}{\sqrt{\frac{fs^2}{\sigma^2}}/\sqrt{f}} \leq \mu \sqrt{n}\right) = \gamma \quad (34)$$

where  $f$  is the degree of freedom,  $f = n-1$  in this case that  $k_{\text{eff}}$ 's are independent of any variables. The non-central Student's t-distribution is defined as the distribution of a random variable  $t$  that follows the distribution below:

$$t = \frac{N + \delta}{\chi_f / \sqrt{f}} \quad (35)$$

where  $N$  obeys the standard normal distribution,  $\chi^2$  obeys a chi-squared distribution with  $f$  degrees of freedom, and  $\delta$  is a non-centrality parameter.

As the variables  $\frac{\bar{k} - m}{\sigma/\sqrt{n}}$  and  $\sqrt{\frac{fs^2}{\sigma^2}}$  follow the standard normal distribution and the chi-squared distribution with  $f = n - 1$  degrees of freedom, respectively, the constant  $\mu \sqrt{n}$  will be obtained as the upper limit of integration of  $t$  density with the non-centrality parameter  $\delta = \mu_p \sqrt{n}$ .

**Table 1:  $\mu$  values for typical sample number  $n$  and degrees of freedom  $f = n-1$ , where  $\gamma = 0.975$  and  $P = 0.025$**

$n$	$\mu$	$n$	$\mu$	$n$	$\mu$	$n$	$\mu$	$n$	$\mu$
2	62.558	21	2.978	50	2.535	190	2.226	2000	2.037
3	12.816	22	2.945	55	2.503	200	2.219	3000	2.023
4	7.710	23	2.914	60	2.475	250	2.189	5000	2.008
5	5.975	24	2.887	65	2.451	300	2.168	10000	1.994
6	5.111	25	2.861	70	2.430	350	2.151	□	1.960
7	4.592	26	2.837	75	2.411	400	2.138		
8	4.243	27	2.815	80	2.394	450	2.127		
9	3.992	28	2.794	85	2.379	500	2.118		
10	3.801	29	2.775	90	2.366	550	2.110		
11	3.650	30	2.757	95	2.353	600	2.104		
12	3.528	32	2.723	100	2.342	650	2.098		
13	3.427	34	2.694	110	2.322	700	2.093		
14	3.342	36	2.667	120	2.304	750	2.088		
15	3.268	38	2.643	130	2.289	800	2.084		
16	3.204	40	2.621	140	2.276	850	2.080		
17	3.148	42	2.601	150	2.264	900	2.076		
18	3.099	44	2.583	160	2.253	950	2.073		
19	3.054	46	2.566	170	2.243	1000	2.070		
20	3.014	48	2.550	180	2.235	1500	2.049		

**Table 2: The estimated criticality multiplication factor, ECMF, and the estimated criticality lower-limit multiplication factor, ECLLMF, for the JACS code system applied to the simple uranium/plutonium systems**

Group name <sup>a</sup>	ECMF	ECLLMF	Number of samples	Sample standard deviation
HomLEU <sup>b</sup>	0.986	0.965	40	0.008
HomHEU	0.985	0.954	68	0.013
HomPu	1.008	0.980	71	0.011
HomMOX	1.013	0.980 <sup>c</sup>	45	0.008
HomMIX	1.010	0.980	10	0.008
HetLEU	0.995	0.978	88	0.007
HetPu	1.004	0.964	9	0.010
HetMOX	0.997	0.980	58	0.007
Total			389	

a Hom: homogeneous; Het: heterogeneous; LEU: low-enriched uranium; HEU: highly enriched uranium; MOX: mixed uranium and plutonium oxide; MIX: mixed uranium and plutonium solution.

b The committee for the preparation of the Nuclear Criticality Safety Handbook of Japan reviewed the selected samples; accordingly, ECLM, ECLLMF, a number of samples and sample standard deviation were changed into 0.991, 0.973, 18 and 0.004, respectively.

c Reduced to this value according to the requirement (2), while 0.992 was obtained by the statistical calculation.

**Table 3: The estimated criticality multiplication factor, ECMF, and the estimated criticality lower-limit multiplication factor, ECLLMF, for the MVP code system applied to the simple uranium/plutonium systems**

Group name <sup>d</sup>	ECMF	ECLLMF	Number of samples	Sample standard deviation
HomLEU	1.0073	0.98 <sup>e</sup>	75	0.0050
HomHEU	1.0052	0.98 <sup>e</sup>	55	0.0070
HomPu	1.0044	0.98 <sup>e</sup>	46	0.0077
Hom(Pu+U)	0.9999	0.98 <sup>e</sup>	29	0.0057
HetLEU	1.0026	0.98 <sup>e</sup>	121	0.0064
Het(Pu+U)	0.9991	0.98 <sup>e</sup>	47	0.0053
Total			373	

<sup>d</sup> Hom: homogeneous; Het: heterogeneous; LEU: low-enriched uranium; HEU: highly enriched uranium.

<sup>e</sup> Reduced to this value according to the requirement (2), while 0.9951, 0.9878, 0.9846, 0.9839, 0.9878 and 0.9855 were obtained by the statistical calculation for HomLEU, HomHEU, HomPu, Hom(Pu+U), HetLEU and Het(Pu+U) groups, respectively.

#### 4.6.2.3 Approach for selection of benchmark experiments

##### 4.6.2.3.1 Parameters used for similarity assessment

Grouped by main actinide (uranium, plutonium, uranium and plutonium), homogeneous/heterogeneous; uranium is further divided into low- and high-enriched uranium groups.

Note: The similarity assessment has been made only for reflected systems.

##### 4.6.2.3.2 Criteria and process used for similarity assessment

Expert judgement

#### 4.6.2.4 Implementation of the validation method used to determine bias and bias uncertainty (if available)

##### 4.6.2.4.1 Software tool title

N/A

##### 4.6.2.4.2 Algorithm

N/A

#### 4.6.2.5 Initial data for the bias and bias uncertainty determination

##### 4.6.2.5.1 Number of benchmarks available for calculation-to-experiment comparison

373 benchmark experiment.

##### 4.6.2.5.2 Uncertainties treatment for experimental data

Not considered.

##### 4.6.2.5.3 Other data used in validation method (nuclear data covariance, sensitivity coefficients, etc.)

None.

#### 4.6.2.6 History of the validation methodology

##### 4.6.2.6.1 Primary purpose

To produce basic data (critical masses and volumes of spherical fuel, critical diameters of infinite-long cylindrical fuel, critical thicknesses of infinite plane fuel) of the Japanese Criticality Safety Handbook.

##### 4.6.2.6.2 Experience of use

The methodology has been used in Japan for 20 years.

#### 4.6.2.7 Status of the development/validation

The present method is only applicable when the bias is constant. The extension to the bias that depends on parameters was given in [32]. It was applied to homogeneous systems of low-enriched uranium.

#### 4.6.2.8 Published references supporting the validation methodology

See [31] through [33].

#### 4.6.2.9 Additional information/notes

None.

### 4.7 Korean Institute of Nuclear Safety (KINS), Republic of Korea

Contributors: Gil Soo Lee, Sweng Woong Woo

#### 4.7.1 Criticality calculations

##### 4.7.1.1 Criticality package (codes system) title and version

KENOV.a and KENO VI in SCALE6.

##### 4.7.1.2 Modules utilised for neutron cross-section treatment and neutron transport calculation (methods employed and titles)

- BONAMIST, CENTRM;
- KENO V.a and KENO VI (multi-group Monte Carlo).

##### 4.7.1.3 Nuclear data source and energy structure

238-group library based on ENDF/B-VII evaluation (v7-238).

#### 4.7.2 Validation of criticality calculations

##### 4.7.2.1 Sources of bias and uncertainties

The sources of uncertainty considered include uncertainties of bias, statistical uncertainty in criticality calculation, manufacturing tolerance, and uncertainties originated from nuclear data that were not considered before.

##### 4.7.2.2 Description of the validation methodology

The evaluated  $k_{\text{eff}}$  value from Equation (36) should have a subcritical margin of administrative value. The uncertainty term includes manufacturing tolerance, calculation statistical uncertainty, bias uncertainty, and uncertainty due to using burn-up credit. Bias and bias uncertainty are determined from the calculation results of critical experiments with similar condition.

Recently, we started to work to determine similarity criteria and consider uncertainty in nuclear data. As a result of this, the following components have been considered:

- bias and bias uncertainty established through comparison with experimental benchmarks similar to test application (benchmarks with EALF similar to that for application case and  $c_k > 0.90$  for LEU like applications with thermal fission spectrum);
- uncertainties in nuclear data are included (calculated with covariance and sensitivity data produced by TSUNAMI).

$$k = k_{cal} + \delta k(bias) + \sqrt{\sum [\delta k(uncert)]^2} \quad (36)$$

Bias is determined as the average of calculated  $k_{eff}$  values of critical experiments which are less than 1.

$$\delta k(bias) = 1 - \bar{k} = 1 - \frac{1}{N} \sum_{k_i < 1} (1 - k_i) \quad (37)$$

$$\delta k(bias, uncert) = stdev(k_i) = \sqrt{\frac{1}{n-1} \sum (\bar{k} - k_i)^2} \quad (38)$$

#### 4.7.2.3 Approach for selection of benchmark experiments

- 4.7.2.3.1 Parameters used for similarity assessment
  - EALF
  - Correlation coefficient  $c_k$  [3].
- 4.7.2.3.2 Criteria and process used for similarity assessment  
Expert judgement

#### 4.7.2.4 Implementation of the validation method used to determine bias and bias uncertainty (if available)

- 4.7.2.4.1 Software tool title  
None.
- 4.7.2.4.2 Algorithm  
N/A

#### 4.7.2.5 Initial data for the bias and bias uncertainty determination

- 4.7.2.5.1 Number of benchmarks available for calculation-to-experiment comparison  
The data are available for the following 32 configurations from the ICSBEP Handbook:
  - LEU-COMP-THERM: 4 experiments (8 configurations);
  - IEU-MET-FAST: 6 experiments (6 configurations);
  - PU-SOL-THERM: 3 experiments (18 configurations);
- 4.7.2.5.2 Uncertainties treatment for experimental data  
The uncertainties are accepted as they are documented in the ICSBEP Handbook.

- 4.7.2.5.3 Other data used in validation method (nuclear data covariance, sensitivity coefficients, etc.)

44-group covariance data for neutron cross-sections are available in SCALE6 criticality codes package.

$k_{\text{eff}}$  sensitivity coefficients to neutron cross-sections computed with TSUNAMI-3D code. The sensitivity data are available for 12 benchmarks.

#### 4.7.2.6 History of the validation methodology

- 4.7.2.6.1 Primary purpose

Safety reviews on fissile material storage facilities (fresh and spent fuel storage).

#### 4.7.2.7 Status of the development/validation

Licensee's results have been reviewed, which are for LEU. The uncertainty for nuclear data was not included.

#### 4.7.2.8 Published references supporting the validation methodology

#### 4.7.2.9 Additional information/notes

None.

## 4.8 Oak Ridge National Laboratory (ORNL), US

Participants: Bradley Rearden, Don Mueller

### 4.8.1 Criticality calculations

#### 4.8.1.1 Criticality package (codes system) title and version

The computer software package SCALE 6.0 was used in this project.

#### 4.8.1.2 Modules utilised for neutron cross-section treatment and neutron transport calculation (methods employed and titles)

The SCALE 6.0 TSUNAMI-3D eigenvalue sensitivity and uncertainty analysis sequences were applied in this exercise.

SCALE 6.0 provides the CENTRM and PMC modules for continuous-energy treatment of resonance self-shielding calculations. Point-wise fluxes are computed for 1D cell models in CENTRM, then the point-wise fluxes are used as a weighting function to integrate the point-wise cross-sections in the desired multi-group structure. Unresolved resonances and implicit sensitivity effects are treated with the BONAMIST codes, which utilised full-range Bondarenko factors to generate the implicit sensitivity coefficients.

Transport calculations were performed with the KENO V.a and KENO-VI Monte Carlo neutron transport codes.

#### 4.8.1.3 Nuclear data source and energy structure

The SCALE 6.0 238-group ENDF/B-VII.0 library is used in all calculations.

### 4.8.2 Validation of criticality calculations

#### 4.8.2.1 Sources of bias and uncertainties

The sources of uncertainty considered include uncertainties in the benchmark  $k_{\text{eff}}$  values. Correlations in uncertainties in the benchmark  $k_{\text{eff}}$  values were approximated. Uncertainties and correlations in the computed  $k_{\text{eff}}$  values due to uncertainties in nuclear data were explicitly quantified using the SCALE 6.0 cross-section-covariance data and the

TSUNAMI-3D sensitivity data for each system. Uncertainties in the computed  $k_{\text{eff}}$  values due to Monte Carlo statistics were explicitly treated.

#### 4.8.2.2 Description of the validation methodology

##### ■ 4.8.2.2.1 TSUNAMI techniques for code validation

The TSUNAMI software developed at Oak Ridge National Laboratory (ORNL) provides a unique means of determining the similarity of nuclear criticality experiments to safety applications [34] [35]. The basis of the TSUNAMI validation techniques is that computational biases are primarily caused by errors in the cross-section data, the potential for which are quantified in cross-section-covariance data. The presentation of the TSUNAMI methodologies is based largely on those presented in [35].

TSUNAMI provides two methods to establish the computational bias introduced through cross-section data. For the first method, instead of using one or more average physical parameters to characterise a system, TSUNAMI determines the uncertainty in  $k_{\text{eff}}$ , due to cross-section uncertainties, that is shared between two systems. This shared uncertainty in  $k_{\text{eff}}$  directly relates to the bias shared by the two systems. To accomplish this, the sensitivity of  $k_{\text{eff}}$  to each group-wise nuclide-reaction-specific cross-section is computed for all systems considered in the analysis. Correlation coefficients are developed by propagating the uncertainties in neutron cross-section data to uncertainties in the computed neutron multiplication factor for experiments and safety applications through sensitivity coefficients. The bias in the experiments, as a function of correlated uncertainty with the intended application, is extrapolated to predict the bias and bias uncertainty in the target application. This correlation coefficient extrapolation method is useful where many experiments with uncertainties that are highly correlated to the target application are available.

For the second method, data adjustment or data assimilation techniques are applied to predict computational biases, and more general responses, including but not limited to  $k_{\text{eff}}$ , can be addressed [34]. This technique utilises sensitivity and uncertainty (S/U) data to identify a single set of adjustments to nuclear data and experimental responses, taking into account their correlated uncertainties that will result in the computational models producing response values close to their experimental response value. Then, the same data adjustments are used to predict an unbiased response (e.g.  $k_{\text{eff}}$ ) value for the application and an uncertainty on the adjusted response value. The difference between the originally calculated response value and the new post-adjustment response value represents the bias in the original calculation, and the uncertainty in the adjusted value represents the uncertainty in this bias. If experiments are available to validate the use of a particular nuclide in the application, the uncertainty of the bias for this nuclide is reduced. If similar experiments are not available, the uncertainty in the bias for the given nuclide is high. Thus, with a complete set of experiments to validate important components in the application, a precise bias with a small uncertainty can be predicted. Where the experimental coverage is lacking, a bias can be predicted with an appropriately large uncertainty. The data assimilation method presents many advantages over other techniques in that biases can be projected from an agglomeration of benchmark experiments, each of which may represent only a small component of the bias of the target application. Also, contributors to the computational bias can be analysed on an energy-dependent, nuclide-reaction-specific basis.

TSUNAMI is a suite of tools in which individual components each perform a specific task. These tools are introduced below and explained in detail in subsequent sections.

The TSUNAMI-1D and TSUNAMI-3D analysis sequences compute the sensitivity of  $k_{\text{eff}}$  to energy-dependent cross-section data for each reaction of each nuclide in a system model. The one-dimensional (1D) transport calculations are performed with XSDRNPM, and the three-dimensional (3D) calculations are performed with KENO V.a or KENO-VI [36]. The energy-dependent sensitivity data are stored in a sensitivity data file (SDF) for

subsequent analysis. Additionally, the TSUNAMI-1D and -3D sequences use the energy-dependent cross-section-covariance data to compute the uncertainty in each system's  $k_{\text{eff}}$  value due to the cross-section-covariance data.

TSUNAMI-IP (TSUNAMI Indices and Parameters) uses the SDFs generated from TSUNAMI-1D, -3D, or TSAR for a series of systems to compute correlation coefficients that determine the amount of shared uncertainty between each target application and each benchmark experiment considered in the analysis. TSUNAMI-IP offers a wide range of options for more detailed assessment of system-to-system similarity. Additionally, TSUNAMI-IP can generate input for the Upper Subcritical Limit STATistical Software (USLSTATS) [37] trending analysis and compute a penalty, or additional margin, needed for the gap analysis.

TSURFER (Tool for S/U Analysis of Response Functions Using Experimental Results) is a bias and bias uncertainty prediction tool that implements the Generalised Linear Least-Squares (GLLS) approach to data assimilation and cross-section data adjustment. The data adjustments produced by TSURFER are not used to produce adjusted cross-section data libraries for subsequent use; rather, they are used only to predict biases in application systems.

TSAR (Tool for Sensitivity Analysis of Reactivity Responses) computes the sensitivity of the reactivity change between two  $k_{\text{eff}}$  calculations, using SDFs from TSUNAMI-1D and/or TSUNAMI-3D. TSAR also computes the uncertainty in the reactivity difference due to the cross-section-covariance data.

#### 4.8.2.3 Approach for selection of benchmark experiments

##### 4.8.2.3.1 Parameters used for similarity assessment

When using robust 3D neutron transport techniques to predict the criticality of a system, the most likely sources of computational bias are errors in the nuclear data. The basis of the TSUNAMI validation techniques is that computational biases are primarily caused by errors in the cross-section data, which are quantified and bounded by the cross-section-covariance data. For criticality code validation,  $k_{\text{eff}}$  sensitivity data are computed for the targeted application systems as well as relevant benchmark criticality experiments. The similarity of a benchmark experiment and an application system is quantified using sensitivity and uncertainty analysis techniques described in this section.

- Comparison of sensitivity profiles

It is often instructive to examine the energy-dependent sensitivity data for the application system and benchmark experiments to visually identify important characteristics in the sensitivity data. The Javapeño data-plotting package of SCALE 6 provides convenient interactive plotting of the sensitivity data from multiple data files. The VIBE package of SCALE 6 provides the ability to group collapse the sensitivity data then sort and filter the collapsed data in a tabular form to identify benchmark experiments with sensitivity data most similar to the application system.

- Nuclide-reaction specific integral index  $g$

A sensitivity-based integral index denoted  $g$ , and sometimes referred to as “little  $g$ ,” is based on the coverage of the sensitivity of the application system,  $a$ , by a given benchmark experiment,  $e$ , for a single nuclide-reaction pair. It is defined in terms of the normalised differences of the group-wise sensitivity coefficients for a particular nuclide,  $i$ , and reaction,  $x$ , summed over all energy groups,  $j$ , as:

$$g_x^i = 1 - \frac{\sum_j (S_{x,j}^{a,i} - S_{x,j}^{e,i})}{\sum_j S_{x,j}^{a,i}}, \quad (39)$$

where

$$S_{x,j}^{e',i} = \begin{cases} S_{x,j}^{e,i}, & \text{where } |S_{x,j}^{a,i}| \geq |S_{x,j}^{e,i}| \text{ and } \frac{S_{x,j}^{a,i}}{|S_{x,j}^{a,i}|} = \frac{S_{x,j}^{e,i}}{|S_{x,j}^{e,i}|} \\ S_{x,j}^{a,i}, & \text{where } |S_{x,j}^{a,i}| < |S_{x,j}^{e,i}| \text{ and } \frac{S_{x,j}^{a,i}}{|S_{x,j}^{a,i}|} = \frac{S_{x,j}^{e,i}}{|S_{x,j}^{e,i}|} \\ 0, & \text{otherwise} \end{cases}$$

and the  $j$  summation is performed over all energy groups.

The definition of  $S_{x,j}^{e',i}$  restricts the coverage of the application by the experiment to the portion of the experiment's sensitivity coefficient that does not exceed that of the application in magnitude. Additionally, the application's sensitivity coefficient and that of the experiment must have the same sign. The  $g$  index is useful where the experiment sensitivity has a lower magnitude than that of the application in that it assesses the extent to which the benchmark experiment does not adequately test the cross-section to the extent it is used in the application. The  $g$  index is normalised such that a  $g$  value of 1 indicates complete coverage of the application by the experiment for the particular nuclide-reaction pair. A  $g$  value of zero indicates no coverage of the application by the experiment for the particular nuclide-reaction pair. Even if the sensitivity of the benchmark experiment exceeds that of the application, the index will not exceed 1.0.

- Integral correlation coefficients

As computational biases are primarily caused by errors in the cross-section data, as bounded by the cross-section covariance data, a more rigorous approach to assessing the similarity of two systems for purposes of bias determination is the use of uncertainty analysis to quantify the shared uncertainty between two systems [34]. Coupling the sensitivity data from both systems with the cross-section covariance data, the shared uncertainties between two systems can be represented by a correlation coefficient. This correlation coefficient index, denoted as  $c_k$ , measures the similarity of the systems in terms of related uncertainty.

The mathematical development of the integral index  $c_k$  is presented here based on the development given in [34]. Defining  $\mathbf{S}_k$  to include the  $k_{\text{eff}}$  sensitivities of  $N$  different systems to the cross-section data,  $\alpha$ ,

$$\mathbf{S}_k \equiv \left[ \frac{\alpha_m}{k_n} \frac{\partial k_n}{\partial \alpha_m} \right], n = 1, 2, \dots, N; m = 1, 2, \dots, M, \quad (40)$$

where  $M$  is the number of nuclear data parameters. The uncertainty matrix for all the system  $k_{\text{eff}}$  values,  $\mathbf{C}_{kk}$ , is given as:

$$\mathbf{C}_{kk} = \mathbf{S}_k \mathbf{C}_{\alpha\alpha} \mathbf{S}_k^T, \quad (41)$$

$\mathbf{S}_k$  is an  $N \times M$  matrix;  $\mathbf{C}_{\alpha\alpha}$  is an  $M \times M$  matrix; and the resulting  $\mathbf{C}_{kk}$  matrix is of dimension  $N \times N$ . The diagonal elements of the  $\mathbf{C}_{kk}$  are the relative variance values,  $\sigma_{k_n}^2$ , for each of the systems under consideration, and the off-diagonal elements are the relative covariances between a given application system,  $a$ , and a given benchmark experiment,  $e$ , represented as  $\sigma_{k_{ae}}^2$ . Correlation coefficients provide a common means of normalising shared uncertainties. The correlation coefficient is defined by dividing the covariance terms by the corresponding standard deviations as:

$$c_k = \frac{\sigma_{k_{ae}}^2}{(\sigma_{k_a} \sigma_{k_e})}, \quad (42)$$

such that the single  $c_k$  value represents the correlation of uncertainties between an application and experiment.

These correlations are primarily due to the fact that the uncertainties in the calculated  $k_{\text{eff}}$  values for two different systems are related, since they contain the same materials. Cross-section uncertainties propagate to all systems containing these materials. Systems with the same materials and similar spectra would be correlated, while systems with different materials or spectra would not be correlated. The interpretation of the correlation coefficient is the following: a value of 0.0 represents no correlation between the systems, a value of 1.0 represents full correlation between the systems, and a value of  $-1.0$  represents a full anti-correlation.

- Nuclide-reaction-specific correlation coefficients

It is sometimes desirable to assess the similarity of systems in terms of the shared uncertainties for a single nuclide-reaction pair. The individual  $c_k$  is similar to system-wide  $c_k$  from Equation (42), except that it is normalised between  $-1$  and  $1$  for each for a particular nuclide,  $i$ , and reaction,  $x$ , as E:

$$c_{k_{ae},(i-x)}^{\text{individual}} = \frac{\sigma_{k_{ae},(i-x)}^2}{(\sigma_{k_a,(i-x)} \sigma_{k_e,(i-x)})}, \quad (43)$$

Where:

$\sigma_{k_{ae},(i-x)}^2$  represents the covariance between application  $a$  and experiment  $e$  due to the specified nuclide-reaction pairs;

$\sigma_{k_a,(i-x)}^2$  is the standard deviation in  $k_{\text{eff}}$  for the application due to the specified nuclide-reaction pair;

$\sigma_{k_e,(i-x)}^2$  is the standard deviation in  $k_{\text{eff}}$  for the experiment due to the specified nuclide-reaction pair.

It should be noted that individual  $c_k$  values are only computed for the same nuclide-reaction pair in the application and the experiment. Although cross-reaction and cross-nuclide covariance data are available, the cross-relationship has no physical interpretation for assessing the similarity of systems for a specific nuclide-reaction pair.

#### ■ 4.8.2.3.2 Criteria and process used for similarity assessment

The similarity of the application systems to the benchmark experiments is assessed using the techniques described above as implemented in the TSUNAMI-IP code of SCALE 6.0. When seeking overall application similarity by a given benchmark experiment, past studies have indicated that systems with  $c_k$  values of 0.9 and above are highly similar to the application, those with values of 0.8 – 0.9 are marginally similar, and those with values below 0.8 may not be similar in terms of computational bias [34]. When examining similarity for nuclide-reaction-specific coverage, the comparison of sensitivity profiles provides visual verification of coverage; the  $g$  index can identify under-coverage, where the benchmark is not as sensitive as the application for a given nuclide-reaction pair; and the individual  $c_k$  provides uncertainty weighted similarity assessment.

#### 4.8.2.4 Implementation of the validation method used to determine bias and bias uncertainty (if available)

- 4.8.2.4.1 Software tool title  
SCALE 6.0 TSUNAMI-IP/USLSTATS and TSURFER
- 4.8.2.4.2 Algorithm

Because the uncertainty in  $k_{\text{eff}}$  due to cross-section data uncertainties is directly related to potential computational bias, the  $c_k$  coefficient quantifies the similarity of the two systems in terms of common sources of bias. Where many benchmarks similar to the application are available to quantify all potential sources of bias, linear regression and extrapolation techniques can be applied to determine bias and bias uncertainty values for an application. The USLSTATS package can be applied to determine the computational bias, bias uncertainty, and upper subcritical limit (USL) based on trends in calculated  $k_{\text{eff}}$  values as a function of their similarity to the application as determined by the integral index,  $c_k$ . A linear regression of the ratio of computed-to-measured  $k_{\text{eff}}$  values as a function of  $c_k$  is extrapolated to a value 1.0, which is the  $c_k$  value generated when the application is compared to itself. Thus, the value of the regression line at  $c_k$  of 1.0 is the predicted calculated-to-measured ratio of the application system, from which the computational bias is determined. The statistical analysis techniques of USLSTATS are applied to determine a confidence band in the extrapolated value, which then becomes the uncertainty in the computational bias.

Where analytical methods are used to predict the criticality condition of a design system, the American National Standard ANSI/ANS-8.17-1984 (R1997) [38] requires that the calculated multiplication factor,  $k_s$ , should not exceed a maximum allowable value established as:

$$k_s \leq k_c - \Delta k_s - \Delta k_c - \Delta k_m \quad (44)$$

Where:

$k_s$  = the calculated allowable maximum multiplication factor,  $k_{\text{eff}}$ , of the system being evaluated for normal or credible abnormal conditions or events.

$k_c$  = the mean  $k_{\text{eff}}$  that results from the calculation of the benchmark criticality experiments using a particular computational method. If the calculated  $k_{\text{eff}}$  values for the criticality experiments exhibit a trend with a parameter, then  $k_c$  will be determined by extrapolation on the basis of a best fit to the calculated values. The criticality experiments used as benchmarks in computing  $k_c$  should have physical compositions, configurations, and nuclear characteristics (including reflectors) similar to those of the system being evaluated.

$\Delta k_s$  = an allowance for statistical or convergence uncertainties, or both in the computation of  $k_s$ ; material and fabrication tolerances; and uncertainties due to limitations in the geometric or material representations used in the computational method.

$\Delta k_c$  = a margin for uncertainty in  $k_c$  which includes allowance for uncertainties in the critical experiments; statistical or convergence uncertainties, or both, in the computation of  $k_c$ ; uncertainties due to extrapolation of  $k_c$  outside the range of experimental data; and uncertainties due to limitations in the geometrical or material representations used in the computational method.

$\Delta k_m$  = an additional margin to ensure the subcriticality of  $k_s$ .

Consistent with the requirements of ANSI/ANS-8.17-1984 (R1997), a criticality code is typically validated against a suite of critical experiments to define a USL for design

systems. According to the standard, the computed  $k_{\text{eff}}$  value of a design system (i.e.  $k_s$ ) should not exceed the maximum acceptable value. This is expressed as:

$$k_s + 2\sigma \leq USL = 1.00 + \beta - \Delta\beta - \Delta k_m, \quad (45)$$

where  $\sigma$  is the standard deviation of the computed value,  $k_s$ ;  $\beta$  and  $\Delta\beta$  represent the computational bias and uncertainty in the bias, respectively [39]. For critical experiments, the computational bias is the difference between the mean value of  $k_{\text{eff}}$  calculated for the critical experiments,  $k_c$ , and 1.0 (i.e.  $\beta = k_c - 1.0$ ). In practice, certain critical experiments may exhibit calculated  $k_{\text{eff}}$  values  $> 1.0$ , leading to a positive bias and reducing the required subcritical margin for the design system. However, regulatory impositions typically have not allowed for a positive computational bias; thus,  $\beta$  is either negative or zero. The quantity  $\Delta k_m$  is often referred to as an administrative margin and commonly assigned a value between 2 and 5% in  $k_{\text{eff}}$  (e.g.  $\Delta k_m = 0.05$ ), depending on the application and regulatory guidance.

Two commonly used approaches for the calculation of the USL based on a suite of criticality experiments covering a particular area of applicability are (1) confidence band with administrative margin, referred to as  $USL_1$ , and (2) single-sided uniform-width closed-interval approach, also called the lower tolerance band (LTB) method, and referred to as  $USL_2$  [37]. The statistical analysis commonly used in the computation of  $USL_1$  and  $USL_2$  is only valid within the range of applicability of the chosen trending parameter. However, the approach applied with TSUNAMI always requires at least some extrapolation. As  $USL_2$  is by definition a closed-interval approach, it is never suitable for extrapolation. However, the  $USL_1$  approach can be appropriately defined for extrapolation as presented below and implemented in the SCALE 6 version of USLSTATS.

- Correlation coefficient trending

The  $USL_1$  in [37] applies a statistical calculation of the bias and its uncertainty plus an optional additional margin to a linear fit of critical experiment benchmark data. This approach is illustrated in Figure 10, where the additional margin is set to 0.02, or 2%  $\Delta k/k$ . In this figure, the blue-dashed  $k(x)$  line represents a linear regression fit to a set of calculations based on the calculated-to-experiment (C/E) ratio of  $k_{\text{eff}}$  results from critical experiments. The relative bias in the application ( $\Delta k/k$ ) is given as  $k(x) - 1$ , evaluated at  $k_c = 1.0$ . The green-dashed line represents the lower confidence band for a single additional calculation, a quadratic expression defined below. The width of this band is determined statistically based on the existing data and a specified level of confidence; the greater the standard deviation in the data or the larger the confidence desired, the larger the band width will be. This confidence band,  $w(x)$ , accounts for uncertainties in the experiments and the calculation approach as well as the dispersion of the data points and is therefore a statistical basis for  $\Delta\beta$ , the uncertainty in the value of  $\beta$ . With a  $(1-\gamma_1)$  confidence level,  $w(x)$  is defined as:

$$w(x) = t_{1-\gamma_1} s_p \left[ 1 + \frac{1}{n} + \frac{(x - \bar{x})^2}{\sum_{i=1,n} (x_i - \bar{x})^2} \right]^{\frac{1}{2}}, \quad (46)$$

Where:

$n$  = the number of critical calculations used in establishing  $k(x)$ ;

$t_{1-\gamma_1}$  = the Student-t distribution statistic for  $1-\gamma_1$  and  $n-2$  degrees of freedom;

$\bar{x}$  = the mean value of the independent variable  $x$  in the set of calculations;

$s_p$  = the pooled standard deviation for the set of criticality calculations.

The pooled standard deviation is obtained from the pooled variance ( $s_p = \sqrt{s_p^2}$ ), where  $s_p^2$  is given as:

$$s_p^2 = s_{k(x)}^2 + s_w^2 \tag{47}$$

where  $s_{k(x)}^2$  is the variance (or mean-square error) of the regression fit, and is given by:

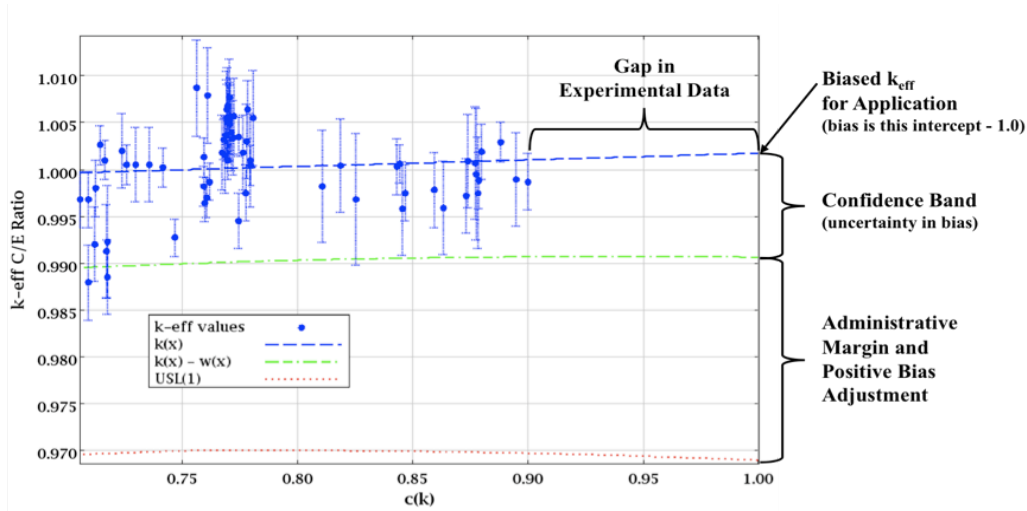
$$s_{k(x)}^2 = \frac{1}{(n-2)} \left[ \sum_{i=1,n} (k_i - \bar{k})^2 \frac{\left\{ \frac{\sum_{i=1,n} (x_i - \bar{x})(k_i - \bar{k})}{\sum_{i=1,n} (x_i - \bar{x})^2} \right\}^2}{\sum_{i=1,n} (x_i - \bar{x})^2} \right], \tag{48}$$

and  $s_w^2$  is the within-variance of the data:

$$s_w^2 = \frac{1}{n} \sum_{i=1,n} \sigma_i^2, \tag{49}$$

where  $\sigma_i$  is the standard deviation associated with  $k_i$ , which could be due to Monte Carlo calculations.

**Figure 10: Illustration of correlation coefficient trending with  $USL_1$**



Note that the function  $w(x)$  is a curvilinear function that will increase in width as a function of extrapolation from the data. Typically,  $w(x)$  is determined at a 95% confidence level.

The red-dashed line in Figure 10 represents  $USL_1$ , which discounts any positive bias and included the administrative margin. The value of  $USL_1$  as a function of the trending parameter,  $x$ , is defined as:

$$USL_1(x) = \begin{cases} 1 - \Delta k_m - w(x) + \beta(x), & \beta(x) < 0 \\ 1 - \Delta k_m - w(x), & \beta(x) \geq 0 \end{cases}, \tag{50}$$

The value of  $USL_1$  for the application is determined by evaluating Equation (50) with  $x = 1.0$ . The data used in the  $USL_1$  determination must pass a normality test before statistical analyses are applied. USLSTATS provides a simple  $\chi^2$  test for normality using five equal-probability bins. Because the current normality test is so simple, data sets that may pass other normality test may fail the USLSTATS normality test. If the data are shown to be

normal by some other means, the statistical treatments of USLSTATS can still be valid, even though the data failed the internal test.

- Gap analysis using TSUNAMI penalty assessment

The set of critical experiments used as benchmarks in the computation of  $\beta$  should be representative of the composition, configuration, and nuclear characteristics of the application system. However, ANSI/ANS-8.1 allows the range of applicability to be extended beyond the range of conditions represented by the benchmark experiments by extrapolating the trends established for the bias. When the extrapolation is large relative to the range of data, the calculation method applied should be supplemented by other methods in order to better estimate the extrapolated bias. Note that large is not defined by the ANSI standard.

A method is available in TSUNAMI-IP to assess an additional margin to subcriticality, or penalty, where sufficient experiments are not available to provide complete coverage for a particular application. The gap between the best-available experiment and the application is illustrated in Figure 10, where the  $c_k$  value of the best-matching experiment is 0.90, indicating that 10% of the cross-section uncertainty in the application is different from that in the closest matching experiment. Although the statistical treatment of USLSTATS accounts for trends in existing data, the lack of similarity indicates that some processes in the application may not be fully accounted for by the experiments included in the analysis. In this case, any possible change in the trend as  $c_k$  approaches 1.0 may not be bounded by a statistical analysis of the C/E values.

The TSUNAMI gap analysis technique quantifies an additional uncertainty component that can be added to the administrative margin to provide an added measure of safety for application systems where validation coverage is lacking. The penalty calculation is based on the criteria for coverage used for the integral index  $g$ . The TSUNAMI penalty calculation quantifies the uncertainty in the application that remains after the best-available coverage from qualified experiments has been applied. As this form of gap analysis is intended as a supplement to  $c_k$  trending analysis, any experiment used in the penalty assessment calculation must pass a qualification test to determine global similarity of the experiment, based on  $c_k$ . Thus, only experiments that exhibit a certain degree of similarity to the application, and thus an expected relevant influence on the trending analysis, can be considered in the penalty calculation. Additionally, a sufficient number of similar experiments are required before any penalty assessment is produced by TSUNAMI-IP.

To compute the penalty, a vector of the minimum differences in the sensitivity coefficients,  $\mathbf{Z}_a$ , for the application with respect to all experiments can be obtained as:

$$\mathbf{Z}_a \equiv \left[ Z_{x,j}^{a,n} \right], n=1, \dots, N, x=1, \dots, X, j=1, \dots \quad (51)$$

Where:

$$Z_{x,j}^{a,n} = S_{x,j}^{a,n} - C_{x,j}^{a,n}$$

$C_{x,j}^{a,n}$  is a composite of the best-available sensitivity data from all experiments and is defined as:

$$C_{x,j}^{a,n} = S_{x,j}^{e',n} \text{ for the experiment that satisfies } \min \left| S_{x,j}^{a,n} - S_{x,j}^{e',n} \right|, e'=1, \dots, E;$$

$N =$  number of nuclides in the application system;

$X =$  number of reactions for each nuclide;

$J =$  number of energy groups;

$E =$  number of experiments meeting the qualification tests.

Once  $\mathbf{Z}_a$  is computed, the portion of the sensitivity of the application that is not covered by the experiments can be used to propagate the uncertainty in the cross-section data to a relative uncertainty in  $k_{eff}$  as:

$$\Delta k_{eff} / k_{eff} = \sqrt{\mathbf{Z}_a \mathbf{C}_{\alpha\alpha} \mathbf{Z}_a^T} \quad (52)$$

In the above equation, the elements of  $\mathbf{Z}_a$  are each expressed in terms of  $(\Delta k_{eff}/k_{eff})/(\Delta\sigma/\sigma)$  and the elements of  $\mathbf{C}_{\alpha\alpha}$  are expressed in terms of relative variances or covariances as  $(\Delta\sigma/\sigma)^2$ , so that the final penalty is expressed as a relative uncertainty in  $k_{eff}$ ,  $\Delta k_{eff}/k_{eff}$ . This relative uncertainty in  $k_{eff}$  due to the gap in experimental coverage can be used to increase the safety margin to provide for extrapolation beyond the range of applicability of available experiments.

- Bias assessment with data adjustment techniques

A new capability for SCALE 6 allows the prediction of computational biases with the nuclear data adjustment tool TSURFER, which is based on the Generalised Linear Least-Squares approach [34]. The data adjustments in TSURFER are not used to produce adjusted cross-section data libraries for subsequent use; rather they are used only to predict biases in application systems. As TSURFER is a general-purpose tool, a computed quantity for which a bias is predicted is referred to as a response. A response is often  $k_{eff}$  but in general could be a reactivity, a reaction rate ratio, or any other quantity of interest that can be both measured in benchmark experiments and calculated through numerical simulation using multi-group cross-section data. TSURFER identifies a single set of adjustments to nuclear data and experimental values, all bounded by their uncertainties, that will result in the computational models all producing response values close to their experimental response value. Then the same data adjustments are used to predict an unbiased response value for the application and an uncertainty on the adjusted response value. The difference between the originally calculated response value and the new post-adjustment response value represents the bias in the original calculation, and the uncertainty in the adjusted value represents the uncertainty in this bias. If similar experiments are available to validate the use of a particular nuclide in the application, the uncertainty of the bias for this nuclide is reduced. In TSURFER, experiments that are dissimilar from the application can still provide useful information for bias assessment if at least one material demonstrates similar sensitivities to those of the application. If similar experiments are not available to validate a particular nuclide, a high uncertainty in the bias for the given nuclide will result. Thus, with a complete set of experiments to validate important components in the application, a precise bias with a small uncertainty can be predicted. Where the experimental coverage is lacking, a bias can be predicted with an appropriately large uncertainty. As users gain experience with TSURFER, it may become a preferred tool for rigorous bias and bias uncertainty determination, particularly for applications for which nearly identical critical experiments are not available. However, the results of TSURFER analyses rely on the availability of quality uncertainty and correlation data for both nuclear data and benchmark experiments.

- TSURFER computational methodology

TSURFER applies the Generalised Linear Least-Squares (GLLS) technique to produce the adjusted cross-section values that are used for bias prediction. A recent detailed derivation of the GLLS formalism is given in [34]. The general formalism allows cross-correlations between the initial integral experiment measurements and the original nuclear data, such as would be present if the calculations used a previously “adjusted” library of nuclear data. Since this is not normally done in SCALE, correlations between the benchmark experiment measurements and the cross-section data in the multi-group libraries are not considered in the TSURFER code; therefore, the GLLS equations presented here are somewhat simplified compared to the more general expressions in [34].

At present, the SCALE cross-section-covariance data files characterise nuclear data uncertainties in terms of relative covariances. Therefore, the initial development that follows is for relative, rather than absolute, response sensitivity and uncertainty parameters. It is then shown how to express the quantities in absolute form for reactivity analysis and mixed relative-absolute form for combined  $k_{\text{eff}}$  and reactivity analysis.

The methodology consists of calculating values for a set of  $I$  integral responses ( $k_{\text{eff}}$ , reactivity differences, reaction rates, etc.), some of which have been measured in selected benchmark experiments. Responses with no measured values are then selected as applications, whose biases will be predicted based on the measured quantities. The set of measured response values  $\{m_i; i=1,2,\dots, I\}$  can be arranged into an  $I$ -dimension column vector designated as  $\mathbf{m}$ . By convention the (unknown) experimental values corresponding to applications are represented by the corresponding calculated values. The measured integral responses have uncertainties – possibly correlated – due to uncertainties in the system parameter specifications. The  $I \times I$  covariance matrix describing the relative experimental uncertainties is defined to be  $\mathbf{C}_{\text{mm}}$ .

Experimental uncertainties are typically defined in the description of benchmark experiments. Often the sources of the uncertainties are detailed and the contribution to the overall uncertainty in the response value is described. These uncertainties are important to TSURFER analysis, as the reported benchmark response value is only as precise as techniques used in its evaluation allow. It makes little sense to adjust cross-section data to precisely match an imprecise response value. Therefore, TSURFER adjusts not only the cross-section data within their uncertainties but also adjusts the experimental values within their uncertainties, constrained by their correlations.

Discrepancies between the calculated and measured responses are defined by the  $I$  dimensional column vector:

$$\mathbf{d} = \left\{ d_i = \frac{k_i(\boldsymbol{\alpha}) - m_i}{k_i(\boldsymbol{\alpha})}, i = 1, \dots, I \right\} \quad (53)$$

where  $k_i(\boldsymbol{\alpha})$  is the computed  $k_{\text{eff}}$  value for system  $i$  using the prior, unadjusted, cross-section data,  $\boldsymbol{\alpha}$ , and  $m_i$  is the measured  $k_{\text{eff}}$  of system  $i$ . In TSURFER, the components of  $\mathbf{d}$  corresponding to application responses are set to zero because applications have no measured values. Using the standard formula for propagation of error and assuming no correlations between  $k$  and  $m$ , the relative uncertainty matrix for the discrepancy vector  $\mathbf{d}$  can be expressed as the  $I \times I$  matrix:

$$\mathbf{C}_{\text{dd}} = \mathbf{C}_{\text{kk}} + \mathbf{F}_{\text{m/k}} \mathbf{C}_{\text{mm}} \mathbf{F}_{\text{m/k}} = \mathbf{S}_{\text{k}} \mathbf{C}_{\boldsymbol{\alpha}\boldsymbol{\alpha}} \mathbf{S}_{\text{k}}^T + \mathbf{F}_{\text{m/k}} \mathbf{C}_{\text{mm}} \mathbf{F}_{\text{m/k}}, \quad (54)$$

where  $\mathbf{F}_{\text{m/k}}$  is an  $I \times I$  diagonal matrix containing  $m/k$  factors, that is, E/C factors (ratio of experimental to calculated response values). The inverse of the matrix  $\mathbf{C}_{\text{dd}}$  appears in several expressions presented later in this section.

The goal of the GLLS method is to vary the nuclear data ( $\boldsymbol{\alpha} \rightarrow \boldsymbol{\alpha}'$ ) and the measured integral responses ( $\mathbf{m} \rightarrow \mathbf{m}'$ ), such that they are most consistent with their respective uncertainty matrices,  $\mathbf{C}_{\boldsymbol{\alpha}\boldsymbol{\alpha}}$  and  $\mathbf{C}_{\text{mm}}$ . This is done by minimising chi-square, expressed as:

$$\begin{aligned} \chi^2 &= \left[ \frac{\boldsymbol{\alpha}' - \boldsymbol{\alpha}}{\boldsymbol{\alpha}} \right]^T \mathbf{C}_{\boldsymbol{\alpha}\boldsymbol{\alpha}}^{-1} \left[ \frac{\boldsymbol{\alpha}' - \boldsymbol{\alpha}}{\boldsymbol{\alpha}} \right] + \left[ \frac{\mathbf{m}' - \mathbf{m}}{\mathbf{m}} \right]^T \mathbf{C}_{\text{mm}}^{-1} \left[ \frac{\mathbf{m}' - \mathbf{m}}{\mathbf{m}} \right] \\ &= [\Delta\boldsymbol{\alpha}]^T \mathbf{C}_{\boldsymbol{\alpha}\boldsymbol{\alpha}}^{-1} [\Delta\boldsymbol{\alpha}] + [\Delta\mathbf{m}]^T \mathbf{C}_{\text{mm}}^{-1} [\Delta\mathbf{m}] \end{aligned} \quad (55)$$

where  $\Delta\alpha_i = \frac{\alpha'_i - \alpha_i}{\alpha_i}$  and  $\Delta m_i = \frac{m'_i - m_i}{m_i}$ . Equation (55) is rearranged to give:

$$\chi^2 = [\boldsymbol{\sigma}_\alpha^{-1} \Delta \boldsymbol{\alpha}]^T \mathbf{R}_{\alpha\alpha}^{-1} [\boldsymbol{\sigma}_\alpha^{-1} \Delta \boldsymbol{\alpha}] + [\boldsymbol{\sigma}_m^{-1} \Delta \mathbf{m}]^T \mathbf{R}_{mm}^{-1} [\boldsymbol{\sigma}_m^{-1} \Delta \mathbf{m}] \quad (56)$$

Equation (56) expresses the variations in the nuclear data and measured responses in units of their respective standard deviations, that is,  $[\boldsymbol{\sigma}_\alpha^{-1} \Delta \boldsymbol{\alpha}]$  and  $[\boldsymbol{\sigma}_m^{-1} \Delta \mathbf{m}]$ .

Chi-square is a quadratic form indicating the squared magnitude of the combined data variations with respect to their uncertainties. This is easily seen for the simple case in which  $[\mathbf{R}_{\alpha\alpha}]^{-1}$  and  $[\mathbf{R}_{mm}]^{-1}$  are identity matrices, so that Equation (56) is reduced to only the diagonal contributions:

$$\chi^2 \rightarrow \sum_{n=1}^M \left( \frac{\alpha'_n - \alpha_n}{\tilde{\sigma}_{\alpha_n}} \right)^2 + \sum_{i=1}^I \left( \frac{m'_i - m_i}{\tilde{\sigma}_{m_i}} \right)^2 \quad (57)$$

The first term on the right side of Equation (57) is equal to the sum of the squares of the individual nuclear data variations expressed in units of their standard deviations, while the second term represents a similar quantity for the measured integral responses. In the general case where correlations exist, the inverse matrices in Equation (56) are not diagonal, and the value of chi-square must be evaluated using the indicated matrix multiplication.

Thus it can be seen that the GLLS method determines adjustments in the nuclear data and experimental measurements that (a) make the calculated and measured responses agree [i.e.  $\mathbf{k}' = \mathbf{k}'(\boldsymbol{\alpha}') = \mathbf{m}'$ , within the limitations of first-order sensitivity theory] and (b) minimise Equation (57) so that the adjustments are most consistent with the data uncertainties. Although many possible combinations of data variations may make  $\mathbf{k}' = \mathbf{m}'$ , there is a unique set that also minimises  $\chi^2$ .

The following variations minimise Equation (57), subject to the constraint  $\mathbf{k}'(\boldsymbol{\alpha}') = \mathbf{m}'$  and the linearity condition  $[\Delta \mathbf{k}] = \mathbf{S}_{k\alpha} [\Delta \boldsymbol{\alpha}]$  where  $\Delta k_i = \frac{k'_i - k_i}{k_i}$ :

$$\Delta \boldsymbol{\alpha} = -[\mathbf{C}_{\alpha\alpha} \mathbf{S}_{k\alpha}^T \mathbf{C}_{dd}^{-1}] \mathbf{d} \quad (58)$$

$$\Delta \mathbf{m} = [\mathbf{C}_{mm} \mathbf{F}_{m/k} \mathbf{C}_{dd}^{-1}] \mathbf{d} \quad (59)$$

In the above equations the initial response discrepancy vector  $\mathbf{d}$  is operated on by the transformation matrix in square brackets to obtain the desired variations in nuclear data and integral measurements; thus, it is the discrepancy components that drive the adjustments. If the linearity assumption is valid, then the changes in the calculated responses are found to be:

$$\Delta \mathbf{k} = \mathbf{F}_{m/k} \Delta \mathbf{m} - \mathbf{d} = \mathbf{S}_k \Delta \boldsymbol{\alpha} \quad (60)$$

Equation (60) relates the adjustments in calculated responses, measured responses, and nuclear data.

As previously discussed, consolidation of the calculated and measured responses reduces the prior uncertainties for  $\boldsymbol{\alpha}$ ,  $\mathbf{m}$ , and  $\mathbf{k}$  because additional knowledge has been incorporated. This is indicated by their modified covariance matrices  $\mathbf{C}_{\alpha'\alpha'}$ ,  $\mathbf{C}_{m'm'}$ ,  $\mathbf{C}_{k'k'}$  respectively, given by:

$$\mathbf{C}_{\alpha'\alpha'} = \mathbf{C}_{\alpha\alpha} - [\mathbf{C}_{\alpha\alpha} \mathbf{S}_k^T \mathbf{C}_{dd}^{-1} \mathbf{S}_k \mathbf{C}_{\alpha\alpha}] \quad (61)$$

$$\mathbf{C}_{m'm'} = \mathbf{C}_{mm} - [\mathbf{C}_{mm} \mathbf{F}_{m/k} \mathbf{C}_{dd}^{-1} \mathbf{F}_{m/k} \mathbf{C}_{mm}] \quad (62)$$

$$\mathbf{C}_{k'k'} = \mathbf{C}_{kk} - [\mathbf{C}_{kk} \mathbf{C}_{dd}^{-1} \mathbf{C}_{kk}], \quad (63)$$

If all the responses on the TSURFER input are relative-formatted, then the adjusted data and response values edited by TSURFER are obtained from Equations (58)-(59), while the square roots of diagonal elements in Equations (61)-(63) correspond to the relative values for adjusted uncertainties in the nuclear data and in the experiment responses, respectively.

The adjustment formulas must be modified slightly to be consistent with the absolute-formatted responses. In the following expressions, absolute response covariance and response sensitivity data are denoted by a tilde:

$$\tilde{\mathbf{d}} = \mathbf{k}(\boldsymbol{\alpha}) - \mathbf{m} \quad (64)$$

$$\tilde{\mathbf{C}}_{dd} = \tilde{\mathbf{C}}_{kk} + \mathbf{C}_{mm} = \tilde{\mathbf{S}}_k \mathbf{C}_{\alpha\alpha} \tilde{\mathbf{S}}_k^T + \tilde{\mathbf{C}}_{mm} \quad (65)$$

$$\Delta \tilde{\boldsymbol{\alpha}} = \boldsymbol{\alpha}' - \boldsymbol{\alpha} = -[\mathbf{C}_{\alpha\alpha} \tilde{\mathbf{S}}_k^T \tilde{\mathbf{C}}_{dd}^{-1}] \tilde{\mathbf{d}} \quad (66)$$

$$\Delta \tilde{\mathbf{m}} = \mathbf{m}' - \mathbf{m} = [\tilde{\mathbf{C}}_{mm} \tilde{\mathbf{C}}_{dd}^{-1}] \tilde{\mathbf{d}} \quad (67)$$

$$\Delta \tilde{\mathbf{k}} = \mathbf{k}' - \mathbf{k} = (\mathbf{m}' - \mathbf{m}) - \mathbf{d} = \mathbf{S}_k (\boldsymbol{\alpha}' - \boldsymbol{\alpha}) \quad (68)$$

Relative covariances for the posterior values of the nuclear data and measured responses are given as:

$$\mathbf{C}_{\alpha'\alpha'} = \mathbf{C}_{\alpha\alpha} - [\mathbf{C}_{\alpha\alpha} \tilde{\mathbf{S}}_k^T] \tilde{\mathbf{C}}_{dd}^{-1} [\tilde{\mathbf{S}}_k \mathbf{C}_{\alpha\alpha}] \quad (69)$$

$$\tilde{\mathbf{C}}_{m'm'} = \tilde{\mathbf{C}}_{mm} - [\tilde{\mathbf{C}}_{mm} \tilde{\mathbf{C}}_{dd}^{-1} \tilde{\mathbf{C}}_{mm}] \quad (70)$$

If all the input from responses to TSURFER are absolute-formatted, the adjusted data and response values edited by TSURFER are obtained from Equations (66)-(70), while the square roots of diagonal elements in Equations (69)-(70) correspond to the absolute values for adjusted uncertainties in the nuclear data and in the experiment responses, respectively.

The adjustment formulas again must be modified slightly given a set of mixed relative/absolute-formatted responses. In the following expressions, mixed response covariance and response sensitivity data are denoted by a caret, and  $\hat{\mathbf{F}}_{m/k}$  is an  $l \times l$  diagonal matrix containing  $m/k$  factors for relative-formatted responses or a value of one for absolute-formatted responses:

$$\hat{d}_i = \begin{cases} \frac{k(\boldsymbol{\alpha})_i - m_i}{k(\boldsymbol{\alpha})_i} & i_{th} \text{ response is relative - formatted} \\ k(\boldsymbol{\alpha})_i - m_i & i_{th} \text{ response is absolute - formatted} \end{cases} \quad (71)$$

$$\Delta \hat{m}_i = \begin{cases} \frac{m'_i - m_i}{m_i} & \text{relative} \\ m'_i - m_i & \text{absolute} \end{cases} \quad (72)$$

$$\Delta \hat{\mathbf{k}}_i = \begin{cases} \frac{\mathbf{k}'(\boldsymbol{\alpha}')_i - \mathbf{k}(\boldsymbol{\alpha})_i}{\mathbf{k}(\boldsymbol{\alpha})_i} & \text{relative} \\ \mathbf{k}(\boldsymbol{\alpha})_i - \mathbf{k}(\boldsymbol{\alpha})_i & \text{absolute} \end{cases} \quad (73)$$

$$\hat{\mathbf{C}}_{dd}^{-1} = \hat{\mathbf{C}}_{kk} + \hat{\mathbf{F}}_{m/k} \hat{\mathbf{C}}_{mm} \hat{\mathbf{F}}_{m/k}^T = \hat{\mathbf{S}}_k \mathbf{C}_{dd} \hat{\mathbf{S}}_k^T + \hat{\mathbf{F}}_{m/k} \hat{\mathbf{C}}_{mm} \hat{\mathbf{F}}_{m/k}^T \quad (74)$$

$$\Delta \hat{\boldsymbol{\alpha}} = -[ \mathbf{C}_{dd} \hat{\mathbf{S}}_k^T \hat{\mathbf{C}}_{dd}^{-1} ] \hat{\mathbf{d}} \quad (75)$$

$$\Delta \hat{\mathbf{m}} = [ \hat{\mathbf{C}}_{mm} \hat{\mathbf{F}}_{m/k} \hat{\mathbf{C}}_{dd}^{-1} ] \hat{\mathbf{d}} \quad (76)$$

$$\Delta \hat{\mathbf{k}} = \hat{\mathbf{S}}_k \Delta \hat{\boldsymbol{\alpha}} \quad (77)$$

Covariances for the posterior values of the nuclear data and measured responses are given as:

$$\mathbf{C}_{\boldsymbol{\alpha}'\boldsymbol{\alpha}'} = \mathbf{C}_{\boldsymbol{\alpha}\boldsymbol{\alpha}} - [ \mathbf{C}_{\boldsymbol{\alpha}\boldsymbol{\alpha}} \hat{\mathbf{S}}_k^T ] \hat{\mathbf{C}}_{dd}^{-1} [ \hat{\mathbf{S}}_k \mathbf{C}_{\boldsymbol{\alpha}\boldsymbol{\alpha}} ] \quad (78)$$

$$\hat{\mathbf{C}}_{m'm'} = \hat{\mathbf{C}}_{mm} - [ \hat{\mathbf{C}}_{mm} \hat{\mathbf{F}}_{m/k} \hat{\mathbf{C}}_{dd}^{-1} \hat{\mathbf{F}}_{m/k} \hat{\mathbf{C}}_{mm} ] \quad (79)$$

If responses on the TSURFER input are both relative-formatted and absolute-formatted, the adjusted data and response values edited by TSURFER are obtained from Equations (71)-(77) while the square roots of diagonal elements in Equations (77)-(79) correspond to the relative or absolute values for adjusted uncertainties in the nuclear data and in the experiment responses, respectively.

- Consistency relations and chi-square filtering

Using relative sensitivities, variations for  $\Delta \mathbf{m}$  and  $\Delta \boldsymbol{\alpha}$  defined by Equations (58) and (59) are those that give the smallest value of the quadratic form of  $\chi^2$ . This minimum  $\chi^2$  value is found by substituting Equations (58) and (59) into Equation (55) as:

$$\chi_{\min}^2 = \mathbf{d}^T \mathbf{C}_{dd}^{-1} \mathbf{d} = \mathbf{d}^T [ \mathbf{C}_{kk} + \mathbf{F}_{m/k} \mathbf{C}_{mm} \mathbf{F}_{m/k} ]^{-1} \mathbf{d} \quad (80)$$

It is interesting to observe that the discrepancy vector  $\mathbf{d}$  defined by Equation (71) does not depend upon adjustments in nuclear data or integral experiments and physically expresses a measure of the initial discrepancies ( $\mathbf{d}$ ) in all responses, compared to their combined calculation and experiment uncertainties ( $\mathbf{C}_{kk} + \mathbf{F}_{m/k} \mathbf{C}_{mm} \mathbf{F}_{m/k}$ ). Equation (79) can be viewed as an inherent limit on the consistency of the GLLS adjustment procedure. If the initial calculated and measured responses are not consistent with their stated uncertainties, then adjustments in nuclear data and experiment values obtained by TSURFER cannot be consistent either.

TSURFER provides an option for  $\chi^2$  filtering to ensure that a given set of benchmark experiments is consistent, that is, that the input responses have an acceptable  $\chi^2_{\min}$  defined by Equation (79). The code progressively removes individual experiments until the calculated  $\chi^2_{\min}$  is less than a user input threshold. Each iteration removes one experiment estimated to have the greatest impact on  $\chi^2$  per degree of freedom. The method used to assess individual contributions to  $\chi^2_{\min}$  is specified by the user from the options given below.

#### Independent chi-square [40]

The consistency of the  $i^{\text{th}}$  measured and calculated response values, disregarding any other integral response, is equal to the discrepancy in the measured and calculated value squared divided by the variance of the discrepancy of the  $i^{\text{th}}$  response:

$$\chi_{ind,i}^2 = \frac{(k_i - m_i)^2}{s_{k_i}^2 + s_{m_i}^2}. \quad (81)$$

Equation (80) is strictly valid only when no correlations exist, but it may be a useful approximation to estimate the experiment having the greatest impact on chi-square per degree of freedom. Hence, this expression is called the independent chi-square approximation in TSURFER. This approximation is executed quickly since no matrix inversions are required.

#### Diagonal chi-square

The diagonal chi-square approach uses diagonal values of the original inverse  $\mathbf{C}_{dd}$  matrix to estimate the experiment having the greatest impact on chi-square per degree of freedom:

$$\chi_{dia,i}^2 \equiv (k_i - m_i)^2 \mathbf{C}_{dd}^{-1}(i,i). \quad (82)$$

In this method the correlations in all responses are taken into account to some extent. The original  $\mathbf{C}_{dd}^{-1}$  is used in each iteration; therefore, the diagonal chi-square method requires only a single matrix inversion.

#### Iterative-diagonal chi-square

This approach is identical to the diagonal chi-square method, except that an updated value of  $\mathbf{C}_{dd}^{-1}$  is computed for each iteration to re-evaluate the total chi-square from Equation (80). Thus, one matrix inversion is performed per iteration.

#### Delta chi-square

The most rigorous method to determine the impact of an individual response on the overall consistency is called the delta chi-square method in TSURFER. This method [40] calculates the change in chi-square whenever a particular response is omitted for the analysis; that is, omitting the  $i^{\text{th}}$  response results in:

$$\Delta\chi_i^2 = [\mathbf{d}^T \mathbf{C}_{dd}^{-1} \mathbf{d}] - [\mathbf{d}_{\neq i}^T (\mathbf{C}_{dd}^{\neq i})^{-1} \mathbf{d}_{\neq i}] \quad (83)$$

where  $\mathbf{d}_{\neq i}$  and  $\mathbf{C}_{dd}^{\neq i}$  are, respectively, the discrepancy vector and discrepancy covariance with response  $i$  omitted. While Equation (81) is the most rigorous method, it also requires the most computation effort. A matrix inversion must be performed for every omitted response, in each iteration.

It has been observed that independent chi-square and diagonal chi-square options execute quickly but often eliminate more experiments than necessary to obtain the target chi-square value. The diagonal chi-square option is somewhat faster than the iterative-diagonal chi-square option but also sometimes omits more than the minimum number of experiments. The delta chi-square option is currently the default in TSURFER.

- Expressions for computational bias

The computational bias is defined in TSURFER as the observed difference between a calculated and measured response. In conventional validation studies, such as those using USLSTATS, the expected bias in an application response (for which there is no measurement, by definition) often is estimated as the sample mean of the biases for a set of benchmark experiments and the uncertainty in the application bias is estimated by the sample standard deviation of the experimental biases.

The GLLS technique provides another method to compute the bias of an application response. The application response bias  $\beta_a$  is defined as the expected deviation of the original calculated response  $k_a$  from the best estimate of the measured response, which is unknown but has some probability distribution. Note that if the application response actually did have a prior measured value  $m_a$ , then the best estimate for the experiment value would be the final adjusted value  $m'_a$  obtained from the GLLS procedure. For this reason, the notation  $m'_a$  is used here to represent the (unknown) best estimate for the application's projected measured response, so that:

$$\beta_a = E[k_a - m'_a] \quad (84)$$

where  $E$  is the expectation operator. The application's projected measured value can be expressed as  $m'_a = k_a(\alpha') - \delta m_a$ , where  $\delta m_a$  represents the difference between the best-computed response obtained with the adjusted data  $\alpha'$  and the expected value of the actual measurement. Therefore Equation (82) can be expressed as:

$$\beta_a = E[k_a - k_a(\alpha') + \delta m_a] = k_a - k_a(\alpha') + E[\delta m_a] \quad (85)$$

It should be noted that all experiment responses have  $\delta m_i = 0$ , because the GLLS procedure forces  $\mathbf{k}' = \mathbf{m}'$  within the approximation of first-order theory. However,  $\delta m_a$  ( $= k'_a - m'_a$ ) for the application is not guaranteed to be zero, since there is no known measured value. Nevertheless, the application response calculated using the best cross-sections  $\alpha'$  should approach the desired (unknown) measured value if a sufficient number of experiments similar to the application of interest are considered; so that under these conditions  $E[\delta m_a] \rightarrow 0$  for the application as well [34]. More details concerning the suitable degree of similarity and the sufficient number of experiments necessary for convergence of the GLLS methodology are discussed in other publications [34].

Assuming an adequate benchmark database such that  $E[\delta m_a] \sim 0$ , Equation (77) simplifies to:

$$\beta_a = k_a - k_a(\alpha') \sim -(k_a) \mathbf{S}_a^T \Delta \alpha \quad (86)$$

or, stated in absolute terms:

$$\beta_a \approx -\tilde{\mathbf{S}}_a^T \Delta \alpha \quad (87)$$

- Bias uncertainty

In most cases, some gaps exist in the benchmark database so that  $E[\delta m_a] \neq 0$ . In this case, the adjusted cross-section covariance data are used to produce a post-adjustment uncertainty, which is the uncertainty in the adjusted response value, and thus the uncertainty in the computational bias. Similar to uncertainty due to nuclear data, the post-adjustment uncertainty for the application is computed as:

$$\sigma_{k_a}^2 = \mathbf{S}_a \mathbf{C}_{\alpha\alpha'} \mathbf{S}_a^T, \quad (88)$$

and the uncertainty in the bias is:

$$\Delta \beta_a = (\mathbf{S}_a \mathbf{C}_{\alpha\alpha'} \mathbf{S}_a^T)^{1/2} \quad (89)$$

The individual nuclide-reaction-specific contributors to the bias uncertainty can be computed from the individual processes that make up the post-adjustment cross-section-covariance data. When folded with the application sensitivity data for the same processes, gaps in the benchmark database that contribute to the uncertainty in the bias are revealed.

#### 4.8.2.5 Initial data for the bias and bias uncertainty determination

- 4.8.2.5.1 Number of benchmarks available for calculation-to-experiment comparison

For this exercise, 275 critical experiments from the ICSBEP Handbook with SCALE 6.0 238-group ENDF/B-VII.0 data were available for use. The calculations were performed with  $k_{\text{eff}}$  converged to approximately 0.0005  $\Delta k/k$ . The selected benchmarks experiments, shown in Table 4, provide a representative sampling of many fuel and moderator conditions from the ICSBEP Handbook. Table 4 shows the benchmark  $k_{\text{eff}}$  and benchmark  $k_{\text{eff}}$  uncertainty values obtained from the DICE database using the ORNL tool VIBE, the calculated  $k_{\text{eff}}$  and calculated uncertainty due to cross-section covariance data. The observed computational bias (calculated-benchmark) and the uncertainties due to cross-section data are shown in Figure 11.

**Table 4: Benchmark experiments used by ORNL**

Benchmark experiment	Benchmark $k_{eff}$	Benchmark $k_{eff}$ uncertainty (%)	Calculated $k_{eff}$	Uncertainty due to cross-section data (%)
HEU-MET-FAST-005-001	1.0000	0.3600	0.9958	1.5714
HEU-MET-FAST-005-002	1.0007	0.3597	0.9948	1.7180
HEU-MET-FAST-005-003	0.9996	0.3601	0.9946	1.6917
HEU-MET-FAST-005-004	0.9989	0.3604	0.9883	1.6683
HEU-MET-FAST-005-005	0.9980	0.3607	0.9978	1.5772
HEU-MET-FAST-005-006	0.9987	0.3605	0.9969	1.5609
HEU-MET-FAST-008-001	0.9989	0.1602	0.9955	1.0660
HEU-MET-FAST-009-001	0.9992	0.1501	0.9936	1.2178
HEU-MET-FAST-009-002	0.9992	0.1501	0.9944	1.2269
HEU-MET-FAST-010-001	0.9992	0.1501	0.9962	1.2007
HEU-MET-FAST-010-002	0.9992	0.1501	0.9966	1.1965
HEU-MET-FAST-011-001	0.9989	0.1502	0.9946	1.0463
HEU-MET-FAST-013-001	0.9990	0.1502	0.9962	1.1075
HEU-MET-FAST-016-001	0.9996	0.1801	0.9987	1.3516
HEU-MET-FAST-016-002	0.9996	0.1801	0.9999	1.3729
HEU-MET-FAST-017-001	0.9993	0.1401	0.9963	1.6004
HEU-MET-FAST-018-001	1.0000	0.1400	1.0003	1.0931
HEU-MET-FAST-019-001	1.0000	0.3000	1.0070	1.1533
HEU-MET-FAST-020-001	1.0000	0.3000	1.0008	1.1723
HEU-MET-FAST-021-001	1.0000	0.2400	1.0057	1.1421
HEU-MET-FAST-024-001	0.9990	0.1502	0.9969	1.0795
HEU-MET-FAST-030-001	1.0000	0.0900	1.0015	2.3024
HEU-MET-FAST-038-001	0.9999	0.0700	1.0034	2.2821
HEU-MET-FAST-038-002	0.9999	0.0900	1.0034	2.3036
HEU-SOL-THERM-001-001	1.0004	0.5998	0.9984	0.9394
HEU-SOL-THERM-001-002	1.0021	0.7185	0.9965	0.9549
HEU-SOL-THERM-001-003	1.0003	0.3499	1.0014	0.9389
HEU-SOL-THERM-001-004	1.0008	0.5296	0.9987	0.9571
HEU-SOL-THERM-001-005	1.0001	0.4900	0.9974	0.8325
HEU-SOL-THERM-001-006	1.0002	0.4599	1.0011	0.8449
HEU-SOL-THERM-001-007	1.0008	0.3997	0.9967	0.9364
HEU-SOL-THERM-001-008	0.9998	0.3801	0.9976	0.9383

Benchmark experiment	Benchmark $k_{eff}$	Benchmark $k_{eff}$ uncertainty (%)	Calculated $k_{eff}$	Uncertainty due to cross-section data (%)
HEU-SOL-THERM-001-009	1.0008	0.5396	0.9947	0.9534
HEU-SOL-THERM-001-010	0.9993	0.5404	0.9924	0.8324
HEU-SOL-THERM-013-001	1.0012	0.2597	0.9990	0.5793
HEU-SOL-THERM-013-002	1.0007	0.3597	0.9984	0.5692
HEU-SOL-THERM-013-003	1.0009	0.3597	0.9946	0.5625
HEU-SOL-THERM-013-004	1.0003	0.3599	0.9959	0.5586
HEU-SOL-THERM-014-001	1.0000	0.2800	0.9949	0.8120
HEU-SOL-THERM-014-002	1.0000	0.5200	1.0102	0.7241
HEU-SOL-THERM-014-003	1.0000	0.8700	1.0186	0.6435
HEU-SOL-THERM-016-001	1.0000	0.3600	0.9903	0.8681
HEU-SOL-THERM-016-002	1.0000	0.6900	1.0049	0.7614
HEU-SOL-THERM-016-003	1.0000	0.7900	1.0253	0.6720
HEU-SOL-THERM-028-001	1.0000	0.2300	0.9965	0.7674
HEU-SOL-THERM-028-002	1.0000	0.3400	0.9969	0.6735
HEU-SOL-THERM-028-003	1.0000	0.2600	0.9984	0.7869
HEU-SOL-THERM-028-004	1.0000	0.2800	0.9988	0.6940
HEU-SOL-THERM-028-005	1.0000	0.3100	0.9930	0.7839
HEU-SOL-THERM-028-006	1.0000	0.2300	0.9975	0.7095
HEU-SOL-THERM-028-007	1.0000	0.3800	0.9970	0.7749
HEU-SOL-THERM-028-008	1.0000	0.2700	0.9965	0.7344
HEU-SOL-THERM-028-009	1.0000	0.4900	0.9961	0.8299
HEU-SOL-THERM-028-010	1.0000	0.5300	0.9954	0.7051
HEU-SOL-THERM-028-011	1.0000	0.5100	0.9975	0.8370
HEU-SOL-THERM-028-012	1.0000	0.4600	0.9945	0.7380
HEU-SOL-THERM-028-013	1.0000	0.5800	0.9964	0.8355
HEU-SOL-THERM-028-014	1.0000	0.4600	0.9978	0.7745
HEU-SOL-THERM-028-015	1.0000	0.6400	1.0047	0.8325
HEU-SOL-THERM-028-016	1.0000	0.5200	1.0012	0.7895
HEU-SOL-THERM-028-017	1.0000	0.6600	0.9967	0.8217
HEU-SOL-THERM-028-018	1.0000	0.6000	0.9973	0.7938
HEU-SOL-THERM-029-001	1.0000	0.6600	0.9994	0.8733
HEU-SOL-THERM-029-002	1.0000	0.5800	1.0023	0.7871
HEU-SOL-THERM-029-003	1.0000	0.6800	0.9956	0.7777
HEU-SOL-THERM-029-004	1.0000	0.7400	0.9933	0.6932

Benchmark experiment	Benchmark $k_{eff}$	Benchmark $k_{eff}$ uncertainty (%)	Calculated $k_{eff}$	Uncertainty due to cross-section data (%)
HEU-SOL-THERM-029-005	1.0000	0.6700	0.9988	0.6980
HEU-SOL-THERM-029-006	1.0000	0.6500	0.9989	0.7440
HEU-SOL-THERM-029-007	1.0000	0.6300	1.0002	0.7927
HEU-SOL-THERM-030-001	1.0000	0.3900	0.9960	0.8221
HEU-SOL-THERM-030-002	1.0000	0.3200	0.9980	0.7332
HEU-SOL-THERM-030-003	1.0000	0.3100	0.9959	0.6977
HEU-SOL-THERM-030-004	1.0000	0.6400	0.9993	0.8724
HEU-SOL-THERM-030-005	1.0000	0.5800	0.9964	0.8146
HEU-SOL-THERM-030-006	1.0000	0.5900	0.9994	0.7903
HEU-SOL-THERM-030-007	1.0000	0.6400	0.9985	0.7240
IEU-MET-FAST-002-001	1.0000	0.3000	1.0045	1.8279
IEU-MET-FAST-003-001	1.0000	0.1900	1.0043	1.2570
IEU-MET-FAST-004-001	1.0000	0.3200	1.0091	1.2983
IEU-MET-FAST-005-001	1.0000	0.2300	1.0127	1.3169
IEU-MET-FAST-009-001	1.0000	0.5300	1.0079	1.1415
IEU-MET-FAST-010-001	0.9954	0.2411	1.0035	2.5931
IEU-MET-FAST-012-001	1.0007	0.2698	1.0130	1.9561
LEU-COMP-THERM-001-001	0.9998	0.3101	0.9981	0.5972
LEU-COMP-THERM-001-002	0.9998	0.3101	0.9977	0.5813
LEU-COMP-THERM-001-003	0.9998	0.3101	0.9986	0.5713
LEU-COMP-THERM-001-004	0.9998	0.3101	0.9978	0.5802
LEU-COMP-THERM-001-005	0.9998	0.3101	0.9945	0.5652
LEU-COMP-THERM-001-006	0.9998	0.3101	0.9972	0.5749
LEU-COMP-THERM-001-007	0.9998	0.3101	0.9967	0.5635
LEU-COMP-THERM-001-008	0.9998	0.3101	0.9966	0.5676
LEU-COMP-THERM-002-001	0.9997	0.2001	0.9976	0.6439
LEU-COMP-THERM-002-002	0.9997	0.2001	0.9981	0.6413
LEU-COMP-THERM-002-003	0.9997	0.2001	0.9984	0.6337
LEU-COMP-THERM-002-004	0.9997	0.2001	0.9980	0.6040
LEU-COMP-THERM-002-005	0.9997	0.2001	0.9963	0.5926
LEU-COMP-THERM-017-003	1.0000	0.3100	0.9983	0.5521
LEU-COMP-THERM-017-004	1.0000	0.3100	0.9975	0.5221
LEU-COMP-THERM-017-005	1.0000	0.3100	0.9994	0.5312
LEU-COMP-THERM-017-006	1.0000	0.3100	0.9990	0.5358

Benchmark experiment	Benchmark $k_{eff}$	Benchmark $k_{eff}$ uncertainty (%)	Calculated $k_{eff}$	Uncertainty due to cross-section data (%)
LEU-COMP-THERM-017-007	1.0000	0.3100	0.9980	0.5366
LEU-COMP-THERM-017-008	1.0000	0.3100	0.9970	0.5423
LEU-COMP-THERM-017-009	1.0000	0.3100	0.9961	0.5557
LEU-COMP-THERM-017-010	1.0000	0.3100	0.9968	0.5368
LEU-COMP-THERM-017-011	1.0000	0.3100	0.9971	0.5371
LEU-COMP-THERM-017-012	1.0000	0.3100	0.9966	0.5421
LEU-COMP-THERM-017-013	1.0000	0.3100	0.9976	0.5445
LEU-COMP-THERM-017-014	1.0000	0.3100	0.9979	0.5461
LEU-COMP-THERM-017-015	1.0000	0.2800	0.9960	0.5521
LEU-COMP-THERM-017-016	1.0000	0.2800	0.9977	0.5530
LEU-COMP-THERM-017-017	1.0000	0.2800	0.9983	0.5538
LEU-COMP-THERM-017-019	1.0000	0.2800	0.9976	0.5566
LEU-COMP-THERM-017-020	1.0000	0.2800	0.9973	0.5580
LEU-COMP-THERM-017-021	1.0000	0.2800	0.9966	0.5622
LEU-COMP-THERM-017-022	1.0000	0.2800	0.9948	0.5703
LEU-COMP-THERM-017-023	1.0000	0.2800	0.9980	0.5615
LEU-COMP-THERM-017-024	1.0000	0.2800	0.9981	0.5671
LEU-COMP-THERM-017-025	1.0000	0.2800	0.9962	0.5584
LEU-COMP-THERM-017-028	1.0000	0.2800	0.9974	0.5412
LEU-COMP-THERM-017-029	1.0000	0.2800	0.9980	0.5439
LEU-COMP-THERM-026-003	1.0018	0.6189	1.0091	0.6067
LEU-COMP-THERM-040-010	1.0000	0.4600	0.9932	0.5419
LEU-COMP-THERM-042-001	1.0000	0.1600	0.9961	0.5492
LEU-COMP-THERM-042-002	1.0000	0.1600	0.9950	0.5386
LEU-COMP-THERM-042-003	1.0000	0.1600	0.9971	0.5322
LEU-COMP-THERM-042-004	1.0000	0.1700	0.9973	0.5344
LEU-COMP-THERM-042-005	1.0000	0.3300	0.9976	0.5325
LEU-COMP-THERM-042-006	1.0000	0.1600	0.9979	0.5475
LEU-COMP-THERM-042-007	1.0000	0.1800	0.9963	0.5395
LEU-SOL-THERM-002-001	1.0038	0.3985	1.0004	0.5356
LEU-SOL-THERM-002-002	1.0024	0.3691	0.9962	0.5609
LEU-SOL-THERM-002-003	1.0024	0.4389	1.0015	0.5507
LEU-SOL-THERM-003-001	0.9997	0.3901	0.9962	0.6182
LEU-SOL-THERM-003-002	0.9993	0.4203	0.9934	0.5950

Benchmark experiment	Benchmark $k_{eff}$	Benchmark $k_{eff}$ uncertainty (%)	Calculated $k_{eff}$	Uncertainty due to cross-section data (%)
LEU-SOL-THERM-003-003	0.9995	0.4202	0.9991	0.5877
LEU-SOL-THERM-003-004	0.9995	0.4202	0.9931	0.5843
LEU-SOL-THERM-003-005	0.9997	0.4801	0.9975	0.5311
LEU-SOL-THERM-003-006	0.9999	0.4900	0.9979	0.5237
LEU-SOL-THERM-003-007	0.9994	0.4903	0.9960	0.5175
LEU-SOL-THERM-003-008	0.9993	0.5204	1.0002	0.4924
LEU-SOL-THERM-003-009	0.9996	0.5202	0.9974	0.4912
LEU-SOL-THERM-004-001	0.9994	0.0800	1.0002	0.6028
LEU-SOL-THERM-004-002	0.9999	0.0900	1.0018	0.5903
LEU-SOL-THERM-004-003	0.9999	0.0900	0.9991	0.5771
LEU-SOL-THERM-004-004	0.9999	0.1000	1.0014	0.5637
LEU-SOL-THERM-004-005	0.9999	0.1000	1.0024	0.5540
LEU-SOL-THERM-004-006	0.9994	0.1101	1.0012	0.5459
LEU-SOL-THERM-004-007	0.9996	0.1100	1.0015	0.5384
MIX-COMP-FAST-001-001	0.9866	0.2331	0.9992	1.2713
MIX-COMP-MIXED-001-001	0.9999	0.5601	0.9922	0.9653
MIX-COMP-MIXED-001-002	0.9996	0.5302	0.9909	0.9666
MIX-COMP-MIXED-001-003	1.0011	0.3896	1.0029	0.9598
MIX-COMP-MIXED-001-004	1.0004	0.3599	1.0019	0.9584
MIX-COMP-MIXED-001-005	1.0005	0.4298	1.0058	0.9590
MIX-COMP-MIXED-001-006	0.9970	0.4213	1.0027	0.9575
MIX-COMP-MIXED-001-007	0.9990	0.3804	1.0008	0.9557
MIX-COMP-MIXED-001-008	0.9985	0.4407	1.0015	0.9567
MIX-COMP-MIXED-001-009	1.0001	0.4600	1.0011	0.9548
MIX-COMP-MIXED-001-010	0.9988	0.4505	1.0043	0.9553
MIX-COMP-MIXED-001-011	0.9998	0.4001	1.0055	0.9551
MIX-COMP-MIXED-001-012	0.9995	0.3702	1.0072	0.9559
MIX-COMP-MIXED-001-013	1.0007	0.3997	1.0056	0.9546
MIX-COMP-MIXED-001-014	0.9989	0.3904	1.0057	0.9566
MIX-COMP-MIXED-001-015	1.0004	0.4098	1.0059	0.9542
MIX-COMP-MIXED-001-016	1.0009	0.4096	1.0059	0.9539
MIX-COMP-MIXED-001-017	1.0001	0.4100	1.0065	0.9616
MIX-COMP-MIXED-001-018	1.0010	0.4096	1.0049	0.9593
MIX-COMP-MIXED-001-019	1.0007	0.3797	1.0041	0.9576

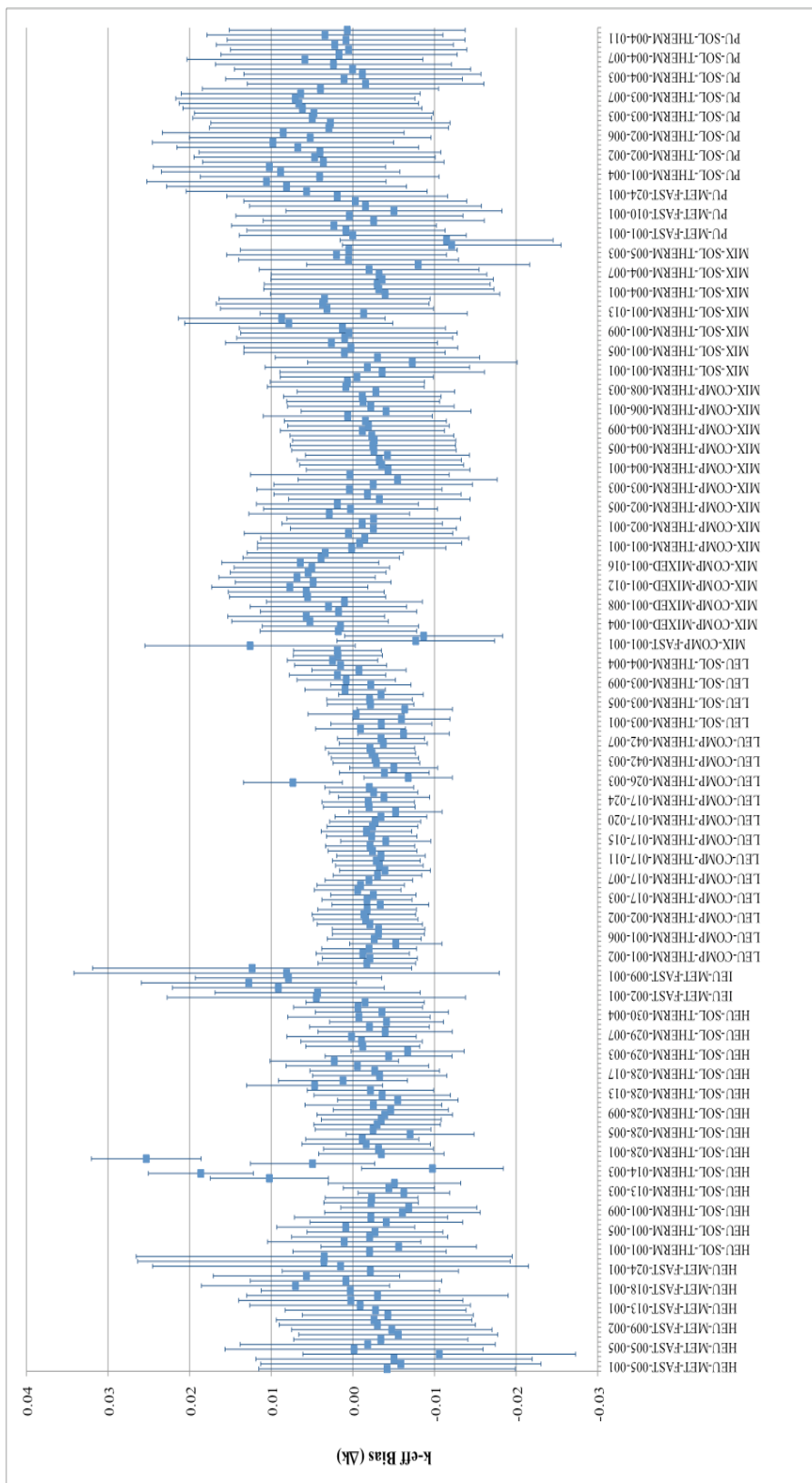
Benchmark experiment	Benchmark $k_{eff}$	Benchmark $k_{eff}$ uncertainty (%)	Calculated $k_{eff}$	Uncertainty due to cross-section data (%)
MIX-COMP-THERM-001-001	1.0000	0.2500	1.0002	1.1541
MIX-COMP-THERM-001-002	1.0000	0.2600	0.9992	1.2509
MIX-COMP-THERM-001-003	1.0000	0.3200	0.9985	1.2745
MIX-COMP-THERM-001-004	1.0000	0.3900	1.0005	1.2772
MIX-COMP-THERM-002-001	1.0024	0.5986	0.9999	1.0191
MIX-COMP-THERM-002-002	1.0009	0.4696	0.9998	0.9836
MIX-COMP-THERM-002-003	1.0042	0.3087	1.0017	1.0684
MIX-COMP-THERM-002-004	1.0024	0.2394	1.0053	0.9873
MIX-COMP-THERM-002-005	1.0038	0.2491	1.0041	1.0698
MIX-COMP-THERM-002-006	1.0029	0.2692	1.0048	0.9948
MIX-COMP-THERM-003-001	1.0028	0.7180	0.9996	1.1152
MIX-COMP-THERM-003-002	1.0019	0.5889	1.0001	1.1487
MIX-COMP-THERM-003-003	1.0000	0.5400	1.0004	1.1332
MIX-COMP-THERM-003-004	1.0027	0.3092	1.0002	1.2200
MIX-COMP-THERM-003-005	1.0049	0.2687	0.9994	1.2258
MIX-COMP-THERM-003-006	1.0000	0.2300	1.0004	1.2171
MIX-COMP-THERM-004-001	1.0000	0.4600	0.9957	1.0022
MIX-COMP-THERM-004-002	1.0000	0.4600	0.9965	1.0043
MIX-COMP-THERM-004-003	1.0000	0.4600	0.9968	1.0068
MIX-COMP-THERM-004-004	1.0000	0.3900	0.9958	1.0049
MIX-COMP-THERM-004-005	1.0000	0.3900	0.9974	1.0075
MIX-COMP-THERM-004-006	1.0000	0.3900	0.9975	1.0121
MIX-COMP-THERM-004-007	1.0000	0.4000	0.9974	1.0003
MIX-COMP-THERM-004-008	1.0000	0.4000	0.9977	1.0034
MIX-COMP-THERM-004-009	1.0000	0.4000	0.9988	1.0055
MIX-COMP-THERM-004-010	1.0000	0.5100	0.9981	0.9892
MIX-COMP-THERM-004-011	1.0000	0.5100	0.9985	0.9924
MIX-COMP-THERM-005-001	1.0008	0.2198	1.0014	1.0364
MIX-COMP-THERM-006-001	1.0016	0.5092	0.9975	1.0422
MIX-COMP-THERM-007-002	1.0024	0.3891	1.0002	1.0231
MIX-COMP-THERM-008-001	0.9997	0.3201	0.9984	0.9364
MIX-COMP-THERM-008-002	1.0008	0.2998	0.9996	0.9650
MIX-COMP-THERM-008-003	1.0023	0.3791	0.9995	0.9674
MIX-COMP-THERM-008-004	1.0015	0.4693	1.0024	0.9617

Benchmark experiment	Benchmark $k_{eff}$	Benchmark $k_{eff}$ uncertainty (%)	Calculated $k_{eff}$	Uncertainty due to cross-section data (%)
MIX-COMP-THERM-008-005	1.0022	0.5588	1.0029	0.9465
MIX-COMP-THERM-008-006	1.0028	0.6482	1.0023	0.9405
MIX-SOL-THERM-001-001	1.0000	0.1600	0.9964	1.2529
MIX-SOL-THERM-001-002	1.0000	0.1600	0.9982	1.2530
MIX-SOL-THERM-001-003	1.0000	0.1600	0.9927	1.2831
MIX-SOL-THERM-001-004	1.0000	0.1600	0.9970	1.2523
MIX-SOL-THERM-001-005	1.0000	0.1600	1.0010	1.2331
MIX-SOL-THERM-001-006	1.0000	0.1600	1.0002	1.3101
MIX-SOL-THERM-001-007	1.0000	0.1600	1.0026	1.2986
MIX-SOL-THERM-001-008	1.0000	0.1600	1.0010	1.3228
MIX-SOL-THERM-001-009	1.0000	0.1600	1.0005	1.3257
MIX-SOL-THERM-001-010	1.0000	0.1600	1.0013	1.2635
MIX-SOL-THERM-001-011	1.0000	0.5200	1.0079	1.2747
MIX-SOL-THERM-001-012	1.0000	0.5200	1.0087	1.2665
MIX-SOL-THERM-001-013	1.0000	0.1600	0.9987	1.2691
MIX-SOL-THERM-002-001	1.0000	0.2400	1.0032	1.3054
MIX-SOL-THERM-002-002	1.0000	0.2400	1.0037	1.3041
MIX-SOL-THERM-002-003	1.0000	0.2400	1.0035	1.2938
MIX-SOL-THERM-004-001	1.0000	0.3300	0.9960	1.4047
MIX-SOL-THERM-004-002	1.0000	0.3300	0.9968	1.4091
MIX-SOL-THERM-004-005	1.0000	0.2900	0.9970	1.3842
MIX-SOL-THERM-004-006	1.0000	0.2900	0.9964	1.3626
MIX-SOL-THERM-004-007	1.0000	0.2600	0.9968	1.3212
MIX-SOL-THERM-004-008	1.0000	0.2600	0.9980	1.3469
MIX-SOL-THERM-005-001	1.0000	0.3700	0.9920	1.3671
MIX-SOL-THERM-005-002	1.0000	0.3700	1.0005	1.3470
MIX-SOL-THERM-005-003	1.0000	0.3700	1.0020	1.3470
MIX-SOL-THERM-005-004	1.0000	0.3700	1.0005	1.3287
MIX-SOL-THERM-005-005	1.0000	0.3700	0.9879	1.3392
MIX-SOL-THERM-005-006	1.0000	0.3700	0.9885	1.3048
PU-MET-FAST-001-001	1.0000	0.2000	1.0000	1.3900
PU-MET-FAST-002-001	1.0000	0.2000	1.0008	1.2139
PU-MET-FAST-006-001	1.0000	0.3000	1.0023	1.2548
PU-MET-FAST-008-001	1.0000	0.0600	0.9974	1.3551

Benchmark experiment	Benchmark $k_{eff}$	Benchmark $k_{eff}$ uncertainty (%)	Calculated $k_{eff}$	Uncertainty due to cross-section data (%)
PU-MET-FAST-010-001	1.0000	0.1800	1.0004	1.3912
PU-MET-FAST-018-001	1.0000	0.3000	0.9950	1.3235
PU-MET-FAST-022-001	1.0000	0.2100	0.9985	1.4202
PU-MET-FAST-023-001	1.0000	0.2000	0.9997	1.3662
PU-MET-FAST-024-001	1.0000	0.2000	1.0019	1.3522
PU-SOL-THERM-001-001	1.0000	0.5000	1.0057	1.4764
PU-SOL-THERM-001-002	1.0000	0.5000	1.0081	1.4691
PU-SOL-THERM-001-003	1.0000	0.5000	1.0106	1.4651
PU-SOL-THERM-001-004	1.0000	0.5000	1.0041	1.4616
PU-SOL-THERM-001-005	1.0000	0.5000	1.0088	1.4607
PU-SOL-THERM-001-006	1.0000	0.5000	1.0102	1.4236
PU-SOL-THERM-002-001	1.0000	0.4700	1.0036	1.4791
PU-SOL-THERM-002-002	1.0000	0.4700	1.0047	1.4773
PU-SOL-THERM-002-003	1.0000	0.4700	1.0040	1.4809
PU-SOL-THERM-002-004	1.0000	0.4700	1.0067	1.4803
PU-SOL-THERM-002-005	1.0000	0.4700	1.0098	1.4783
PU-SOL-THERM-002-006	1.0000	0.4700	1.0052	1.4795
PU-SOL-THERM-002-007	1.0000	0.4700	1.0085	1.4804
PU-SOL-THERM-003-001	1.0000	0.4700	1.0029	1.4644
PU-SOL-THERM-003-002	1.0000	0.4700	1.0027	1.4659
PU-SOL-THERM-003-003	1.0000	0.4700	1.0050	1.4634
PU-SOL-THERM-003-004	1.0000	0.4700	1.0048	1.4628
PU-SOL-THERM-003-005	1.0000	0.4700	1.0062	1.4633
PU-SOL-THERM-003-006	1.0000	0.4700	1.0066	1.4661
PU-SOL-THERM-003-007	1.0000	0.4700	1.0070	1.4644
PU-SOL-THERM-003-008	1.0000	0.4700	1.0064	1.4632
PU-SOL-THERM-004-001	1.0000	0.4700	1.0040	1.4480
PU-SOL-THERM-004-002	1.0000	0.4700	0.9984	1.4495
PU-SOL-THERM-004-003	1.0000	0.4700	1.0011	1.4508
PU-SOL-THERM-004-004	1.0000	0.4700	0.9988	1.4522
PU-SOL-THERM-004-005	1.0000	0.4700	1.0000	1.4473
PU-SOL-THERM-004-006	1.0000	0.4700	1.0024	1.4459
PU-SOL-THERM-004-007	1.0000	0.4700	1.0059	1.4450
PU-SOL-THERM-004-008	1.0000	0.4700	1.0017	1.4467

<b>Benchmark experiment</b>	<b>Benchmark <math>k_{eff}</math></b>	<b>Benchmark <math>k_{eff}</math> uncertainty (%)</b>	<b>Calculated <math>k_{eff}</math></b>	<b>Uncertainty due to cross-section data (%)</b>
PU-SOL-THERM-004-009	1.0000	0.4700	1.0005	1.4481
PU-SOL-THERM-004-010	1.0000	0.4700	1.0022	1.4527
PU-SOL-THERM-004-011	1.0000	0.4700	1.0008	1.4571
PU-SOL-THERM-004-012	1.0000	0.4700	1.0034	1.4457
PU-SOL-THERM-004-013	1.0000	0.4700	1.0007	1.4455

Figure 11: Observed  $k_{\text{eff}}$  biases and uncertainties due to cross-sections for 275 benchmark experiments



#### 4.8.2.5.2 Uncertainties treatment for experimental data

The experimental uncertainties were extracted from the DICE database of ICSBEP Handbook using the ORNL VIBE tool. The TSURFER GLLS techniques require an evaluation of correlations in experimental uncertainties. As correlations in the experimental uncertainties are not available for most experiments in the ICSBEP Handbook, an approximation was used where experiments from the same evaluation were treated as 70% correlated, and uncertainties for benchmarks from different evaluations were treated as uncorrelated. Careful quantification of the experimental correlations is important for safety calculations. However, for this example of the methodology, the approximate experimental correlations will be adequate.

#### 4.8.2.5.3 Other data used in validation method (nuclear data covariance, sensitivity coefficients, etc.)

##### 4.8.2.5.3.1 Sensitivity coefficients

Sensitivity coefficients were computed for each system considered in this study using the TSUNAMI tools of SCALE 6.0 with ENDF/B-VII.0 cross-section data in the 238-energy-group structure for the sensitivity of  $k_{\text{eff}}$  to the reactions listed in Table 5, if appropriate cross-section data are available. The Evaluated Nuclear Data File (ENDF) MT identifier for each of these sensitivity types is also given [41]. The MT of zero assigned to scattering is arbitrary, as a sum of scattering reaction does not exist in the ENDF specification.

**Table 5: Sensitivity types computed by TSUNAMI-1D and -3D**

MT	Reaction	TSUNAMI identifier
0	Sum of scattering	scatter
1	Total	total
2	Elastic scattering	elastic
4	Inelastic scattering	n,n'
16	n, 2n	n, 2n
18	Fission	fission
101	Neutron disappearance	capture
102	n, $\gamma$	n,gamma
103	n,p	n,p
104	n,d	n,d
105	n,t	n,t
106	n, $^3\text{He}$	n,he-3
107	n, $\alpha$	n,alpha
452	$\bar{\nu}$	nubar
1018	$\chi$	chi

##### 4.8.2.5.3.2 Cross-section-covariance data

The SCALE 6.0 cross-section covariance library is a single comprehensive library with a total of 401 materials in the SCALE 44-energy-group structure. The SCALE covariance

library data correspond to 44-group relative uncertainties assembled from a variety of sources, including evaluations from ENDF/B-VII, ENDF/B-VI, JENDL-3.1, and more than 300 approximated uncertainties from a collaborative project performed by Brookhaven National Laboratory (BNL), Los Alamos National Laboratory (LANL), and Oak Ridge National Laboratory (ORNL).

Because SCALE includes separate multi-group cross-section libraries processed from ENDF/B-V, ENDF/B-VI.8, and ENDF/B-VII.0, the application of a single “generic” covariance library to all multi-group cross-section libraries obviously raises questions about consistency with any given data evaluation. In reality, many of the approximate uncertainty data in the library are based on simplifying approximations that do not depend on specific ENDF evaluations, and thus can be applied to all cross-section libraries within the limitations of the assumed methodology. In other cases where a covariance evaluation has been taken from a specific nuclear data file (e.g. ENDF/B-VII, ENDF/B-VI, or JENDL-3.3), it is assumed that the same relative (rather than absolute) uncertainties can be applied to all cross-section libraries, even if these are not strictly consistent with the nuclear data evaluations. This may be questionable for some older evaluations in the ENDF/B-V data, but it should be reasonable for the SCALE ENDF/B-VI and VII cross-section libraries. The assumption is partially justified by the fact that different evaluations often use many of the same experimental measurements, since there is a limited amount of this information available. Also, because most important nuclear data are now known rather well, newer evaluations in many instances correspond to rather modest variations from previous ones, and are expected to lie within the earlier uncertainties. The nuclear data evaluations from ENDF/B-VII, ENDF/B-VI, JEF-3.1, and JENDL-3.3 tend to agree well for many nuclides. Similar results are found for many types of cross-sections; thus, it seems reasonable to assume that the uncertainties in these data are similar.

It should be noted that there is no inherently “true” uncertainty that can be defined unambiguously for nuclear data. For example, in theory, two independent evaluations could produce similar nuclear data with much different uncertainties. While differences in nuclear data evaluations have direct impact on calculations that can be affirmed by comparisons with benchmark experiments, there is no such procedure that can be used to quantify the reliability of uncertainty estimates. In general, the SCALE covariance library should be viewed as a best-estimate assessment of data uncertainties based upon the specific methodology described in the following section. This methodology is certainly not unique, and it can be argued that other approaches could have been used. Nevertheless, it can be concluded that the SCALE covariance library is a reasonable representation of the nuclear data uncertainties, given the current lack of information, and it is the only available comprehensive library that has been created in a well-defined, systematic manner.

- Evaluated covariances from nuclear data files

A rigorous, modern evaluation of nuclear data typically utilises a regression algorithm that adjusts parameters in a nuclear physics model (e.g. Reich-Moore resonance formula, optical model, etc.) to fit a set of differential experimental measurements that have various sources of statistical and systematic uncertainties [42]. Information from the regression analysis of the model parameters can be propagated to uncertainties and correlations in the evaluated differential data. In this manner, the differential nuclear data and covariances are consistent and coupled together by an evaluation process. Unfortunately, only a relatively few cross-section evaluations have produced “high-fidelity” covariances in this rigorous manner. All other nuclear data uncertainties must be estimated from approximations in which the uncertainty assessment is decoupled from the original evaluation procedure.

- Approximate covariance data

At the other end of the spectrum from high-fidelity data, “low-fidelity” (lo-fi) covariances are defined to be those that are estimated independently of a specific data evaluation. The approximate covariance data in SCALE are based on results from a collaborative project funded by the Department of Energy Nuclear Criticality Safety Programme to generate lo-fi covariances over the energy range from  $10^{-5}$  eV to 20 MeV for materials without covariances in ENDF/B-VII.0. Nuclear data experts at BNL, LANL, and ORNL devised simple procedures to estimate data uncertainties in the absence of high-fidelity covariance evaluations. The result of this project is a set of covariance data in ENDF/B file 33 format that can be processed into multi-group covariances [43]. In this documentation, these data are called the “BLO” [BNL-LANL-ORNL] uncertainty data, which were generated as described below.

ORNL used uncertainties in integral experiment measurements of thermal cross-sections, resonance integrals, and potential cross-sections to approximate the standard deviations of capture, fission, and elastic scattering reactions for the thermal (<0.5 eV) and resonance ranges (0.5 eV–5 keV). Full energy correlation was assumed for the covariances within each of these respective ranges [44] [45]. The integral measurement uncertainty values were tabulated by Mughabghab in the *Atlas of Neutron Resonances: Resonance Parameters and Thermal Cross-Sections* [46]. The lo-fi relative uncertainty is computed as the absolute uncertainty in the integral parameter (i.e. thermal cross-section or resonance integral) taken from the Atlas, divided by the average of the measured parameter and the calculated value computed from ENDF/B-VII differential data:

$$U = \frac{\Delta_I}{0.5 \times (X_I + X_D)} , \quad (90)$$

Where:

$U$  is the relative lo-fi uncertainty included in SCALE;

$\Delta_I$  is the absolute uncertainty in the integral measurement, obtained from Mughabghab;

$X_I$ ,  $X_D$  are the measured and computed (from ENDF/B differential data) integral parameter values, respectively.

In some cases the integral measurement value from the Mughabghab Atlas [46] and the corresponding value computed from the ENDF/B-VII differential evaluation are inconsistent-defined here as having a difference greater than two standard deviations in the measured and computed integral parameters. In these cases, the lo-fi relative standard deviation is defined as half the difference, relative to the average of the measured and calculated values:

$$U = \frac{|X_I - X_D|}{X_I + X_D} ; \text{ for } |X_I - X_D| > 2\Delta_I \quad (91)$$

In some instances, this expression may exceed 100%. For these cases, a 100% uncertainty was assigned. Also, the Atlas does not include uncertainties in integral measurements for a few isotopes, which typically are not of great interest for most applications. For these nuclides, the least significant digit of the integral uncertainty has been set to five.

BNL and LANL provided estimates in the fast energy range from 5 keV–20 MeV for covariances of capture, fission, elastic, inelastic, ( $n,2n$ ) cross-sections, and prompt  $\bar{\nu}$ . BNL used optical model calculations with estimated uncertainties in model parameters to

compute covariances in the fast range for about 300 structural isotopes, fission products, and non-fissionable heavy nuclei. Estimated uncertainties in model parameters were based on previous work and expert judgement [47]. Covariances for 14 actinide isotopes were obtained from earlier work done by BNL for Subgroup-26 (SG-26) [48]. The SG-26 actinide covariances cover the full energy range, including thermal, resonance, and fast regions. Thermal data uncertainties tend to be overestimated by the SG-26 approach, which is based on propagating resonance parameter uncertainties, therefore, the thermal data covariances are represented by ORNL's integral uncertainty technique.

LANL produced covariances in the fast range for an additional 47 actinide materials. The LANL actinide covariances were based on empirical estimates of nuclear reaction models [49]. Full energy range covariances were also produced by LANL for 16 light isotopes ranging from hydrogen to fluorine [50]. These included high-fidelity covariances from R-matrix analyses for  $^1\text{H}$ ,  $^6\text{Li}$ , and  $^{10}\text{B}$ , along with lo-fi uncertainties for the other materials, based on approximations such as least-squares fitting to experimental data, statistical model calculations at higher energies, or sometimes simply best-judgement estimation [43].

- Modifications to covariance data

In generating earlier covariance libraries for SCALE 5.1, a number of obvious omissions or inconsistencies were identified and corrected in the ENDF/B-VI covariance evaluations, and these modifications are retained in the current SCALE covariance library. Two modifications were also made to the ENDF/B-VII evaluated  $\bar{\nu}$  covariances. These  $\bar{\nu}$  uncertainties are believed to be more realistic. The ENDF/B-VII.0  $^{235}\text{U}$  thermal  $\bar{\nu}$  uncertainty of 0.71% was revised to the JENDL-3.3 value of 0.31%. In addition, the thermal  $\bar{\nu}$  uncertainty in the pre-released ENDF/B-VII.1  $^{233}\text{U}$  evaluation was modified to the value in a recent ORNL data evaluation [51]. This ORNL  $^{233}\text{U}$  cross-section evaluation also provided the thermal and resonance cross-sections for the pre-released ENDF/B-VII.1 data.

Several modifications were also made to the uncertainties obtained from the BLO data. The energy boundary between the thermal and resonance covariance blocks was modified from 0.5 eV to 0.625 eV in order to coincide with a 44-group boundary. The BLO lo-fi data do not include thermal or resonance range uncertainties for isotope reactions that do not have integral uncertainties given in the Mughabghab text. These occur mainly for relatively unimportant data such as elastic cross-sections of several fission products. In these cases the uncertainties were estimated by different approaches. For example, the thermal data uncertainty was sometimes used to represent the epithermal uncertainty if it was not available in the Mughabghab tabulation, and sometimes the high-energy uncertainty was extended to lower energies. The BLO thermal uncertainties for  $^1\text{H}$  capture and elastic and for  $^{16}\text{O}$  elastic were modified to the JENDL-3.3 values of 0.5% and 0.1%, respectively. Similarly, the uncertainty in the  $^{10}\text{B}$  ( $n, \alpha$ ) thermal cross-section was modified to the ENDF/B-VI value of about 0.2%, since this is more consistent with the Mughabghab integral uncertainty. The uncertainty in the  $^{149}\text{Sm}$  resonance capture integral is not provided in the 2006 edition of Mughabghab's text, therefore, it was set to the value of 5.7%, which was obtained from an earlier tabulation by Mughabghab [52].

- Covariance data for fission spectra

The methodology used to construct multi-group fission spectrum ( $\chi$ ) covariance matrices is described in [53]. In this approach, the fission spectrum is represented as either a Watt or Maxwellian distribution. These energy distributions are widely used to represent fission spectra and have been commonly employed in many ENDF/B evaluations. For example, Watt and Maxwellian expressions were used almost exclusively to describe fission spectra in ENDF/B-V and also for many ENDF/B-VI evaluations. More recent evaluations for some important fissionable nuclides have replaced the simple Watt and Maxwellian analytical expressions by distributions such as

the Madland-Nix spectrum obtained from more phenomenological nuclear fission models. However, it is assumed here that uncertainties based on an appropriate Watt or Maxwellian representation of the fission spectrum can be transferred to the actual fission spectra contained in the different multi-group cross-section libraries.

- Contents of the SCALE 6 covariance library

Covariance data were processed with the ORNL PUFF-IV [54] code to generate the production library distributed with SCALE 6.0. The SCALE covariance library provides uncertainty data in the 44-group uncertainty data for a total of 401 materials, including some duplication for materials with multiple thermal scattering kernels.

The contents of the SCALE 6.0 covariance library are summarised in Table 6. In this table, the following nomenclature is used:

- ENDF/B-VII.0: evaluated covariance data released with ENDF/B-VII.0;
- ENDF/B-VII-p: recently evaluated data proposed for future release of ENDF/B-VII.1;
- ENDF/B-VI: evaluated covariance data released with ENDF/B-VI;
- JENDL-3.3: evaluated covariance data in JENDL-3.3;
- BLO approximate data: lo-fi covariances from BLO project;
- BLO LANL evaluation: LANL R-matrix evaluation from BLO project;
- SG-26: approximate covariances from WPEC Subgroup-26.

**Table 6: Sources of covariance data in the SCALE 6 covariance library**

Data source	Materials
ENDF/B-VII.0	<sup>152,154-158,160</sup> Gd, <sup>191,193</sup> Ir, <sup>7</sup> Li, <sup>99</sup> Tc, <sup>232</sup> Th
ENDF/B-VII-p	<sup>197</sup> Au, <sup>209</sup> Bi, <sup>59</sup> Co, <sup>23</sup> Na, <sup>93</sup> Nb, <sup>58</sup> Ni, <sup>239</sup> Pu, <sup>48</sup> Ti, <sup>233,235,238</sup> U, V
ENDF/B-VI	<sup>27</sup> Al, <sup>241</sup> Am, C, C-graphite, <sup>50,52-54</sup> Cr, <sup>65</sup> Cu, <sup>156</sup> Dy, <sup>54,56-58</sup> Fe, In, <sup>55</sup> Mn, <sup>60-62,64</sup> Ni, <sup>206-208</sup> Pb, <sup>242</sup> Pu, <sup>185,187</sup> Re, <sup>45</sup> Sc, Si, <sup>28-30</sup> Si, <sup>89</sup> Y
JENDL 3.3	<sup>11</sup> B, <sup>240,241</sup> Pu
JENDL 3.3+BLO	<sup>16</sup> O
SG-26	<sup>234,236</sup> U, <sup>242,242m</sup> Am, <sup>242-245</sup> Cm, <sup>237</sup> Np, <sup>238</sup> Pu
BLO LANL evaluation +JENDL 3.3	<sup>10</sup> B, <sup>1</sup> H, H-ZrH, H-poly, Hfreegas
BLO LANL evaluation	<sup>6</sup> Li
BLO Approximate Data	<sup>225-227</sup> Ac, <sup>107,109,110m,111</sup> Ag, <sup>243,244,244m</sup> Am, <sup>36,38,40</sup> Ar, <sup>74-75</sup> As, <sup>130,132,133,135-138,140</sup> Ba, <sup>7,9</sup> Be, <sup>249,250</sup> Bk, <sup>79,81</sup> Br, <sup>Ca</sup> , <sup>40,42-44,46,48</sup> Ca, <sup>Cd</sup> , <sup>106,108,110-114,115m,116</sup> Cd, <sup>136,138,139-144</sup> Ce, <sup>249-254</sup> Cf, <sup>Cl</sup> , <sup>35,37</sup> Cl, <sup>241,246-250</sup> Cm, <sup>58,58m</sup> Co, <sup>133-137</sup> Cs, <sup>63</sup> Cu, <sup>158,160-164</sup> Dy, <sup>162,64,166-168,170</sup> Er, <sup>253-255</sup> Es, <sup>151-157</sup> Eu, <sup>19</sup> F, <sup>255</sup> Fm, <sup>Ga</sup> , <sup>69,71</sup> Ga, <sup>153</sup> Gd, <sup>70,72-74,76</sup> Ge, <sup>2,3</sup> H, <sup>Dfreegas</sup> , <sup>3,4</sup> He, <sup>Hf</sup> , <sup>174,176-180</sup> Hf, <sup>196,198-202,204</sup> Hg, <sup>165</sup> Ho, <sup>127,129-131,135</sup> I, <sup>113,115</sup> In, <sup>K</sup> , <sup>39-41</sup> K, <sup>78,80,82-86</sup> Kr, <sup>138-140</sup> La, <sup>175,176</sup> Lu, <sup>Mg</sup> , <sup>24-26</sup> Mg, <sup>Mo</sup> , <sup>92,97-100</sup> Mo, <sup>14,15</sup> N, <sup>94,95</sup> Nb, <sup>142-148,150</sup> Nd, <sup>59</sup> Ni, <sup>235,236,238,239</sup> Np, <sup>17</sup> O, <sup>31</sup> P, <sup>231-233</sup> Pa, <sup>204</sup> Pb, <sup>102,104-108,110</sup> Pd, <sup>147,148,148m,149,151</sup> Pm, <sup>141-143</sup> Pr, <sup>236,237,243,244,246</sup> Pu, <sup>85-87</sup> Rb, <sup>103,105</sup> Rh, <sup>96,98-106</sup> Ru, <sup>S</sup> , <sup>32-34,36</sup> S, <sup>121,123-126</sup> Sb, <sup>74,76-80,82</sup> Se, <sup>144,147-154</sup> Sm, <sup>112-120,122-125</sup> Sn, <sup>84,86-90</sup> Sr, <sup>181,182</sup> Ta, <sup>159,160</sup> Tb, <sup>120,122-126,127m,128,129m,130</sup> Te, <sup>227-230,233,234</sup> Th, <sup>Ti</sup> , <sup>46,47,49,50</sup> Ti, <sup>232,237,239-241</sup> U, <sup>W</sup> , <sup>182-184,186</sup> W, <sup>123,124,126,128-136</sup> Xe, <sup>90,91</sup> Y, <sup>Zr</sup> , <sup>90-96</sup> Zr

Some important uncertainties, in the form of standard deviations in group-wise cross-section values for  $^{235}\text{U}$  fission,  $^1\text{H}$  elastic scattering,  $^{239}\text{Pu}$  fission,  $^{235}\text{U}$  nubar, and  $^{239}\text{Pu}$  nubar, are shown in Figure 12. Additional uncertainties for reaction with high uncertainties at fast energies,  $^{238}\text{U}$  n, gamma and  $^{238}\text{U}$  inelastic scattering, are shown in Figure 13. Cross-sections with higher uncertainties are more likely to be in error and cause computational biases. Systems that are sensitive to these highly uncertain reactions may have large computational biases.

**Figure 12: Some important uncertainties in the SCALE 6.0 covariance library**

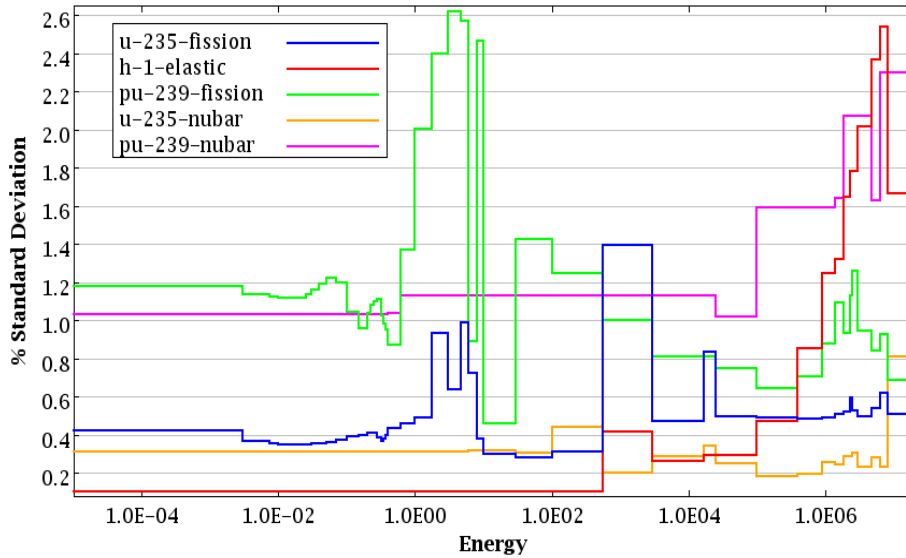
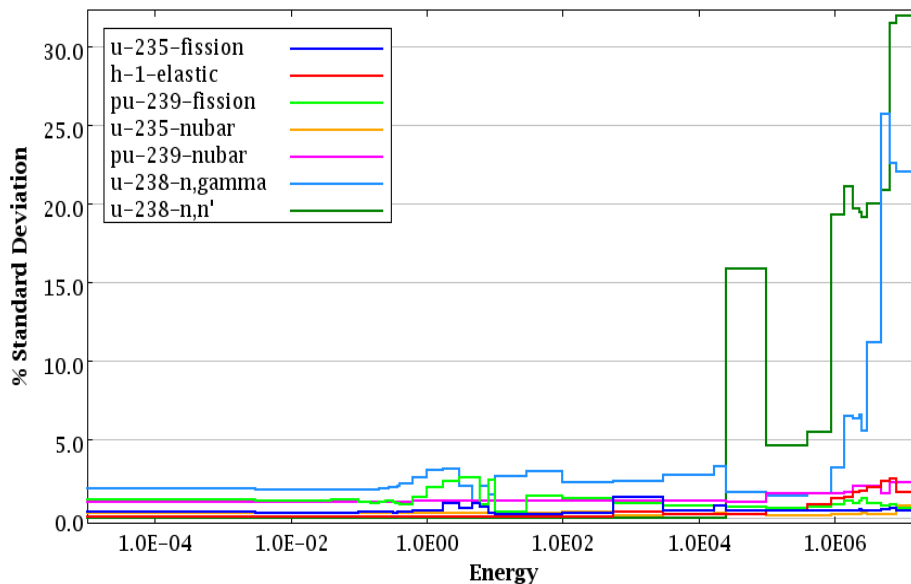


**Figure 13: Additional uncertainties in the SCALE 6.0 covariance library**



#### 4.8.2.6 History of the validation methodology

##### ■ 4.8.2.6.1 Primary purpose

The sensitivity and uncertainty analysis methods of SCALE were developed for the validation of criticality safety calculations using a physics-based approach instead of more traditional heuristic approaches. From its conceptualisation, the TSUNAMI methods were intended to extend the area of applicability of existing benchmark data to systems where limited applicable data are available for validation. TSUNAMI is also intended to identify gaps in validation coverage and serve as a tool to assist in the design of experiments to fill the gaps. Where gaps exist, and it is not feasible to conduct experiments to fill the gaps, the uncertainty data computed by TSUNAMI can be used to provide bounding estimates on computational biases due to invalidated components.

##### ■ 4.8.2.6.2 Experience of use

TSUNAMI was first publicly released with SCALE 5.0 in 2004. There are licensed users of SCALE in 40 nations, and industry, research while regulatory bodies have used TSUNAMI for many purposes including validation of criticality safety calculations, detailed examination of the physics of fissile material systems, and design of critical experiments.

#### 4.8.2.7 Status of the development/validation

The TSUNAMI methods are in a mature development state, having been used in license applications and reviews, in numerous analytical studies, and in experiment design.

#### 4.8.2.8 Published references supporting the validation methodology

Many references are provided in the text describing the TSUNAMI techniques. A few select references related to applications of TSUNAMI are provided in [55] through [69].

#### 4.8.2.9 Additional information/notes

Practitioners who are interested in using the SCALE/TSUNAMI techniques for validation are recommended to attend a SCALE training course for sensitivity and uncertainty analysis techniques. These courses are typically offered twice per year at ORNL and once per year in Europe, hosted by the OECD/NEA Data Bank. Additionally, practitioners are directed to the TSUNAMI primer provided in the reference section above.

The level of effort to apply TSUNAMI for the validation of system is highly dependent on the application under consideration. The first step required is calculation and verification of the sensitivity coefficients for the application system. This can require only a few minutes for simple systems that can be accurately represented using 1D models to several days to accurately model complex systems. The next step is to carry out comparison against existing benchmark experiments. Sensitivity data must be available for each benchmark. As with the application modelling, the time required to generate sensitivity data for each benchmark is highly dependent on the complexity of the experiment. The SCALE team is actively generating sensitivity data for distribution through the ICSBEP Handbook to alleviate this time consuming task.

Once sufficient sensitivity data are available, the validation tools can typically be applied in a matter of hours to determine the bias and bias uncertainty and perform gap analysis. Once sensitivity data were available for the five test systems and 275 benchmarks used in this current exercise, the validation data were generated in approximately two hours.

## 4.9 Paul Scherrer Institute (PSI), Switzerland

Contributors: A.Vasiliev, E.Kolbe, M.A.Zimmermann, H.Ferroukhi

### 4.9.1 Criticality calculations

#### 4.9.1.1 Criticality package (codes system) title and version

Monte Carlo radiation transport code MCNPX (version 2.5.0 at present).

#### 4.9.1.2 Modules utilised for neutron cross-section treatment and neutron transport calculation (methods employed and titles)

Point-wise neutron data libraries and Monte Carlo code MCNPX.

#### 4.9.1.3 Nuclear data source and energy structure

ENDF/B-VII.0 and JEFF-3.1 general-purpose neutron data libraries in ACE format, as distributed by the RSICC and OECD/NEA Data Bank, respectively.

### 4.9.2 Validation of criticality calculations

#### 4.9.2.1 Sources of bias and uncertainties

Assumed sources of uncertainty are: 1) uncertainties in neutron cross-section data, 2) uncertainties in benchmark  $k_{\text{eff}}$  values (due to uncertainties/model simplifications in the benchmark configurations/dimensions, materials, measurement uncertainties, methodical uncertainties introduced in the benchmark evaluation process), 3) methodical uncertainty in  $k_{\text{eff}}$  calculations with MCNPX code (statistical uncertainties).

#### 4.9.2.2. Description of the validation methodology

The validation methodology is based on the calculation of benchmark experiments and a subsequent evaluation of the obtained  $k_{\text{eff}}^{\text{calc}}/k_{\text{eff}}^{\text{bench}}$  values. The source of the criticality benchmarks is the International Handbook of Evaluated Criticality Safety Benchmark Experiments.

#### 4.9.2.3 Approach for selection of benchmark experiments

##### 4.9.2.3.1 Parameters used for similarity assessment

The benchmarks selected for method validation should be representative relative to a test application in terms of the fuel form, typical dimensions and physical properties (neutron spectrum). The benchmarks should also be accurately evaluated. As the field of criticality safety assessment at PSI is currently limited to the analysis of configurations with LWR fuel assemblies, the following parameters are currently considered relevant for the benchmark selection:

- fuel rod arrays arrangement (e.g. square lattices);
- moderator material (e.g. water);
- fuel rods pitch size;
- moderation ratio;
- presence/material of a soluble absorber;
- presence of solid reflectors;
- presence/material of solid absorbers;
- distance between separate arrays of fuel rods, if any;
- benchmark  $k_{\text{eff}}$  uncertainty (should be reasonably small, e.g. less than 500 pcm);

- benchmarks selected should be known as not containing strongly correlated cases;
- only three-dimensional benchmarks are considered.

#### 4.9.2.3.2 Criteria and process used for similarity assessment

Strictly, the initial benchmark selection is based on expert judgement, but based on the comprehensive analysis of the parameters specified in the previous subsection. The approach is assumed to be rigorous and efficient if a significant number of benchmark configurations directly corresponding by the design characteristics to the test application are available. This is the case for criticality safety evaluations of LWR storage pools and transport casks.

At the next stage, spectrum-related parameters of the calculated benchmarks and the test case are compared to ensure the similarity of the physical properties of the systems. The set of parameters includes (following ICSBEP Handbook recommendations):

- the energy corresponding to the average neutron lethargy causing fission (EALF);
- the average neutron energy causing fission (AFGE);
- the neutron gas temperature in the thermal energy range ( $T_n$ );
- the percentage of neutron flux, fissions, and captures that occur in a three-(thermal, intermediate, fast) and thirty-group energy mesh;
- the percentage of fissions (e.g. of  $^{235}\text{U}$ ,  $^{238}\text{U}$ ) and captures by isotopes ( $^{235}\text{U}$ ,  $^{238}\text{U}$ ,  $^{16}\text{O}$ ,  $^1\text{H}$ ,  $^{10}\text{B}$ ,  $^{27}\text{Al}$ ) over the core region;
- the number of average fission neutrons produced per neutron absorbed in the core ( $\nu\Sigma_f/\Sigma_a$ ).

Afterwards a statistical analysis of outliers in the calculated benchmarks set is performed to check for eventual incorrect benchmark evaluations.

Then the benchmarks sample is subdivided into groups with some similar characteristics, like presence/absence of boron absorber plates,  $\text{UO}_2$  or MOX fuel, etc. Calculation results of such benchmark subgroups are evaluated individually in order to test for significant discrepancies in the calculation results for these subgroups (i.e. evidence that the calculation results from different subgroups belong to different hypothetical populations). In the validation performed up to now for criticality safety evaluations of LWR storage pools and transport casks based on the “LEU-COMP-THERM” benchmarks from ICSBEP Handbook, all the benchmark cases were found to belong to a single hypothetical population and thus constitute one general validation sample.

The range of applicability of the performed validation studies is determined on the basis of ranges of the design and calculated spectrum-related benchmarks parameters.

#### 4.9.2.4 Implementation of the validation method used to determine bias and bias uncertainty (if available)

##### 4.9.2.4.1 Software tool title

None.

##### 4.9.2.4.2 Algorithm

The average calculational bias is determined based on the validation sample of the  $k_{\text{eff}}^{\text{calc}}/k_{\text{eff}}^{\text{bench}}$  values as following:

$$Bias = \left\langle \frac{k_{eff}^{calc}}{k_{eff}^{bench}} \right\rangle - 1 \quad (92)$$

$$\text{where } \left\langle \frac{k_{eff}^{calc}}{k_{eff}^{bench}} \right\rangle = \frac{1}{w} \sum_{n=1}^N w_n \left( \frac{k_{eff}^{calc}}{k_{eff}^{bench}} \right)_n ; \quad w = \sum_{n=1}^N w_n ; \quad w_n = \frac{1}{\sigma_n^2}$$

The bias uncertainty may be expressed in terms of the  $k_{eff}^{calc}/k_{eff}^{bench}$  sample estimated standard deviation:

$$s = \sqrt{\frac{\frac{1}{(N-3^*)} \sum_{n=1}^N \frac{1}{\sigma_n^2} \left( \left( \frac{k_{eff}^{calc}}{k_{eff}^{bench}} \right)_n - \left\langle \frac{k_{eff}^{calc}}{k_{eff}^{bench}} \right\rangle \right)^2}{\frac{1}{(N)} \sum_{n=1}^N \frac{1}{\sigma_n^2}}} \quad (93)$$

$$\text{where } \sigma_n = \left( \frac{k_{eff}^{calc}}{k_{eff}^{bench}} \right)_n \sqrt{\left( \frac{\sigma^{bench}}{k_{eff}^{bench}} \right)_n^2 + \left( \frac{\sigma^{MC}}{k_{eff}^{calc}} \right)_n^2} ;$$

\*Instead of (N-1), this gives the best estimate of the standard deviation when a Gaussian distribution is assumed (see ICSBEP Guide to the Expression of Uncertainties from the (ICSBEP Handbook)).

It is assumed that the hypothetical  $k_{eff}^{calc}/k_{eff}^{bench}$  population follows a normal probability distribution; accordingly any further statistical evaluations of the  $k_{eff}^{calc}/k_{eff}^{bench}$  properties, like tolerance bounds to cover certain population proportions with certain confidence levels will be performed under this assumption. Distribution-free estimates (including associated uncertainties) may be provided additionally for comparative purposes.

#### 4.9.2.5 Initial data for the bias and bias uncertainty determination

##### 4.9.2.5.1 Number of benchmarks available for calculation-to-experiment comparison

Following the benchmark selection criteria, 149 benchmark experiments were selected from the *International Handbook of Evaluated Criticality Safety Benchmark Experiments* for validation studies of criticality calculations for LWR compact storage pools and transport casks. The validation set includes cases with UO<sub>2</sub> and MOX fuel, with and without absorbing materials (boron, boroflex, etc.), with different number of fuel rod arrays, etc. No evidence for the subdivision of the total validation set into different groups with different properties has been found.

##### 4.9.2.5.2 Uncertainties treatment for experimental data

In the given approach, the uncertainties of the experimental data are taken from the ICSBEP Handbook benchmark specifications as the  $k_{eff}^{bench}$  uncertainties. It is assumed that these correspond to random uncertainties at the 1 $\sigma$  level, if not specified explicitly in the Handbook. The benchmark uncertainties are accounted for in the method bias and uncertainty evaluations according to Equations (92)-(93). Furthermore, they may be accounted for later at the definition of the upper subcriticality limit (USL) for the final criticality safety evaluations, which is not discussed in the given document.

- 4.9.2.5.3 Other data used in validation method (nuclear data covariance, sensitivity coefficients, etc.)

None.

#### 4.9.2.6 History of the validation methodology

- 4.9.2.6.1 Primary purpose

The purpose of the validation methodology is to provide data to be used for criteria to establish subcriticality and range of applicability for criticality safety evaluations for systems with fissionable materials of interest, which in the given case are configurations of the LWR fuel assemblies, e.g. LWR compact storage pools and transport casks.

- 4.9.2.6.2 Experience of use

The presented above general validation methodology has been applied for criticality safety evaluations for a new external wet storage pool for a Swiss PWR nuclear power plant.

#### 4.9.2.7 Status of the development/validation

The methodology is being continuously developed.

#### 4.9.2.8 Published references supporting the validation methodology

See [70] [71].

#### 4.9.2.9 Additional information/notes

The recommended qualification for practitioners using this methodology is the same as for the criticality safety calculations and evaluations.

In [71] five continuous-energy neutron cross-section libraries based on ENDF/B-VI.8, JEF-2.2, JENDL-3.3, and the recently released ENDF/B-VII.0 and JEFF-3.1 data files were evaluated. It was found that the latest ENDF/B-VII.0 and JEFF-3.1 libraries lead to very small biases and improve the older libraries. Therefore, ENDF/B-VII.0 and JEFF-3.1 were applied in the PSI-methodology described above.

In [70] we found that the estimates of the lower tolerance bound of the  $k_{\text{eff}}^{\text{calc}}/k_{\text{eff}}^{\text{bench}}$  distribution obtained applying either a distribution-free or a Gaussian approach agreed very closely. As discussed earlier, we make use of Gaussian-based estimators for the  $k_{\text{eff}}^{\text{calc}}/k_{\text{eff}}^{\text{bench}}$  population parameters.

Regarding practical applications, a comprehensive explicit  $k_{\text{eff}}^{\text{calc}}$  uncertainty analysis for the system being analysed is not considered, although all foreseen uncertainties are assumed to be reliably covered by the final value of the USL [70], which includes a predefined “administrative margin”. The USL value is defined once for the given methodology and the specific systems of interest (LWR storage pools and transport casks).

The given approach is assumed to be conservative. The ways to reduce an excessive conservatism in the present approach are increasing the number of the benchmark experiments used for the methodology validation, as well as selection of benchmarks with high quality evaluations.

## 5. Conclusions and plans for further studies

The present report provides an overview of current activities performed by the OECD/NEA Expert Group on Uncertainty Analysis for Criticality Safety Assessment. At the current stage, the work of the group is focused on approaches for validation of criticality calculations. An overview of the approaches and software tools is provided by the participants of the expert group.

A summary of the description of the criticality safety validation methods is given in Table 7. It shows the contributors, criticality codes, nuclear data libraries, methods for similarity assessment, those for bias and bias uncertainty determination, and software tools developed for validation. All the participants used three-dimensional (3D) Monte Carlo codes for neutron transport calculation. Explicit geometry description and advanced algorithms used in Monte Carlo codes help minimise errors due to modelling and the computation algorithm. For these codes, nuclear data may be the major contributor to the overall  $k_{\text{eff}}$  uncertainty. Estimation and treatment of these errors is therefore an imperative task for the validation of criticality calculations. The different methods of cross-section processing and choices of multi-group approximations used by the participants can also contribute to the overall  $k_{\text{eff}}$  error. This part of uncertainty can be either estimated by comparing with continuous energy results based on the same nuclear data evaluation or taken into account by using the same cross-sections when calculating  $k_{\text{eff}}$  sensitivities to cross-section data, if the sensitivities are used for bias and bias uncertainty determination.

A key element in criticality safety code validation is the selection of appropriate experimental benchmarks. It is important on the one hand for the similarity assessment of benchmarks and on the other hand to ensure that the  $k_{\text{eff}}$  uncertainties for the benchmarks are well evaluated and that correlations between the benchmarks are established. To assess similarity, most participants used their expert judgement supported by analysis of numerous physical characteristics (for example, those reported in the ICSBEP Handbook), or a sensitivity/uncertainty-based integral similarity index. The  $k_{\text{eff}}$  sensitivity to multi-group neutron cross-sections is typically applied in similarity assessments or/and in validation algorithms. Monte Carlo codes with explicit 3D geometry are commonly used to compute the sensitivities along with one- or two-dimensional deterministic methods. The most significant diversity in the methods is observed for the similarity assessment stage. This may indicate that the issue of suitable criteria and optimal methods for similarity assessment remains open. The majority of the contributors pay attention to the benchmark quality when selecting them for the validation study, in particular to factors such as magnitude of and confidence in total uncertainty, demonstrated repeatability and reproducibility, information on all components of the total uncertainty, correlations between uncertainties for different benchmarks in the same or in different series, consistency with other high-quality benchmarks, simplicity of the benchmark, availability of additional diagnostic measurements (e.g. reaction rates and ratios, neutron flux, neutron leakage) .

A wide range of the methods are used to establish  $k_{\text{eff}}$  bias and bias uncertainty. They include expert judgement; statistical treatment of the ratio of calculated to experimental  $k_{\text{eff}}$  values; trending analysis; Bayesian Monte Carlo regression analysis; and methods based on the Generalised Linear Least-Squares method. The following sources of biases

and uncertainties are typically evaluated: nuclear data, computational methods, measurement, and benchmark modelling approximations.

Validation databases comprise mainly configurations from the ICSBEP Handbook and sometimes include experiments from other sources. Both critical and reactor type measurements, such as reaction rates or reactivities, are used for the validation studies. The number of benchmark, for which enough data are available to be used for the validation, varies significantly: from tens to more than four thousand. It should be noted that the methods based on expert judgement, rather than detailed statistical treatment, tend to use a much smaller number of selected benchmarks as part of the explicit derivation of code bias and uncertainty. However, it should be noted that this type of approach is generally performed by practitioners with extensive experience, and that by definition they will be cognizant of the code performance for a wide range and large number of benchmarks.

Some of methods/tools have been recently developed and require significant effort to test their performances, while others have been used in areas different from criticality safety. For example, the GLLSM approach has been applied in fast reactor design and safety, nuclear data validation and other areas where a considerable amount of time and effort was made to test the approach. Nevertheless, to be recommended for criticality safety assessment, their initial data and their reliabilities require thorough validation. Of particular importance is that experimental uncertainties (and correlations between the uncertainties) have been properly evaluated, so that the weighting procedure used in the fitting process is applied correctly.

Phase I exercise was conducted in order to illustrate the predictive capabilities of the described criticality validation approaches, including selection of validation benchmarks from the ICSBEP Handbook, similarity assessment, and bias and bias uncertainty definition. The results of the benchmark will be presented in the second part of the report.

Evaluations of  $k_{\text{eff}}$  sensitivities to multi-group neutron cross-sections typically contribute to similarity assessments or/and to the validation algorithm. Monte Carlo codes with explicit 3D geometry are commonly used to compute the sensitivities along with one- or two-dimensional deterministic methods. The EG exercise Phase III benchmark has been proposed to compute  $k_{\text{eff}}$  sensitivities to cross-section data for configurations selected from the ICSBEP Handbook as a useful step towards testing the sensitivity calculation methods.

Methodologies that establish uncertainties related to operational, technological and manufacturing parameters for applications/design systems are also studied under an exercise in Phase II benchmark.

**Table 7: Summary table: participants, criticality codes, nuclear data, criticality validation methods, and software tools**

Organisation Country	Criticality calculation		Validation of criticality calculation		
	Code	Nuclear data	Similarity assessment	Method for bias and bias uncertainty establishment	Software tool
<b>AREVA</b> Germany	SCALE 5.1 [3] Monte Carlo	ENDF/B-V 44-gr. or 238-gr ENDF/B-VI 238-gr.	S/U-based parameter $\alpha_k$ [34] Expert judgement	Bayesian MC regression analysis [4]	TSUNAMI-IP MOCADATA
<b>CEA</b> France	CRISTAL [72] (TRIPOLI-4.3) Monte Carlo	JEF-2.2 CE (Continuous energy)	Benchmark quality S/U-based parameter (Sensitivity calculated using APOLLO2 code and multi-group cross-sections), and representativity factors, Expert judgement	Representativity method (GLLSM based)	R.I.B. [73]
<b>EMS</b> Sweden	SCALE 5.1 [3] Monte Carlo	ENDF/B-VI 238-gr.	Expert judgement based on benchmark quality, S/U-based parameter $\alpha_k$ , Other parameters may be used.	Expert judgement, including consideration of benchmark quality and correlations [19]	TSUNAMI-IP
<b>JAEA</b> Japan	MVP II [74] Monte Carlo	JENDL-3.2 CE	Expert judgement	Statistical method	None
<b>IPPE</b> Russian Federation	MMKKENO [Error! Reference source not found.] Monte Carlo	ABBN 299-gr. Subgroups	Benchmark quality, Sensitivity comparison, $\chi^2$ filter Expert judgement	GLLSM based	INDECS [22]
<b>IRSN</b> France	CRISTAL [72] (APOLLO2- MORET 4) Monte Carlo	CEA93.V6 (JEF-2.2 172-gr.)	Physical parameters & Expert judgement	Trending analysis (trend vs combined parameters)	MACSENS [30]
<b>KINS</b> Republic of Korea	SCALE 6.0 [75] Monte Carlo	ENDF/B-VII.0 238-gr.	EALF, S/U-based parameter $\alpha_k$ , Expert judgement	Statistical method	TSUNAMI-IP
<b>ORNL</b> US	SCALE 6.0 [75] Monte Carlo	ENDF/B-VII.0 238-gr.	H/X, EALF and others or S/U- based parameter $\alpha_k$	Trending analysis	USLSTATS TSUNAMI-IP
			S/U-based parameter $\alpha_k$ $\chi^2$ filter	GLLSM based	TSURFER
<b>PSI</b> Switzerland	MCNPX [76] Monte Carlo	ENDF/B-VII.0 CE JEFF-3.1 CE	Expert judgement, benchmark quality and analysis of physical parameters	Statistical method	None

## 6. References

- [1] OECD/NEA (2008), International Handbook of Evaluated Criticality Safety Benchmark Experiments, NEA/NSC/DOC(95)03.
- [2] [www.oecd-nea.org/science/wpncs/UACSA/](http://www.oecd-nea.org/science/wpncs/UACSA/).
- [3] SCALE (2009), "A Modular Code System for Performing Standardized Computer Analyses for Licensing Evaluation", Version 5.1, ORNL/TM-2005/39, 11/1/2006; Version 6.0, ORNL/TM-2005/39.
- [4] J.C. Neuber, A. Hoefler, "Application of Monte Carlo methods to the evaluation of the criticality safety acceptance criterion", *International Conference on the Physics of Reactors*, 14-19 September 2008, Interlaken, Switzerland.
- [5] J.C. Neuber, AXEL HOEFER, "Frequentist and Bayesian Approach in Criticality Safety Uncertainty Evaluations", *Paper No. 33 of the Topical Meeting of the ANS Nuclear Criticality Safety Division 2009, Realism, Robustness and the Nuclear Renaissance*, 13-17 September 2009, Richland, Washington US.
- [6] O. Buss, A. Hoefler, J.C. Neuber, M. Schmid, "Hierarchical Monte-Carlo approach to bias estimation for criticality safety calculations", *International Conference on the Physics of Reactors*, 9-14 May 2010, Pittsburgh, US.
- [7] J.C. Neuber, A. Hoefler, MOCADATA "Monte Carlo Aided Design and Tolerance Analysis: General hierarchical Bayesian procedure for calculating the bias and the a posteriori uncertainty of neutron multiplication factors including usage of TSUNAMI in a hierarchical Bayesian procedure for calculating the bias and the a posteriori uncertainty of  $k_{\text{eff}}$ ", *International Workshop on Advances in Applications of Burn-up Credit for Spent Fuel Storage, Transport, Reprocessing, and Disposition*, organised by the Nuclear Safety Council of Spain (CSN) in cooperation with the International Atomic Energy Agency (IAEA), Córdoba, Spain, 27-30 October, 2009.
- [8] W.T. Eadie, D. Drijard, F.E. James, M. Roos, B. Sadoulet (1971), *Statistical Methods in Experimental Physics*, North Holland Publishing Company Oxford.
- [9] A. Gelman, J.B. Carlin, H.S. Stern, D.B. Rubin (2003), "Bayesian Data Analysis", Second Edition, Chapman and Hall, London.
- [10] H. Jeffreys (1961), "Theory of Probability", Third Edition, Oxford University Press.
- [11] V.V. Orlov et al. (1980), "Problems of Fast Reactors Physics Related to Breeding", *Atomic Energy Review*, 18 4, pp. 989-1077.
- [12] J.C. Cabrillat et al. (1988), "Use of Superphénix Integral Data for the Adjustment and Uncertainty Evaluation of Reactor Design Quantities", *Proc. Int. Conf. Specialist' Mtg.*, Jackson Hole, USA, 23-24 September 1988, p. 125, Nuclear Energy Agency Committee on Reactor Physics.
- [13] S. Cathalau et al. (1995), "Qualification of the JEF2.2 Cross Sections in the Epithermal and Thermal Energy Ranges Using a Statistical Approach", *NSE*, 121, pp. 326-333.
- [14] A. Santamarina et al. (2004), "Qualification of the APOLLO2.5/CEA93.V6 code for UOX and MOX fuelled PWR", *Proc. Int. Conf. on The Physics of Reactors, PHYSOR 2002*, Seoul, 7-10 October on CD-ROM, American Nuclear Society.

- [15] A. Courcelle, A. Santamarina (2004), "JEF 2.2 Nuclear Data Statistical Adjustment Using Post-Irradiation Experiments", *Proc. Int. Conf. on The Physics of Fuel Cycles and Advanced Nuclear Systems*, PHYSOR, Chicago, USA 25-29 April 2004, on CD-ROM, American Nuclear Society.
- [16] C. Venard et al. (2005), "Calculation Error and Uncertainty due to Nuclear Data Application to MOX Fissile Media", *NCSD 2005*, Knoxville, USA, 18-22 September 2005, on CD-ROM, American Nuclear Society.
- [17] A. Santamarina et al. (2008), "Advanced Neutronics tool for BWR Design Calculations", *Nuclear Engineering and Design*, 238, pp 1965-1974.
- [18] A. Santamarina et al. (2009), "APOLLO2.8: a validated code package for PWR neutronics calculations", *Proc. Int. Conf. on Advances in Nuclear Fuel Management*, ANFM-IV, Hilton Head Island, USA, 12-15 April 2009, on CD-ROM, American Nuclear Society.
- [19] OECD/NEA, "Reference Values for Nuclear Criticality Safety: Homogeneous and Uniform UO<sub>2</sub>, "UNH", PuO<sub>2</sub> and "PuNH", Moderated and Reflected by H<sub>2</sub>O", *A demonstration study by an Expert Group of the Working Party on Nuclear Criticality Safety*, NEA No. 5433. <http://www.nea.fr/html/science/pubs/2006/nea5433>.
- [20] G. Zherdev et al. (2007), "Use of the SKALA code package for computing Criticality and its Uncertainty", *Proc. of ICNC'07 Conference*, St. Petersburg.
- [21] A. Bliskavka (2001), CONSYST/MMKKENO, "Monte Carlo Code for Modelling Nuclear Reactors Using Multi-Group Approximation", Preprint IPPE-2887, Obninsk.
- [22] G. Manturov (1984), INDECS Code Package, *Nuclear Science and Technology*, Series: Nuclear Data, Issue 5(59), Moscow, p. 20.
- [23] T. Ivanova et al. (2003), "Use of International Criticality Safety Benchmark Evaluation Project Data for Validation of the ABBN Cross-Section Library with the MMKKENO Code", *Nucl. Sci. Eng.*, 145, p. 247.
- [24] T. Ivanova et al. (2003), Influence of the Correlations of Experimental Uncertainties on Criticality Prediction, *Nucl. Sci. Eng.*, 145, p. 97.
- [25] A. Bliskavka, K. Raskach, A. Tsiboulia (2005), "Algorithm of calculation of  $k_{\text{eff}}$  sensitivities to group cross-sections using Monte Carlo method and features of its implementations in the MMKKENO code", *Proc. of M&C2005 Conference*, Avignon, France, on CD-ROM.
- [26] Y. Golovko et al. (2007), "Selection of consistent Set of Critical Experiments from the ICSBEP Handbook and Evaluation of Accuracy of Calculational Prediction of Criticality", *Proceedings of International Conference on Nuclear Criticality Safety (ICNC'07)*, St. Petersburg, Vol. II, pp. 6-11.
- [27] T. Ivanova, M. Nikolaev, K. Raskach, E. Rozhikhin, An. Tsiboulia (2003), "Analysis of the Entire Set of the HEU-SOL Type Experiments from the ICSBEP Handbook for Correlation and Systematic Error", *Proc. of ICNC 2003*, Mito, Japan, 20-24 October 2003, Volume I, pp. 327-333.
- [28] T. Ivanova, M. Nikolaev, G. Manturov, K. Raskach, E. Rozhikhin, An. Tsiboulia (2003), "Estimation of Accuracy of Criticality Prediction of Highly Enriched Uranium Homogeneous Systems on the Basis of Analysis of Data from ICSBEP Handbook", *Proc. of ICNC 2003*, Mito, Japan, 20-24 October 2003, Volume I, pp. 283-288.
- [29] T. Ivanova, M. Nikolaev, E. Rozhikhin, A. Tsiboulia (1999), "Validation of the KENO/ABBN-93 package based on data from the International Handbook of Evaluated Criticality Safety Benchmark Experiments", *Proc. of ICNC 1999*, Versailles, France, 20-24 September 1999, Volume II, pp. 722-730.
- [30] F. Fernex, Y. Richet, E. Letang (2005), "MACSENS: a New MORET Tool to Assist Code Bias Estimation", *Proc. NCSD2005*, Knoxville.
- [31] H. Okuno, Y. Naito (1987), "Evaluation of Calculational Errors with the Nuclear Criticality Safety Analysis Code System JACS", *JAERI-M 87-057*.

- [32] J. Katakura, H. Okuno, Y. Naito (1997), "The preliminary edition of nuclear criticality safety handbook of Japan (2) - Criticality codes and their validation", *Proc. of International Seminar on Nuclear Criticality Safety*, 19-23 October 1987, Tokyo, Japan, 138-144.
- [33] H. Okuno (2007), "Development of a statistical method for evaluation of estimated criticality lower-limit multiplication factor depending on uranium enrichment and H/uranium-235 atomic ratio", *J. Nucl. Sci. Technol.*, 44, 137-146.
- [34] B.L. Broadhead et al. (2004), "Sensitivity and Uncertainty-based Criticality Safety Validation Techniques", *Nucl. Sci. Eng.* 146, 340-366.
- [35] B.T. Rearden, M.L. Williams, M. A. Jessee, D.E. Mueller, D.A. Wiarda (2011), "Sensitivity and Uncertainty Analysis Capabilities and Data in SCALE", *Nucl. Technol.*
- [36] S. Goluoglu et al. (2011), "Monte Carlo Criticality Methods and Analysis Capabilities in SCALE", *Nucl. Technol.*
- [37] J.J. Lichtenwalter et al. (1997), "Criticality Benchmark Guide for Light-Water-Reactor Fuel in Transportation and Storage Packages", NUREG/CR-6361 (ORNL/TM-13211), Oak Ridge National Laboratory, Oak Ridge, Tenn.
- [38] American Nuclear Society (1984), "American National Standard for Criticality Safety Criteria for the Handling, Storage and Transportation of LWR Fuel Outside Reactors", ANSI/ANS-8.1, La Grange Park, III.
- [39] H.R. Dyer, C.V. Parks (1997), "Recommendations for Preparing the Criticality Safety Evaluation of Transport Packages", NUREG/CR-5661 (ORNL/TM-11936), prepared for the U.S. Nuclear Regulatory Commission by Oak Ridge National Laboratory, Oak Ridge, Tenn.
- [40] Y. Yeivin, J.J. Wagschal, J.H. Marable, C.R. Weisbin (1980), "Relative Consistency of ENDF/B-IV and V with Fast Reactor Benchmarks", *Proc. Int. Conf. on Nuclear Cross Sections for Technology*, J.L. Fowler, C.H. Johnson, C.D. Bowman, eds., NBS SP 594.
- [41] National Nuclear Data Centre (2009), ENDF-6 Formats Manual: Data Formats and Procedures for the Evaluated Nuclear Data File ENDF/B-VI and ENDF/B-VII, ENDF-102, Brookhaven National Laboratory, Upton, New York.
- [42] N.M. Larson, L.C. Leal, H. Derrien, G. Arbanas, R.O. Sayer, D. Wiarda (2006), "A Systematic Description of the Generation of Covariance Matrices", *Proc. of PHYSOR-2006, American Nuclear Society Topical Meeting on Reactor Physics: Advances in Nuclear Analysis and Simulation*, 10-14 September 2006, Vancouver, British Columbia, Canada.
- [43] R. Little, T. Kawano, G.D. Hale, M.T. Pigni, M. Herman, P. Obložinský, M.L. Williams, M.E. Dunn, G. Arbanas, D. Wiarda, R.D. McKnight, J.N. McKamy, J.R. Felty (2008), "Low-fidelity Covariance Project", *Nuclear Data Sheets*, Vol. 109, Issue 12, December 2008, pp. 2828-2833.
- [44] M.L. Williams, B.L. Broadhead, M.E. Dunn, B.T. Rearden (2007), "Approximate Techniques for Representing Nuclear Data Uncertainties", pp. 744-752 in *Proc. of the Eighth International Topical Meeting on Nuclear Applications and Utilization of Accelerators (ACCAPP '07)*, 30 July - 2 August 2007, Pocatello, Idaho.
- [45] M.L. Williams, B.T. Rearden (2008), "SCALE-6 Sensitivity/Uncertainty Methods and Covariance Data", *Nuclear Data Sheets*, Vol. 109, Issue 12, December 2008, pp. 2796-2800.
- [46] S.F. Mughabghab (2006), "Atlas of Neutron Resonances: Resonance Parameters and Thermal Cross Sections", Elsevier, Amsterdam.
- [47] M.T. Pigni, M. Herman, P. Obložinsky (2009), "Extensive set of cross section covariance estimates in the fast neutron region", *Nucl. Sci. Eng.* 162(1), 25-40.
- [48] D. Rochman, M. Herman, P. Obložinsky, S.F. Mughabghab (2007), "Preliminary Cross Section and Nubar Covariances for WPEC Subgroup 26", BNL-77407-2007-IR.
- [49] T. Kawano, P. Talou, P.G. Young, G. Hale, M.B. Chadwick, R.C. Little (2008), "Evaluation of Covariances for Actinides and Light Elements at LANL", *Nuclear Data Sheets*, Vol. 109, Issue 12, December 2008, pp. 2817-2821.

- [50] G. Hale, "Covariances from Light-Element R-Matrix Analyses", *Nuclear Data Sheets*, Vol. 109, Issue 12, December 2008, pp. 2812-2816.
- [51] L.C. Leal, D. Wiarda, B.T. Rearden, H. Derrien (2008), "<sup>233</sup>U Cross-Section and Covariance Data Update for SCALE 5.1 Libraries", ORNL/TM-2007/115, Oak Ridge National Laboratory, Oak Ridge, Tenn.
- [52] S.F. Mughabghab (2003), "Thermal Neutron Capture Cross Sections Resonance Integrals and G-Factors", INDC (NDS)-440, International Atomic Energy Agency.
- [53] B.L. Broadhead, J.J. Wagschal (2004), "The Fission Spectrum Uncertainty,"95821.pdf in *Proc. of PHYSOR 2004, The Physics of Fuel Cycles and Advanced Nuclear Systems: Global Developments*, 25-29 April 2004, Chicago, Illinois.
- [54] D. Wiarda, M.E. Dunn (2006), "PUFF-VI: A Code for Processing ENDF Uncertainty Data Into Multi-group Covariance Matrices", ORNL/TM-2006/147, Oak Ridge National Laboratory.
- [55] B.T. Rearden, D.E. Mueller, S.M. Bowman, R.D. Busch, S.J. Emerson (2009), "TSUNAMI Primer: A Primer for Sensitivity/Uncertainty Calculations with SCALE", ORNL/TM-2009/027, Oak Ridge National Laboratory, Oak Ridge, Tenn.
- [56] G. Radulescu, D.E. Mueller J.C. Wagner (2009), "Sensitivity and Uncertainty Analysis of Commercial Reactor Criticals for Burn-up Credit", *Nucl. Technol.* 167(2), 268-287.
- [57] D.E. Mueller, B.T. Rearden, D.F. Hollenbach (2009), "Application of the SCALE TSUNAMI Tools for the Validation of Criticality Safety Calculations Involving <sup>235</sup>U", ORNL/TM-2008/196, Oak Ridge National Laboratory, Oak Ridge, Tenn.
- [58] D.E. Mueller, B.T. Rearden (2008), "Using Cross-Section Uncertainty Data to Estimate Biases", *Trans. Am. Nucl. Soc.* 99, 389-390.
- [59] J.A. Roberts, D.E. Mueller (2008), "Designing Critical Experiments in Support of Full Burn-up Credit", *Trans. Am. Nucl. Soc.* 99, 391-393.
- [60] L. Leal, D. Mueller, G. Arbanas, D. Wiarda, H. Derrien (2008), "Impact of the <sup>235</sup>U Covariance Data In Benchmark Calculations", *Proceedings of the International Conference on the Physics of Reactors (PHYSOR '08), "Nuclear Power: A Sustainable Resource"*, Casino-Kursaal Conference Centre, Interlaken, Switzerland, 14-19 September 2008.
- [61] D.E. Mueller, K.R. Elam, P.B. Fox (2008), "Evaluation of the French Haut Taux de Combustion (HTC) Critical Experiment Data", NUREG/CR-6979 (ORNL/TM-2007/083), prepared for the U.S. Nuclear Regulatory Commission by Oak Ridge National Laboratory, Oak Ridge, Tenn.
- [62] B.T. Rearden, D.E. Mueller (2008), "Recent Use of Covariance Data for Criticality Safety Assessment", *Nuclear Data Sheets* 109, 2739-2744.
- [63] J.R. Parry, J.D. Bess, B.T. Rearden, G.A. Harms (2008), "Assessment of Zero Power Critical Experiments and Needs for a Fission Surface Power System", INL/EXT-08-14678, Idaho National Laboratory.
- [64] G. Radulescu, D.E. Mueller, J.C. Wagner (2007), "Sensitivity and Uncertainty Analysis of Commercial Reactor Criticals for Burn-up Credit", NUREG/CR-6951 (ORNL/TM-2006/87), prepared for the U.S. Nuclear Regulatory Commission by Oak Ridge National Laboratory, Oak Ridge, Tenn.
- [65] G. Radulescu, D.E. Mueller, S. Goluoglu, D.F. Hollenbach, P.B. Fox (2007), "Range of Applicability and Bias Determination for Postclosure Criticality of Commercial Spent Nuclear Fuel", ORNL/TM-2007/127, Oak Ridge National Laboratory, Oak Ridge, Tenn.
- [66] C.V. Parks, J.C. Wagner, D.E. Mueller, I.C. Gauld (2007), "Full Burn-up Credit in Transport and Storage Casks--Benefits and Implementation", *Radwaste Solutions* 14(2), 32-41.
- [67] U.S. Nuclear Regulatory Commission Office of Nuclear Material Safety and Safeguards, Division of Fuel Cycle Safety and Safeguards (FCSS) Interim Staff Guidance (ISG)-10, "Justification of Minimum Margin of Subcriticality for Safety", FCSS ISG-10, Rev. 0, 15 June 2006.

- [68] C.M. Hopper, J.A. Bucholz, R.M. Westfall, C.V. Parks (2005), "Applications of SCALE 5 TSUNAMI for Critical Experiment Benchmark Design, Interpretation, and Estimation of Biases and Uncertainties for Space Power Reactor Designs and Safety Analyses", *American Nuclear Society Embedded Topical Meeting - 2005 Space Nuclear Conference*, p 676-685.
- [69] S. Goluoglu, K.R. Elam, B.T. Rearden, B.L. Broadhead, C.M. Hopper (2004), "Sensitivity Analysis Applied to the Validation of the 10B Capture Reaction in Nuclear Fuel Casks", NUREG/CR-6845 (ORNL/TM-2004/48), prepared for the U.S. Nuclear Regulatory Commission by Oak Ridge National Laboratory, Oak Ridge, Tenn.
- [70] A. Vasiliev, E. Kolbe, M.A. Zimmermann (2008), "Towards the development of upper subcriticality limits on the basis of benchmark criticality calculations", *Annals of Nuclear Energy* 35, 1764-1773.
- [71] E. Kolbe, A. Vasiliev, H. Ferroukhi, M.A. Zimmermann (2008), "Consistent evaluation of modern nuclear data libraries for criticality safety analyses of thermal compound low-enriched-uranium systems", *Annals of Nuclear Energy*, doi:10.1016/j.anucene.2008.04.009.
- [72] J-M. Gomit et al. (2005), CRISTAL V1: "Criticality Package for Burn-up Credit Calculation", *Proc. of NCSD 2005 Meeting: Integrating Criticality Safety into the Resurgence of Nuclear Power*, Knoxville, Tennessee, 19-22 September 2005, on CD-ROM, American Nuclear Society, LaGrange Park, IL.
- [73] C. Venard et al. (2009), "The R.I.B. Tool for the Determination of Computational Bias and Associated Uncertainty in the CRISTAL Criticality-Safety Package", *Proc. of NCSD 2009 Meeting: Realism, Robustness and the Nuclear Renaissance*, Richland, Washington, 13-17 September 2009, on CD-ROM, American Nuclear Society, LaGrange Park, IL.
- [74] Y. Nagaya et al. (2005), "MVP/GMVP II : General Purpose Monte Carlo Codes for Neutron and Photon Transport Calculations based on Continuous Energy and Multi-group Methods", JAERI 1348.
- [75] SCALE: "A Modular Code System for Performing Standardized Computer Analyses for Licensing Evaluation", ORNL/TM-2005/39, Version 6, Vols. I-III, Oak Ridge National Laboratory, Oak Ridge, Tenn., January 2009, available from Radiation Safety Information Computational Centre at Oak Ridge National Laboratory as CCC-750.
- [76] D.B. Pelowitz (Ed.), "MCNPX User's Manual", Version 2.5.0, LA-CP-05-0369, (LANL, 2005).
- [77] J.C. Neuber (2010), "Advances in Burn-up Credit Criticality Safety Analysis Methods and Applications", International Conference on Management of Spent Fuel from Nuclear Power Reactors", 31 May – 4 June 2010, Vienna, organised by IAEA in co-operation with OECD/NEA, Paper No. IAEA-CN178-KN23, [www-ns.iaea.org/meetings/rw-summaries/vienna-2010-mngement-spent-fuel.asp](http://www-ns.iaea.org/meetings/rw-summaries/vienna-2010-mngement-spent-fuel.asp) (Session 7, Germany).
- [78] J.C. Neuber, A. Hofer, J. M. Conde (2007), "Statistical Evaluation of the Isotopic Bias in Burn-Up Credit Criticality Analysis of Spent Nuclear Fuel Systems", *Proceedings of the 8<sup>th</sup> International Conference on Nuclear Criticality Safety ICNC 2007*, St. Petersburg, Russia, Vol. II pp. 124-130 (Re-print of the ICNC2007 Proceedings sponsored by AREVA).
- [79] O. Buss, A. Hofer, J.C. Neuber (2011), "NUDUNA – Nuclear Data Uncertainty Analysis", *Proceedings of the International Conference on Nuclear Criticality 2011, ICNC2011*.
- [80] J.C. Neuber, A. Hofer, O. Buss (2011), "CONCERT: A complete uncertainty analysis tool for criticality safety analysis", *Proceedings of the International Conference on Nuclear Criticality 2011, ICNC2011*.
- [81] NJOY 99, <http://t2.lanl.gov/codes/njoy99/index.html>.
- [82] D. Wiarda, M.E. Dunn (2006), "PUFF-IV: A Code for Processing ENDF Uncertainty Data into Multi-group Covariance Matrices", ORNL/TM-2006/147.

## Appendix A: Glossary of EG UACSA

A single term can sometimes be used with more or less varying meanings. On the other hand, multiple terms can sometimes be used to mean the same thing. Sometimes the meaning is clear from the environment where the term is applied. However, sometimes the interpretation of a term could be incorrect or cause a delay in the understanding of the message. To reduce misunderstandings and to simplify communication, the OECD/NEA/NSC/WPNCs Expert Group on Uncertainty Analysis in Criticality Safety Assessment (UACSA) has agreed on the glossary in this and in future documents and discussions.

The glossary is limited to providing simplified descriptions to help the reader in situations where confusion from use of multiple interpretations of a term or from using multiple terms for the same intention may be possible. More extensive descriptions, including mathematical equations and expressions, may be given in other referenced documents.

### Accuracy

The closeness of computations or estimates to the best-estimate (“true”) value. Directly associated with the term bias. Often used together with precision and the associated term uncertainty.

### Adjustment of data

Some of the more advanced methods for validation build on techniques for adjusting data to obtain agreement between calculation and measurement results. It considers potential variations in nuclear data that minimise the differences in measured and calculated  $k_{eff}$  for a set of the experimental benchmarks, taking into account uncertainties and correlations in nuclear data and in the benchmark  $k_{eff}$ . Reliable methods result in adjustments that confirm known expected measurement biases or that will eventually lead to improved measurements and their evaluations. The adjustment may be similar to a manual bias correction, except that it is based on rigorous technique and built into the software.

### Administrative Margin (AM)

Margin in  $k_{eff}$  applied in addition to bias and bias uncertainty allowances to ensure subcriticality. The AM is a reflection of the confidence in the criticality validation. Terms with similar meanings to be avoided include arbitrary margin, safety margin and subcritical margin.

### Allowance

Allowance is a term often used in criticality safety to bound bias corrections, bias uncertainties or both. If uncertainties are included, the probability distribution should be specified. Use of an allowance will not result in a best-estimate specification.

**Application**

An application is normally used to represent a system/scenario for which the result has not been measured or determined in any other way. A measurement can be treated as an application to support evaluation of the evaluated bias and uncertainty of the measurement. A measurement with a reliable result can also be used to determine the performance of a validation method.

**Benchmark**

A benchmark is a well-defined specification of a problem with a best-estimate solution. A benchmark is intended for testing of a method's capability to provide an adequate solution. An ICSBEP Handbook benchmark has an exact specification with a best-estimate result, allowing for some uncertainty in the result. Other types of benchmarks may have specifications that include uncertainties, leading to results that include corresponding and probably additional uncertainties.

**Benchmark experiment**

A benchmark experiment is sufficiently well characterised to support development of one or more useful calculation benchmarks.

**Benchmark uncertainty**

A benchmark uncertainty is a combination of experiment uncertainties and benchmark simplification uncertainties. The total benchmark uncertainty can be specified by the random effect uncertainty and a number of systematic effect uncertainties. Different benchmarks may be correlated through systematic effect uncertainties.

**Bias**

The bias is the difference between an estimated specification or result, using a well-defined method, and a best-estimate specification or result. It is equivalent to a deviation relative to the best-estimate value. When applicable, both sign and magnitude of the difference need to be specified. An overestimation leads to a positive (sign) bias while an underestimation leads to a negative (sign) bias.

**Bias allowance**

A consideration of the bias in a method or parameter. It can be a combination of bias correction and bias uncertainty. A conservative approach in a criticality safety evaluation is to set a negative bias allowance (influence of a positive bias) for  $k_{eff}$  to zero.

**Bias correction**

A bias correction is the bias with a reversed sign. It is needed to give a best-estimate value, as opposed to a bias allowance which may be used to give a conservative value.

**Bias uncertainty allowance**

After an estimation of a bias is made, an uncertainty normally applies to its accuracy. An allowance for this uncertainty is needed to represent the uncertainty in the

determination of a limiting value. The consideration of an uncertainty allowance changes an expression to a probability range even though it can be expressed as a single value.

### Calculation bias

A calculation bias is the difference between a calculation result and a best-estimate result, i.e. e.g. calculated  $k_{eff}$  – benchmark  $k_{eff}$ . It is often the result of a deliberate approximation and not necessarily an error.

### Calculation uncertainty

A statistical method like Monte Carlo results in a statistical uncertainty. A deterministic method results in a convergence uncertainty.

### Central Limit Theorem (CLT)

In probability theory, the classical central limit theorem (CLT) states conditions under which the mean of a sufficiently large number of independent random variables, each with finite mean and variance, will be approximately normally distributed. The central limit theorem requires the random variables to be identically distributed, unless certain conditions are met.

A practical interpretation of the general CLT allows random variables that are not identically distributed, as long as the total variance is much larger than any single variance related to a non-normal distribution. The validity of the assumption needs to be verified.

### Correlation

Correlation between two variables means that at least one of them influences the other in some parameter range. The correlation can be deterministic (known reason) or statistical. A statistical definition can be made using the covariance definition. The correlation parameter is defined as  $\rho_{\mu_i} = \mu_{i\phi} / (\mu_{i1}\mu_{\phi\phi})^{1/2}$ . If the variances and covariances are determined correctly, the correlation parameter is within the range  $-1 \leq \rho_{i\phi} \leq 1$ .

A correlation may be linear or more complicated.

Even if two parameter changes are independent, the resulting variable (function) changes can be dependent on each other. If the resulting effect is the change in  $k_{eff}$ , the correlation from two independent parameter changes, such as those of fissile mass and water mass, is obtained through the changes in the neutron flux.

### Covariance

Covariance is a measure of an uncertainty in a variable due to common uncertainties in this and in another variable. It is a second order moment of the probability function (like the variance, while the mean is the first order moment). If the variance is expressed as  $\mu_{ii} = \langle (\xi_i - \mu_{0i})^2 \rangle$  then the covariance can be expressed as  $\mu_{i\phi} = \langle (\xi_i - \mu_{0i})(\xi_\phi - \mu_{0\phi}) \rangle$ . Variances and covariances should be determined from comparable observations. Misleading conclusions can be obtained if the observed results are due to variation in one variable at a time, with other variables at constant “base values”. Non-linearity complicates this issue. Even if the dependence of a variable on each single parameter is linear, the dependence on combinations of two or more parameters may not be linear.

**Criticality safety assessment**

One task is to determine and apply logic data (in a broad sense), and calculation methods to determine system (scenario) subcriticality. Another task is to determine and apply acceptance criteria to the system being assessed. The assessment establishes how the determination complies with the acceptance criteria.

**Deviation**

See bias. A standard deviation is not a real deviation but an uncertainty that informs about the probability distribution of the true value related to an estimated value.

**Effect**

The effect, as defined here in connection with random and systematic biases and uncertainties, is limited to the final influence. It is important since it makes an important difference to the source of random and systematic biases and uncertainties. A random bias and uncertainty source does not necessarily give a random effect (if it applies to multiple values) and a systematic bias and uncertainty source does not necessarily give a systematic effect (if it is only applied once).

**Error**

Error is here considered as an unintentional bias, i.e. an unintentional deviation with an estimated sign and amplitude. The concept of “systematic error” is avoided due to its history of inconsistent use.

**Precision**

Precision is a measure of the degree of variation of an estimation from the mean value of a large number of estimations but it is never smaller than the rounding uncertainty. Directly associated with the term uncertainty. Minimum precision indicates that the estimation is within the specified range with a very high confidence level. Maximum precision means the best possible single estimation (e.g. determined by the number of digits on a display). Often used together with accuracy and the associated term bias.

**Quality of an experimental benchmark**

The following specifications contribute to the quality of a benchmark: low total uncertainty (from evaluation of the experiment and from simplifications made for the benchmark), demonstrated repeatability (identical configuration and methods), demonstrated reproducibility (different configuration and methods, e.g. at a different site), information on all components of the total uncertainty and correlations between uncertainties for different benchmarks in the same or in different series, consistency with other high-quality benchmarks (when available), simplicity, availability of complementary measurements (such as reaction rates and ratios, neutron flux, neutron leakage), comprehensive documentation.

**Sensitivity**

Response of a system parameter (P) to a change in another system parameter (X). The sensitivity may be expressed as  $S_p$ , the fractional change  $\Delta P$  in the parameter P corresponding to fractional change  $\Delta X$  in the parameter X or as

$$S_p = \frac{\Delta P / P}{\Delta X / X}$$

### **System/Scenario**

The term system is often referred to in connection with validation. It is then intended to cover a specific scenario. This is different than the engineering term that is often used to represent a functional system (e.g. storage system, transport system, containment system). The same engineering system can lead to many scenarios to cover normal and abnormal conditions.

### **Uncertainty**

Uncertainty is a representation of a probability distribution for an estimation related to some value (often the average value of a large number of measurements).

### **Validation**

Validation refers to a method for determination of overall acceptability of a method, technique, document (e.g. approval certificate for transport), etc. The discussions on uncertainty relate validation to testing against benchmarks. The result of a validation may be a bias with an associated uncertainty but may also be a simple “safe” or “unsafe”.

Validation includes establishment of an area of applicability.

### **Verification**

Verification can be a demonstration that a certain algorithm is implemented properly into a method. It can also be documentation that verifies that information (e.g. input data and results from calculations) is correct.

Verification is different to validation. Verification of a document means that it is correct (identical to the original) while validation means that the document contents are acceptable to a reviewer.

## Appendix B: List of authors and contributors

### Authors

T. Ivanova	(IRSN, France)
R. McKnight	(ANL, US)
D. Mennerdahl	(EMS, Sweden)
J.C. Neuber	(AREVA, Germany)
B. Rearden	(ORNL, US)
A. Santamarina	(CEA, France)
A.Vasiliev	(PSI, Switzerland)

### Contributors

A. Hofer	(AREVA, Germany)
C. Venard, C. Mounier	(CEA, France)
Y. Golovko, E. Rozhikhin, A. Tsiboulia	(IPPE, Russian Federation)
F. Férnax, F. Willem	(IRSN, France)
Y. Nagaya	(JAEA, Japan)
G.S. Lee, S.W. Woo	(KINS, Republic of Korea)
D. Mueller	(ORNL, US)
E. Kolbe, M.A. Zimmermann, H. Ferroukhi	(PSI, Switzerland)